EFFECTS OF EGR, WATER/N_2/CO_2 INJECTION AND OXYGEN ENRICHMENT ON THE AVAILABILITY DESTROYED DUE TO COMBUSTION FOR A RANGE OF CONDITIONS AND FUELS

A Thesis

by

HARI SHANKER SIVADAS

Submitted to the Office of Graduate Studies of
Texas A&M University
in partial fulfillment of the requirements for the degree of

MASTER OF SCIENCE

August 2007

Major Subject: Mechanical Engineering

EFFECTS OF EGR, WATER/N_2/CO_2 INJECTION AND OXYGEN ENRICHMENT ON THE AVAILABILITY DESTROYED DUE TO COMBUSTION FOR A RANGE OF CONDITIONS AND FUELS

A Thesis

by

HARI SHANKER SIVADAS

Submitted to the Office of Graduate Studies of
Texas A&M University
in partial fulfillment of the requirements for the degree of

MASTER OF SCIENCE

Approved by:

Chair of Committee,	Jerald A Caton
Committee Members,	Kalyan Annamalai
	James A Silas
Head of Department,	Dennis O'Neal

August 2007

Major Subject: Mechanical Engineering

ABSTRACT

Effects of EGR, Water/N_2/CO_2 Injection and Oxygen Enrichment on the Availability Destroyed due to Combustion for a Range of Conditions and Fuels. (August 2007)

Hari Shanker Sivadas, B.S. Mechanical Engineering, Anna University
Chair of Advisory Committee: Dr. Jerald A.Caton

This study was directed at examining the effects of exhaust gas recirculation (EGR), water/N_2/CO_2 injections and oxygen enrichment on availability destroyed because of combustion in simple systems like those of constant pressure and constant volume.

Higher cooled EGR fractions lead to higher availability destruction for reactant temperatures less than 2000 K. The availability destroyed for 40% EGR at 300 K for constant pressure and constant volume combustion was 36% and 33%, respectively. Neglecting the chemical availability in the products, the equivalence ratio and reactant temperature that corresponded to the lowest availability destruction varied from 0.8 to 1.0 and 800 K to 1300 K, respectively, depending on the EGR fraction. The fraction of the reactant availability destroyed increased with the complexity of the fuel. The trends stayed the same for the different EGR fractions for the eight fuels that were analyzed.

Higher injected water fractions lead to higher availability destruction for reactant temperatures less than 1000 K. The availability destroyed for a 40% injected water fraction at 300 K for constant pressure combustion was 36%. The product temperature ranged from 2300 K to 450 K at a reactant temperature of 300 K for injected fractions from 0% to 90%. For a 40% injected fraction at a reactant temperature of 300 K, water injection and cooled EGR resulted in the greatest destruction of availability (about 36%) with CO_2 injection leading to the least destruction (about 32%).

Constant volume combustion destroyed less availability compared to constant pressure combustion at a reactant pressure of 50 kPa. At a higher reactant pressure of 5000 kPa, constant pressure combustion destroyed less availability compared to constant volume combustion for reactant temperatures past 1000 K. Higher fractions of oxygen in the inlet lead to higher product temperatures that lead to lower availability destruction. For 40% oxygen in inlet, the product temperature increased to 2900 K and the availability destroyed dropped to 25% at a reactant temperature of 300 K for constant pressure combustion.

ACKNOWLEDGEMENTS

I would like to thank my advisor and committee chair, Dr. Jerald A.Caton, for giving me an opportunity to work on the project as part of my graduate research. His support and guidance extended from the early stages of getting familiar with the topic to the development of the program and subsequent interpretation of the results.

I would, also, like to thank my committee members, Dr. Kalyan Annamalai and Dr. James Silas for helping me through the various stages of the project to accomplish the objectives that I had set for myself. I would, also, like to thank Dr. Timothy Jacobs for supporting and guiding me during the past year.

I would like to thank the sponsors, National Energy Technology Laboratory (NETL) for funding the project, thus giving me a chance to study the combustion process and related phenomena. I want to pursue a career in engines research and I thank them for giving me the chance to work on a range of topics directly applicable to IC engines. The contents of this thesis, however, do not necessarily reflect the opinions or views of the sponsors.

Lastly, I would like to thank two of my seniors whose support was greatly appreciated during my graduate study: Praveen Chavannavar, for helping me get familiar with the topic and for helping me during the development of the program and Dushyant Pathak for supporting and advising me during my graduate study.

In closing, I would like to express my gratitude to everyone who helped and supported me during my graduate study at Texas A&M.

TABLE OF CONTENTS

LIST OF FIGURES

FIGURE Page

FIGURE Page

FIGURE Page

LIST OF TABLES

NOMENCLATURE

$(F:A)_{Actual}$	Actual fuel air ratio
a	Number of moles of fuel
a_1	Coefficient 1 for least square polynomial fit for determining thermodynamic properties
a_2	Coefficient 2 for least square polynomial fit for determining thermodynamic properties
a_3	Coefficient 3 for least square polynomial fit for determining thermodynamic properties
a_4	Coefficient 4 for least square polynomial fit for determining thermodynamic properties
a_5	Coefficient 5 for least square polynomial fit for determining thermodynamic properties
a_6	Coefficient 6 for least square polynomial fit for determining thermodynamic properties
a_7	Coefficient 7 for least square polynomial fit for determining thermodynamic properties
$\mathrm{A}_{\mathrm{Abs}}$	Absolute availability
$\mathrm{A}_{\mathrm{Abs,\,f}}$	Absolute flow availability
A_{CA}	Total chemical availability
$\mathrm{A}_{\mathrm{Dest}}$	Availability destroyed
$\mathrm{A}_{\mathrm{Diffusive}}$	Diffusive chemical availability
$\mathrm{A}_{\mathrm{Products}}$	Total availability of the products
$\mathrm{A}_{\mathrm{Reactants}}$	Total availability of the reactants
$\mathrm{A}_{\mathrm{Reactive}}$	Reactive chemical availability
A_{Ref}^{0}	Reference availability
$\mathrm{A}_{Ref,\mathrm{f}}^{0}$	Reference flow availability
$\mathrm{A}_{\mathrm{TMA}}$	Thermo-mechanical availability of system

$A_{\mathrm{TMA,\,f}}$	Flow Thermo-mechanical availability of system
A_{Total}	Total availability of the system
$A_{\mathrm{Total,\,f}}$	Total flow availability of system
A_W	Availability due to work performed
A_T	Availability due to heat transfer
b	Number of moles of air
b_1	Coefficient 8 for least square polynomial fit for determining thermodynamic properties
b_2	Coefficient 9 for least square polynomial fit for determining thermodynamic properties
c_p	Molar constant pressure specific heat
$EGR\%$	EGR Fraction
f_{O_2}	Mole fraction of oxygen in atmosphere
ΔG	Change in Gibbs energy associated with a reaction
gr	Graphite
H	Enthalpy of system
$h_{A/F}$	Specific enthalpy of Air/Fuel stream
h_{EGR}	Specific enthalpy of EGR stream
h_{inlet}	Total specific enthalpy of inlet stream
h_k	Molar specific enthalpy of species k
$Injected\%$	Fraction of species injected
$m_{A/F}$	Mass of Air/Fuel stream
m_{EGR}	Mass of EGR
$m_{Injected}$	Mass of species injected
m_{Inlet}	Total inlet mass

M	Molecular weight of mixture returned by CEA
M_k	Molecular weight of species '*k*'
MW	Molecular weight of mixture including condensed species
MW_{Air}	Molecular weight of air
MW_{Fuel}	Molecular weight of fuel
n	Number of moles
NG	Number of gaseous species in the mixture
NS	Total number of species in the mixture (Including condensed species)
P	Pressure
$\overline{R}$	Universal gas constant
s_k	Molar specific entropy of species *k*
S	Entropy of system
T	Temperature
U	Internal energy of system
$u_{A/F}$	Specific internal energy of Air/Fuel stream
u_{EGR}	Specific internal energy of EGR stream
u_{inlet}	Total specific internal energy of inlet stream
u_k	Molar specific internal energy of species *k*
V	Volume
x	Number of atoms of carbon per fuel molecule
y	Number of atoms of hydrogen per fuel molecule
y_k	Mole fraction of species *k*
z	Number of atoms of oxygen per fuel molecule

Greek symbols

ϕ	Equivalence ratio

μ	Chemical potential

Superscripts

0	Restricted dead state conditions

Subscripts

0	Reference (atmospheric) conditions
k	species index

I. INTRODUCTION

Most of our energy needs today are being met by the combustion of fossil fuels to convert the chemical energy in them into a more useful form. This is evident in energy conversion devices like gas turbines and internal combustion engines.

The combustion process is inherently irreversible due to the presence of a large number of property gradients and this essentially limits the amount of the chemical energy originally present in the fuel that can be converted into work. The first law of thermodynamics quantifies the various energy interactions in a process. The second law attributes a *quality* to the energy interactions and limits the maximum amount of useful work that can be extracted from a system.

This study aims at isolating the amount of work potential or availability that is lost during the combustion process. All other forms of availability transfer have been ignored to isolate the effect of combustion on the availability destroyed. Only simple combustion systems, like constant pressure and constant volume, have been considered here to conduct the second law analysis. Although this is not a true representation of the combustion systems in actual engines and gas turbines, it does provide a good understanding of the inherent irreversibilities associated with the combustion process and aims at quantifying the availability that is lost.

Availability or Exergy

Availability or Exergy represents the work potential of any system as it comes into equilibrium with the environment. No system can extract work greater than the availability of the system without violating the second law of thermodynamics. The total availability of the system is split into the thermo-mechanical component and the chemical component. The thermo-mechanical component represents the availability that can be extracted from a system as it comes into thermal and mechanical equilibrium with the ambient. The ambient temperature and pressure values in this study are 298.15 K and 101.325 kPa, respectively.

This state of thermal and mechanical equilibrium with the environment is called the ‘Restricted Dead State’. At this point, the temperature and pressure is the same as the ambient but the chemical composition might not necessarily be the same as the ambient. Hence there is still a possibility of utilizing the chemical work potential of the species, now at the restricted dead state. This can be done in two steps.

This thesis follows the style and format of Energy.

First, the chemical species are converted into species present in the ambient through a series of oxidation/reduction reactions at the restricted dead state. Secondly, there could still be a concentration gradient between the species and this can be equalized through the use of semi-permeable membranes and work may be gained or required during this process. The first step in extracting the chemical potential of the species can be a significant number especially at richer equivalence ratios, but the second step usually represents a very small work potential.

The absolute thermo-mechanical availability is defined as:

(Closed System) $$\mathrm{A}_{\mathrm{Abs}} = U - T_0 S + P_0 V \tag{1.1}$$

(Open System) $$\mathrm{A}_{\mathrm{Abs,\,f}} = H - T_0 S \tag{1.2}$$

where, *U*, *H*, *S* and *V* are the system internal energy, enthalpy, entropy and volume and T_0 and P_0 are the ambient temperature and pressure, respectively.

The total thermo-mechanical availability is limited by the availability of the ambient (restricted dead state), i.e. the availability of the species under consideration at the ambient conditions. Hence the total thermo-mechanical availability of a system as it comes into temperature and pressure based equilibrium with the ambient is defined as,

(Closed System) $$\mathrm{A}_{\mathrm{TMA}} = (U - U^0) - T_0 (S - S^0) + P_0 (V - V^0) \tag{1.3}$$

(Open System) $$\mathrm{A}_{\mathrm{TMA,\,f}} = (H - H^0) - T_0 (S - S^0) \tag{1.4}$$

where, U^0, H^0, S^0 and V^0 are the system internal energy, enthalpy, entropy and volume at the ambient conditions.

The chemical component of availability that can be extracted by converting all the species present into species in the ambient is called the ‘Reactive chemical availability’ and the chemical component of availability that can be extracted by equalizing the concentration gradients is called the ‘Diffusive chemical availability’ and is again dependent on the composition of the ambient.

$$\mathrm{A}_{\mathrm{Reactive}} = \sum_{k=1}^{n} \Delta G_k^0 \tag{1.5}$$

where, ΔG_k^0 is the change in Gibbs free energy as the species gets converted into species in the ambient.

$$\mathrm{A}_{\text{Diffusive}} = \sum_{k=1}^{n} n_k \overline{R} T_0 \ln \frac{y_k^0}{y_{k0}} \tag{1.6}$$

where, y_k^0 is the mole fraction of the species '*k*' in the restricted dead state and y_{k0} is the mole fraction of the species '*k*' in the ambient.

The total availability of the system is now represented as follows:

$$\mathrm{A}_{\text{Total}} = \mathrm{A}_{\text{TMA}} + \mathrm{A}_{\text{Reactive}} + \mathrm{A}_{\text{Diffusive}} \tag{1.7}$$

$$\mathrm{A}_{\text{Total}} = (U - U^0) - T_0(S - S^0) + P_0(V - V^0) + \sum_{k=1}^{n} \Delta G_k^0 + \sum_{k=1}^{n} n_k \overline{R} T_0 \ln \frac{y_k^0}{y_{k0}} \tag{1.8}$$

(Closed System)

$$\mathrm{A}_{\text{Total, f}} = (H - H^0) - T_0(S - S^0) + \sum_{k=1}^{n} \Delta G_k^0 + \sum_{k=1}^{n} n_k \overline{R} T_0 \ln \frac{y_k^0}{y_{k0}} \tag{1.9}$$

(Open System)

Description of Following Sections

Section II, Literature Review, outlines some of the previous work done in applying the second law to both simple combustion systems and engines. It also reviews some of the previous work done on studying processes like exhaust gas recirculation, water injection, and oxygen enrichment. It describes the motivations and objectives of the current study.

Section III, Development of the Model, describes the constant pressure and constant volume combustion models and outlines the steps involved in the availability analysis. It also lists the different assumptions and approximations of the model. The NASA Lewis polynomial coefficients used in determining the thermodynamic properties are also described. The different sub routines in the main program dealing with the simulations of processes like exhaust gas recirculation, water injection, and oxygen enrichment are also explained.

Section IV, Results and Discussion, presents the results of the availability analysis for the cooled EGR and the water injection processes. The availability analysis for the cooled EGR case was done for both the constant pressure and constant volume combustion systems. The water injection case was limited to the constant pressure combustion case. A section comparing the cooled EGR and water/CO_2/N_2 injections for a constant pressure combustion system is included. The constant pressure and constant volume combustion systems are also compared as part of the results.

Section V, Summary and Conclusion, provides a brief summary and conclusion of the results obtained.

Appendix I, includes the results obtained for the comparison between the frozen and non-frozen cases of cooled EGR along with the results for adiabatic EGR, oxygen enrichment and condensed species equilibrium cases for a constant pressure combustion system. The results presented in section IV and appendix I were arrived at through a comprehensive parametric analysis involving variation of parameters like equivalence ratio, EGR and injection fractions, reactant temperature and the type of fuel.

Appendix II, III and IV lists the NASA Lewis polynomial coefficients for different fuels, composition of the ambient assumed in the model, and the availability values of the different fuels respectively.

II. LITERATURE REVIEW

Review of Previous Work

This section is divided into two parts. The first part deals with the review of studies undertaken with regards to the application of the second law to simulation of simple combustion systems and engines. The second part deals with the review of studies into techniques like exhaust gas recirculation, water injection, and oxygen enrichment.

Second law analysis is an extremely powerful tool when it comes to identifying the sources of irreversibility (loss of availability) in a system. Most studies of thermal systems like combustion engines, gas turbines and power plants have been based on first law analysis. The first law essentially lets one quantify the various energy interactions in the system but does not take into consideration a vital aspect of those energy terms, i.e. the *quality* of the energy. A second law analysis, on the other hand, does incorporate the *quality* aspect of the energy, and hence, gives a better assessment of the efficiency of the system.

In the past, work has been done with regards to applying the second law analysis to both spark ignition and compression ignition engine simulations. A thorough summary of the important studies undertaken in this area has been done by Caton [1] and Rakopoulos and Giakoumis [2]. The latter study also includes the summary of the second law analysis done on turbocharged and naturally aspirated engines, direct or indirect compressions ignition engines and also for steady state and transient engine operations.

Some of the past second law analysis studies have disregarded the chemical availability aspect when performing the availability balance. This is not a complete representation of the second law efficiency. Van Gerpen and Shapiro [3] considered the effect of the chemical availability when performing the second law analysis. They performed a second law analysis for a diesel engine using a single zone combustion model. The availability was split into thermo-mechanical and chemical availabilities. They found that the contribution of the chemical availability was significant when richer equivalence ratios were considered (as high as 90% of the total availability at an equivalence ratio of 2.0). Van Gerpen and Shapiro [4] also conducted a second law analysis for both spark ignition and compression ignition engines using a two zone combustion model. The thermo-mechanical and the chemical availabilities were considered separately in both the burned and the unburned zones. Again they found that the contribution of the chemical availability was significant at the richer equivalence ratios in both the unburned and burned zones for the spark ignition engine and in the burned zone for the compression ignition engine. This was mainly due to the presence of a large amount of species like CO and H_2 which are not present in the reference state, and hence, need to be converted to the reference species before performing a mass exchange with the ambient to equalize the concentrations.

Daw et al. [5] studied an isobaric combustion process with preheating of the fuel and air separately using the energy in the flue gas resulting from the combustion of the fuel and air. They found that the preheating of the fuel and air reduced the combustion irreversibility. Also, the combustion itself was modified to occur progressively and at elevated temperatures thus reducing the irreversibility generated. The flue gas generated still had some unreacted fuel and air. The flue gas at an elevated temperature transfers its energy in a counter flow heat exchanger to the incoming fuel and air streams, thereby preheating them. The flue gas continues to react, converting the remaining fuel and air to products in the preheater. Hence, the combustion occurs progressively and at elevated temperatures reducing the irreversibility. The effect of preheater non idealities was also considered on the availability efficiency which is defined as the ratio of the availability of the hot flue gas to the original fuel availability.

Dunbar and Lior [6] studied the irreversibility of constant pressure combustion in an adiabatic chamber. The main objective of their study was to isolate the irreversibility produced during combustion in three parts: namely due to mixing, internal thermal energy exchange and fuel oxidation. Hydrogen and methane were analyzed as fuels. They suggested four different paths for the constant pressure combustion in an adiabatic chamber. In each of these paths, the irreversibility generated due to mixing, internal thermal energy exchange and fuel oxidation were determined separately. They found that the maximum amount of irreversibility generated during the combustion process was due to the internal thermal energy exchange process for all the four paths considered. Also they noted that with increase in reactant temperature, the irreversibility decreased. They also looked at the possibility of a reversible combustion process by preheating the fuel and air streams to equilibrium temperature and partial pressures without allowing for any chemical reactions. This is not a practical scenario as there are difficulties related to making sure that a chemical reaction does not take place during the preheating process and also material constraints are an issue due to the high equilibrium temperatures after the preheat stage.

Caton [7] conducted a second law analysis for constant volume combustion in an adiabatic chamber with iso octane as fuel. The effects of reactant temperature, pressure and equivalence ratio on the percentage availability destroyed was determined. Both a frozen and an equilibrium set of products were considered in determining the percentage availability destroyed. He found that the reactant temperature was the most significant parameter and an increase in its value led to a significant decrease in the percentage availability destroyed. The reactant pressure had a minimal effect on the availability destruction value. The equivalence ratio was another significant parameter that affected the value of the percentage availability destroyed. An increase in the equivalence ratio, up to a stoichiometric ratio, led to a sharp decrease in the availability destroyed. In this study [7], the chemical availability aspect was neglected.

Chavannavar [8] conducted a second law analysis for constant pressure, volume and temperature combustion cases in an adiabatic chamber for eight different fuels. He studied the effect of the reactant temperature, pressure and equivalence ratio on the percentage availability destroyed. In this study the chemical availability aspect was considered when performing the availability balance and hence represents a truer picture. The chemical availability was divided into ‘Reactive’ and ‘Diffusive’ chemical availabilities. He found that the reactant temperature was again the significant parameter affecting the percentage availability destroyed. Increase in the reactant temperature led to a sharp fall in the destruction value. The effect of the reactant pressure was modest. The equivalence ratio was also a significant parameter in determining the percentage availability destroyed. Two separate cases were considered, one where the chemical availability in the products was considered as useful and another where it was neglected. The availability destroyed increased with decrease in the equivalence ratio from stoichiometric for both cases. For the rich zone, the former case led to a fall in the destruction value and the latter case led to a rise in the destruction value. Hydrogen and acetylene were found to destroy the least availability followed by the alkanes and alcohols. He also studied the effect of reactant dissociation on the availability destroyed. A regression analysis was also conducted with the destruction term as the dependent parameter and the reactant temperature, lower heating value of the fuel and the number atoms in the fuel molecule as the independent parameters. Lastly, the results were compared to the previous work done in this area.

Rakopoulos and Kyritsis [9] conducted a second law analysis to study the effect of the enrichment of natural gas (CH_4) and landfill gas (CH_4 diluted with about 40% CO_2) with hydrogen. The combustion of the hydrogen enriched mixture led to a decrease in the irreversibility generated. This agrees with the lower values of availability destruction obtained for hydrogen combustion in some of the previous works mentioned. Extending the availability analysis to different fuels, Rakopoulos and Kyritsis [10] conducted a second law analysis using methane, dodecane and methanol as fuels in a Lister LV1, four stroke, direct injected, naturally aspirated and air cooled diesel engine. They found that the irreversibility generated due to combustion was the highest for dodecane and correspondingly lower for methane. This also agrees with the findings in the study conducted by Chavannavar [8]. The difference observed was in the case of methanol which destroyed the least availability in this case when compared to Chavannavar [8]. The reason attributed to this was the lower entropy generated for methanol during combustion and a higher injected fuel availability.

With the ever more stringent emission regulations for both on road and off road engines, the need to look at technologies aimed at achieving reductions in pollutants like NOx, CO, HC and PM have become vitally important. Two of the techniques used widely to achieve a reduction in the emission of the above pollutants, especially NOx, are exhaust gas recirculation (EGR) and water injection. Similarly a technique like oxygen enrichment is beneficial in reducing the HC, CO and PM emissions. Studies into the implementation of EGR for both SI and CI engines have been going on for years. In some cases, EGR has been coupled with water injection to achieve increased reductions in NOx emissions. Almost all studies state the reduced combustion temperatures as the main reason for decreased NOx emissions.

Mitchell et al. [11] simulated an EGR process for an optically accessible direct injected diesel engine. CO_2 and N_2 were used as inert diluents injected into the engine intake to simulate an EGR process. Again, the main objective of the study was to quantify the NOx emission reductions achieved due to the intake charge dilution by CO_2 and N_2. Both diluents had the effect of decreasing the concentration of the oxygen in the inlet. CO_2 had an additional effect of significantly increasing the specific heat of the inlet mixture thus leading to reduced combustion temperatures and lower NOx emissions.

Ladommatos et al. [12] simulated an EGR process using CO_2, N_2 and water vapor as inlet charge diluents for a 2.5L, naturally aspirated, direct injected diesel engine. Again, the main effect of the diluents was to reduce the concentration of oxygen in the inlet. CO_2, as in the previous study, also led to an increase in the specific heat of the mixture. The dilution of the inlet charge did lead to significant reductions in the NOx emission mainly due to a reduced oxygen concentration leading to increased ignition delays and lower combustion temperatures. The temperature of the diluted inlet mixture was also increased to simulate a hot EGR process. This offset the benefits obtained in the case without the heating of the diluted charge. The hot EGR case led to a decreased inlet charge density, reduced ignition delays and increased combustion temperatures leading to slightly higher NOx emissions. The case where water vapor was used as an inlet charge diluent represents a water injection system. It can be seen that the main effect with injecting the water is again to reduce the NOx emissions by lowering the combustion temperatures.

Jacobs et al. [13] studied the effects of a cooled EGR setup in a 6 cylinder (inline), 12.5L, Detroit diesel series 60 engine retrofitted with a variable geometry turbocharger (VGT), EGR valve, EGR cooler, EGR mixer and an electronic control module capable of controlling both the EGR and the VGT flow rates. The main objective of the study was to determine the effects of the cooled EGR – VGT setup on fuel economy, NOx emissions, engine performance and system heat rejection. Engine tests were conducted to simulate 3 different sets of driving conditions. All 3 sets showed an adverse effect on brake thermal efficiency with increasing rates of EGR. The fraction of work loss alternated between combustion work loss and pumping loss associated with the transportation of the exhaust gas mixture to the inlet based on the test conditions. The air/fuel ratio also continually decreased with increase in the EGR fraction but did not have a considerable effect on the ignition delay. This was mainly due to the increase in the inlet charge temperature at higher EGR fractions due to inefficient EGR cooling. The NOx emissions showed a decrease with increase in the EGR fraction and the main reason attributed to this was the lower combustion temperatures due to charge dilution leading to an increase in the specific heat capacity of the inlet charge as indicated by Ladommatos et al. [12] and Mitchell et al. [11]. The lowering of oxygen concentration in the inlet charge and the dissociation effects of the molecules in the EGR stream had a minimal effect on reducing NOx emissions. Lastly, the increased EGR fractions led to a greater amount of overall heat rejection mainly due to the EGR cooling.

Previous studies on the use of EGR mainly focused on its effect on NOx emissions. Caton [14] studied the effects of ‘cooled’ and ‘adiabatic’ EGR processes for an SI engine from a second law perspective. He found that the NOx emissions decreased considerably with increasing levels of EGR and this was again attributed to the lower combustion temperatures which are consistent with the previous studies. But more importantly, he quantified the availability destruction due to combustion, heat transfer to the walls and the availability flowing out through the exhaust for the two EGR cases. The cooled and adiabatic EGR cases showed destruction in availability of about 22.5% and 20.7% for an EGR fraction of 20% at an equivalence ratio of 1.0, MBT spark timing, 1400 rpm and a BMEP of 325 kPa. The lower value in the adiabatic case is due to the higher combustion temperatures as the inlet charge temperature is higher. Conversely, the availability loss due to the heat transfer to the cylinder walls is much higher in the adiabatic case due to the higher combustion temperatures. The cooled EGR case led to a higher loss in availability through the exhaust as the temperature difference between the inlet charge temperature and the exhaust temperature is much higher in the cooled EGR case when compared to the adiabatic EGR case. Caton [14] also simulated an ‘Oxygen Enrichment’ case by increasing the percentage of the inlet charge oxygen. This led to a sharp decrease in the availability destroyed due to combustion as the combustion temperatures increased.

Motivations for the Current Study

Although much work has been completed using second law analysis and in the simulation of techniques like EGR, water injection and oxygen enrichment, they have been mainly exclusive of each other. Hence, there existed a need for an analysis that studied the effects of processes like EGR, water injection and oxygen enrichment from a second law perspective to quantify the availability destroyed due to combustion due to the above mentioned processes.

Also, most of the second law analysis studies done so far have concentrated on a limited number of fuels. Chavannavar [8] did look at a set of different fuels from a second law perspective and the same sets of fuels have been analyzed here.

In all the second law analyses completed so far with equilibrium products of combustion, condensed species were never included in the list of product species to be considered while calculating the equilibrium composition. There was a possibility of the presence of 'Solid Carbon' (modeled as soot) under certain rich operating conditions. Hence, there was a need to include the solid species as part of the products while calculating the equilibrium composition and also to study the effect of its presence on the percentage availability destroyed due to combustion. The results are included in appendix I.

A majority of the second law analyses have neglected the chemical availability while computing the availability destroyed due to combustion and this represents an inaccurate picture especially under certain rich operating conditions. Hence this study looked at including both the reactive and diffusive chemical availabilities to compute the availability destroyed due to combustion.

Objectives

The main objective of this work was to study the effects of exhaust gas recirculation, water injection and oxygen enrichment on the efficiency of the combustion process. This was done by performing a second law analysis to calculate the percentage of availability destroyed during the combustion process. A constant enthalpy-pressure and constant internal energy-volume combustion processes were considered to perform the second law analysis.

The availability analysis was completed by varying parameters like reactant temperature, EGR and injected fractions, equivalence ratios and the type of fuel burnt. Extending the analysis to cover a range of hydrocarbon fuels along with hydrogen and alcohols was one of the goals of this work.

The inclusion of the chemical availability in the second law analysis was another objective of this study. It was shown that the chemical availability is a significant factor at the rich equivalence ratios and hence its inclusion represented a complete picture when calculating the percentage availability destroyed.

Lastly, the study also looked at comparing the constant pressure and the constant volume combustion systems. The efficiency of each system was found to be dependent on the operating parameters chosen.

It is hoped that the work done here will aid in obtaining a better understanding of the combustion process and the associated irreversibilities to design more efficient combustion systems in the future.

III. DEVELOPMENT OF THE MODEL

The following section describes the model that was developed to compute the availability destroyed in the combustion process. This section is again divided into two parts, with the first part describing the formulation of the basic model for computing the availability destroyed due to the combustion process. This required the various thermodynamic properties of the reactant and product mixtures to be determined to compute the destruction of availability. The second part of this section describes the different subroutines in the main model which can be invoked by the user to study the effects of EGR, water injection, oxygen enrichment, and presence of condensed species on the availability destroyed due to combustion.

Computation of 'Availability Destroyed'

The thermodynamic parameters were determined using the "7+2" NASA Lewis polynomial coefficients [15] which were developed as the least square fits to the data generated at the NASA Glenn research center. A compilation of the Lewis polynomial coefficients for common fuels have been included in appendix II. The various equations for determining the thermodynamic properties have been listed below and the coefficient values can be plugged into the equations to obtain the properties.

Heat Capacity

$$\frac{c_p}{\overline{R}} = a_1T^{-2} + a_2T^{-1} + a_3 + a_4T + a_5T^2 + a_6T^3 + a_7T^4 \tag{3.1}$$

Enthalpy

$$\frac{h(T)}{\overline{R}T} = -a_1T^{-2} + a_2T^{-1}\ln T + a_3 + a_4\frac{T}{2} + a_5\frac{T^2}{3} + a_6\frac{T^3}{4} + a_7\frac{T^4}{5} + \frac{b_1}{T} \tag{3.2}$$

Entropy

$$\frac{s(T)}{\overline{R}} = -a_1\frac{T^{-2}}{2} - a_2T^{-1} + a_3\ln T + a_4T + a_5\frac{T^2}{2} + a_6\frac{T^3}{3} + a_7\frac{T^4}{4} + b_2 \tag{3.3}$$

The updated coefficients are available on the NASA Glenn website [16].

The program that was developed interfaced with the NASA 'Complex Equilibrium Compositions and Applications' (CEA) developed by Gordan and McBride [17] to determine the equilibrium composition and the required thermodynamic properties at the various temperatures and pressures.

The main program generated the appropriate input file for the CEA to calculate the thermodynamic properties and the equilibrium composition and read the output file generated by the CEA with the calculated product properties and equilibrium composition. The CEA program required the input conditions to be fixed depending on the mode of combustion being considered. The conditions that were fixed in this study were as follows:

- Specified temperature and pressure (TP)
- Specified internal energy and volume (UV) **(Closed system)**
- Specified enthalpy and pressure (HP) **(Open system)**

The main program also required a database of the availabilities of the various chemical species. These were computed using the Gibbs free energy values for simple combustion reactions occurring at ambient conditions. The ambient atmospheric composition considered for this study is included in appendix III. The Gibbs free energy values, taken from Moran and Shapiro [18] and Annamalai and Puri [19] are included in appendix IV. These values can be altered by the user.

Assumptions of the Model

1. Adiabatic combustion conditions were assumed for the constant volume and constant pressure combustion systems.
2. The analysis was done using the ideal gas model.
3. It was assumed that the products of combustion have enough time to attain the equilibrium composition.
4. The temperature and pressure distribution was assumed as uniform (Single zone)
5. No work transfer to or from the system.

Preliminary Calculations

Input parameters for the program included the type of fuel, initial and final reactant temperature and pressure, temperature and pressure increments, mode of combustion, type of combustion products desired, and equivalence ratio. The program handles fuels of the form $C_xH_yO_z$.

The program first calculated the total number of moles in the reactant mixture using the ideal gas equation.

$$PV = n\overline{R}T \tag{3.4}$$

where, P is the system pressure, V is the system volume, T is the system temperature, n is the number of moles of reactants, and $\overline{R}$ is the universal gas constant.

A general combustion reaction is as follows:

$$a(C_xH_yO_z) + b(Air) \rightarrow PRODUCTS \tag{3.5}$$

where, 'a' and 'b' are the number of moles of fuel and air respectively. Initially the program assumed the number of moles of fuel as 1.0 and computed the required stoichiometric amount of air moles needed for complete combustion of the fuel.

$$b = (2ax + \frac{ay}{2} - az) * \frac{1}{2} f_{O_2} \tag{3.6}$$

where, f_{O_2} is the oxygen fraction in the atmosphere.

The oxygen fraction corresponds to the standard atmospheric composition described in the appendix. These fractions can be altered by the user.

Knowing the air and fuels moles along with the equivalence ratio, the actual air fuel ratio on the mass basis was computed.

$$(F:A)_{Actual} = \frac{a * MW_{Fuel}}{b * MW_{Air}} * \phi \tag{3.7}$$

where, MW_{Fuel} and MW_{Air} are the molecular weight of the fuel and air respectively and ϕ is the equivalence ratio.

Knowing the actual fuel air ratio, the actual number of moles of fuel and air were determined.

Calculation of Reactant and Product Mixture Properties and Associated Availabilities

The required reactant mixture enthalpy and internal energy were calculated as follows:

$$H = \sum_{k=1}^{n} n_k h_k(T) \tag{3.8}$$

$$U = \sum_{k=1}^{n} n_k u_k(T) \tag{3.9}$$

The reactant mixture entropy was calculated after taking into account the partial pressures of the various species in the reactant mixture before summing the individual entropies of the reactant species.

$$S = \sum_{k=1}^{n} n_k \left[s_k(T) - \overline{R} \ln y_k \right] \tag{3.10}$$

where, s_k is the absolute molar specific entropy of species 'k' at temperature T and y_k is the mole fraction of species 'k' in the mixture.

Once the thermodynamic properties were determined, the associated reactant absolute thermo-mechanical availabilities were computed.

(Closed System) $$\mathrm{A}_{\mathrm{Abs}} = U - T_0 S + P_0 V \tag{3.11}$$

(Open System) $$\mathrm{A}_{\mathrm{Abs,\,f}} = H - T_0 S \tag{3.12}$$

To calculate the total thermo-mechanical availability of the reactant stream, the reference availabilities at the restricted dead state were determined.

(Closed System) $$\mathrm{A}^0_{Ref} = U^0 - T_0 S^0 + P_0 V^0 \tag{3.13}$$

(Open System) $$\mathrm{A}^0_{Ref,f} = H^0 - T_0 S^0 \tag{3.14}$$

Hence the total thermo-mechanical availability of the system was calculated as follows:

(Closed System) $$\mathrm{A}_{\mathrm{TMA}} = (U - U^0) - T_0(S - S^0) + P_0(V - V^0) \tag{3.15}$$

(Open System) $$\mathrm{A}_{\mathrm{TMA,\,f}} = (H - H^0) - T_0(S - S^0) \tag{3.16}$$

Additionally this study included the chemical availability component into the calculation of the availability destroyed during the combustion process. The chemical availability was split into two parts in this study. The ‘Reactive chemical availability’ represented the change in the Gibbs energy due to the oxidation/reduction of the fuel/product species and the ‘Diffusive chemical availability’ was the work potential that can be extracted as the various species reaches an equilibrium state in terms of concentration with the species in the ambient. The ‘Reactive chemical availability’ on the reactant side was accounted for by the incoming fuel availability and on the product side was calculated by computing the change in Gibbs energy as the incomplete product species was converted into species present in the ambient through oxidation or reduction chemical reactions.

The ‘Reactive chemical availability’ term was calculated as follows:

$$\mathrm{A}_{\mathrm{Reactive}} = \sum_{k=1}^{n} \Delta G_k^0 \tag{3.17}$$

The ‘Diffusive chemical availability’ term was calculated as follows:

$$\mathrm{A}_{\mathrm{Diffusive}} = \sum_{k=1}^{n} n_k \overline{R} T_0 \ln \frac{y_k^0}{y_{k0}} \tag{3.18}$$

The net chemical availability of the reactants is thus the summation of the reactive and diffusive chemical availabilities and it represents the change in chemical potential of the chemical species as they got converted into species in the ambient.

$$\mathrm{A}_{\mathrm{CA}} = \mathrm{A}_{\mathrm{Reactive}} + \mathrm{A}_{\mathrm{Diffusive}} \tag{3.19}$$

$$\mathrm{A}_{\mathrm{CA}} = \sum_{k=1}^{n} n_k (\mu_k^0 - \mu_{k,0}) \tag{3.20}$$

where, μ_k^0 and $\mu_{k,0}$ are the chemical potentials of the species at the restricted dead state and the ambient respectively.

The above equation upon simplification yields the following summation for the total chemical availability of the system.

$$\mathrm{A}_{\mathrm{CA}} = \sum_{k=1}^{n} \Delta G_k^0 + \sum_{k=1}^{n} n_k \overline{R} T_0 \ln \frac{y_k^0}{y_{k0}} \tag{3.21}$$

The total availability of the reactant mixture was calculated as follows:

$$\mathrm{A}_{\mathrm{Total}} = \mathrm{A}_{\mathrm{TMA}} + \mathrm{A}_{\mathrm{Reactive}} + \mathrm{A}_{\mathrm{Diffusive}} \tag{3.22}$$

$$\mathrm{A}_{\mathrm{Total}} = (U - U^0) - T_0(S - S^0) + P_0(V - V^0) + \sum_{k=1}^{n} \Delta G_k^0 + \sum_{k=1}^{n} n_k \overline{R} T_0 \ln \frac{y_k^0}{y_{k0}} \tag{3.23}$$

(Closed System)

$$\mathrm{A}_{\mathrm{Total,\,f}} = (H - H^0) - T_0(S - S^0) + \sum_{k=1}^{n} \Delta G_k^0 + \sum_{k=1}^{n} n_k \overline{R} T_0 \ln \frac{y_k^0}{y_{k0}} \tag{3.24}$$

(Open System)

The next step involved interfacing the main program with the CEA to determine the equilibrium composition and the thermodynamic properties of the products after combustion. The constant volume combustion process fixed the internal energy and density of the system whereas the constant pressure combustion process fixed the enthalpy and pressure of the system.

This study allowed for both complete and equilibrium products of combustion. The complete products of combustion consisted of the following set of species in the product mixture:

- Carbon dioxide, CO_2
- Water vapor, H_2O
- Nitrogen, N_2
- Oxygen, O_2
- Argon, Ar

The equilibrium products of combustion consisted of the following set of species in the product mixture:

- Carbon dioxide, CO_2
- Carbon monoxide, CO
- Oxygen, O_2
- Oxygen atom, O
- Nitrogen, N_2
- Water vapor, H_2O
- Hydroxyl, OH

- Nitrogen oxide, NO
- Nitrogen dioxide, NO_2
- Hydrogen, H_2
- Hydrogen atom, H
- Argon, Ar
- Nitrogen atom, N
- Carbon, C (g)
- Carbon, C_2 (g)
- Carbon, C_3 (g)
- CH
- Methane, CH_4
- Acetylene, C_2H_2
- Solid Carbon, C (gr)

Once the product composition and properties are determined from the CEA, a similar procedure is adopted in calculate the product mixture availabilities.

The availability destroyed was calculated as follows:

$$A_{Dest} = A_{Reactants} - A_{Products} + A_T + A_W \tag{3.25}$$

where, $A_{Reactants}$ is the total availability of the reactant mixture, $A_{Products}$ is the total availability of the product mixture, A_T is the availability due to heat transfer to or from the system and A_W is the availability due to work transfer to or from the system. From the assumptions listed previously, A_T and A_W terms are zero for the combustion systems being considered.

The availability destroyed thus reduced to the following expression:

$$A_{Dest} = A_{Reactants} - A_{Products} \tag{3.26}$$

The percentage destruction of availability due to combustion was calculated as follows:

$$\%\, A_{Dest} = [\frac{A_{Reactants} - A_{Products}}{A_{Reactants}}]*100 \tag{3.27}$$

Description of Subroutines

The main program performs the availability analysis and the different processes being analyzed were included as subroutines in the main program. The user can invoke any of the subroutines to perform the availability analysis. A brief description of the subroutines is provided.

Cooled EGR

'Cooled EGR' refers to a process where a fraction of the exhaust gas is recirculated and cooled to the inlet temperature where it is mixed with the incoming fuel/air stream. The exhaust gas recirculation was done on a mass basis. The EGR fraction was determined using the percentage of the reactant mixture mass that was replaced by the product mixture.

$$EGR\% = \frac{m_{EGR}}{m_{Inlet}} * 100 \tag{3.28}$$

Hence knowing the EGR fraction, the mass of the EGR species was computed. The molar distribution of the product species in the EGR stream was kept the same as the product stream mole fraction of the various species. The fuel and the air moles were adjusted to keep the equivalence ratio constant. The EGR subroutine was run multiple times at a particular set of input conditions for the final product temperature to attain its true value. In most cases the product temperature attained its true value within 5-6 runs.

Adiabatic EGR

'Adiabatic EGR' involved transporting the fraction of the exhaust gas adiabatically and mixing it with the incoming fuel/air stream. This involved an additional component, an energy balance equation on the inlet side to calculate the temperature due to the mixing of the EGR and the fuel/air stream. The new 'Mix Temperature' was arrived at by an iterative means.

(Open system) $$(h_{EGR} * m_{EGR}) + (h_{A/F} * m_{A/F}) = (h_{inlet} * m_{inlet}) \tag{3.29}$$

(Closed system) $$(u_{EGR} * m_{EGR}) + (u_{A/F} * m_{A/F}) = (u_{inlet} * m_{inlet}) \tag{3.30}$$

The LHS of equations (3.29) and (3.30) are known and the energy balance is performed iteratively by varying the temperature at which h_{inlet} and u_{inlet} is calculated. The temperature that satisfies the energy balance is the new 'Mix Temperature'.

Oxygen Enrichment

In this subroutine, the percentage of oxygen in the incoming steam of air was varied depending on the enrichment fraction needed. The nitrogen percentage was correspondingly changed and the percentages of CO_2, H_2O and Ar were kept constant. With the variation in the oxygen fraction, the fuel moles were altered to keep the equivalence ratio fixed.

Water/N_2/CO_2 Injection

This was based on the 'Cooled EGR' model in that the injection was done on a mass basis and the fuel and air moles were accordingly varied to keep the equivalence ratio constant. The only difference in this case was that since there was no species being recirculated there was not a need for multiple runs at a particular set of input conditions for the product temperature to attain a true value.

$$Injected\% = \frac{m_{Injected}}{m_{Inlet}} * 100 \tag{3.31}$$

Condensed Species Equilibrium

Solid carbon, C (gr) was included as a possible product species while preparing the input for the CEA. The main difference in this case was that while calculating the product properties at the restricted dead state with the solid species in the product stream, the corresponding entropy values was calculated for the gaseous species by neglecting the solid species as it does not exert any partial pressure. The CEA program does not return the properties of the solid species at a particular temperature and pressure. Hence the corresponding enthalpy, internal energy and entropy of the solid were calculated separately by reading the corresponding values from a separate file containing the thermodynamic properties of the solid species. The entropy of the solid does not have the partial pressure term that is a part of the gaseous stream calculations.

Also there are two different definitions of molecular weight within the CEA documentation. The difference arises only when condensed species are part of the product mixture. The CEA returns only one of the molecular weights as part of its output. This is outlined in the NASA CEA Analysis documentation by Gordon and McBride [17].

The definition of the molecular weight that the CEA returns as a part of its output is as follows:

$$\mathrm{M} = \frac{\sum_{\mathrm{k=1}}^{\mathrm{NS}} n_k M_k}{\sum_{k=1}^{\mathrm{NG}} n_k} \tag{3.32}$$

where 'M' is the molecular weight of species 'k', NS stands for the total number of species in the mixture (Including condensed species) and NG stands for only the gaseous species in the mixture.

The second definition for the molecular weight from the CEA documentation is as follows:

$$\mathrm{MW} = \frac{\sum_{\mathrm{k=1}}^{\mathrm{NS}} n_k M_k}{\sum_{k=1}^{\mathrm{NS}} n_k} \tag{3.33}$$

This definition includes all the species in the mixture in calculating the molecular weight unlike the previous one which ignores the condensed species in the mixture. In cases where there are no condensed species in the mixture, both 'M' and 'MW' will have the same values.

To calculate the true molecular weight when condensed species are a part of the mixture, the following correction is applied to the molecular weight 'M' returned by default by the CEA.

$$\mathrm{MW} = \mathrm{M}\left(1 - \sum_{k=\mathrm{NG}+1}^{\mathrm{NS}} y_k\right) \tag{3.34}$$

The summation 'NG + 1' to 'NS' refers to the number of the condensed species present in the mixture and y_k refers to the mole fraction of the condensed species.

IV. RESULTS AND DISCUSSION

Cooled 'Exhaust Gas Recirculation' (EGR)

The following section contains the results obtained by simulating a cooled EGR process for combustion under constant pressure and constant volume conditions. Determining the sensitivity of the percentage of EGR on the availability destroyed is the main aim of the study. EGR involves recycling a fraction of the product species (depending on the EGR %) and replacing some of the inlet charge (fuel + air) with the EGR mixture. The EGR % is defined as the ratio of the mass of the EGR species to the total inlet charge mass. The fuel and air mass are adjusted accordingly to maintain the equivalence ratio constant.

The two variations of the EGR process include a cooled EGR and an adiabatic EGR. The latter has not been discussed here but a section has been included in appendix I. It involves transporting the EGR species adiabatically to the inlet. In such a case the inlet temperature changes as the hot EGR stream mixes with the much cooler inlet fuel and air stream. This is not very beneficial when it comes to implementing it in an actual engine as the increased inlet temperature reduces the volumetric efficiency of the engine.

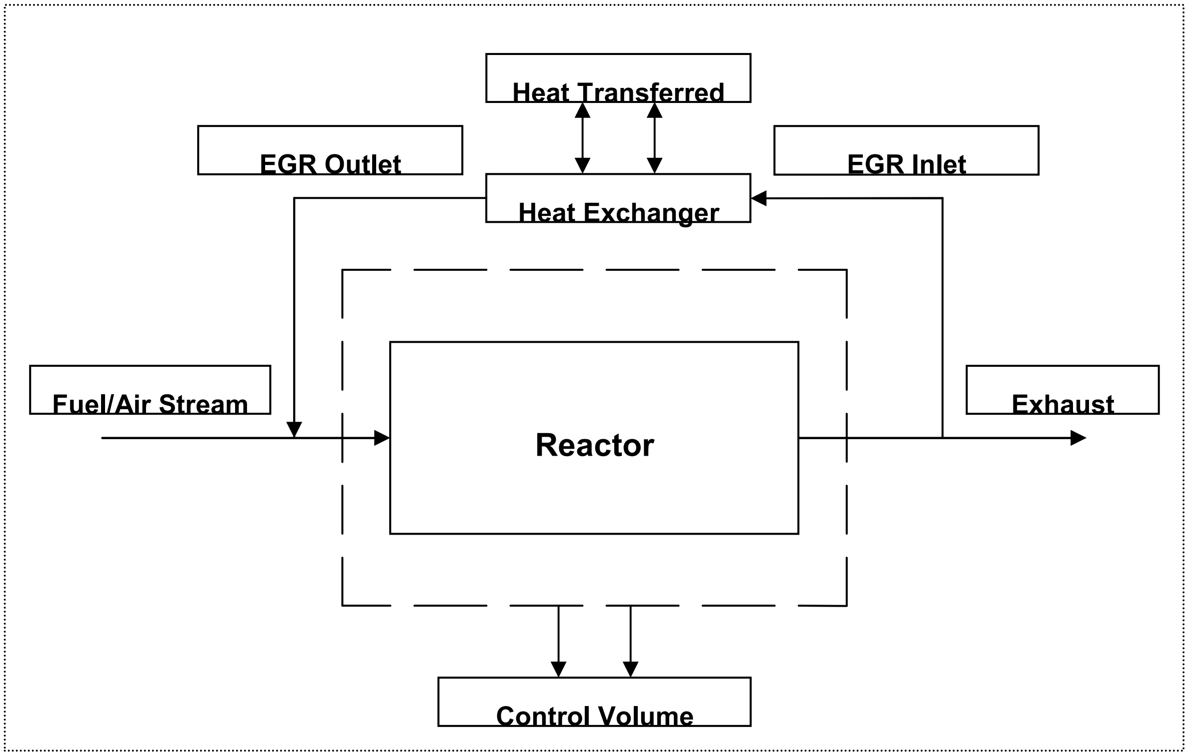

Fig 1. Cooled EGR Setup

In the cooled EGR case depicted in figure 1, the EGR species are cooled to the inlet temperature, i.e. the incoming fuel/air stream temperature, as it is recycled through the use of a suitable cooling mechanism. The word ‘cooled’ can be misleading as there are cases at very high temperatures (without reactant dissociation) where in some of the reactions tend to be endothermic resulting in a product temperature that is lesser than the inlet temperature. In such cases the product species would have to be heated to the inlet temperature according to the definition of the model. The composition of the EGR species can be assumed to be frozen or dynamically changing (non-frozen) as it is cooled to the inlet temperature. Most of the simulations have been done with the frozen EGR composition. This does not necessarily represent a realistic scenario as the EGR species concentration may change as it is cooled down to the inlet temperature. Hence a comparison between the frozen and the non-frozen cases have been completed and the results obtained have been included in appendix I. In addition, the sensitivity of the EGR process to various fuels has also been studied from a second law perspective by tracking the availability destroyed.

The base case conditions adopted for the simulation include a reactant pressure of 500 kPa, an equivalence ratio of 1.0, and iso octane as the fuel. A temperature range between 300 K and 6000 K is selected to clearly demonstrate the effects of EGR on availability destruction. Sensitivity of the availability destruction to the change in the standard parameters has also been examined. EGR percentages of 0%, 20% and 40% have been studied. The results obtained from the 0% EGR case matches with the ones obtained earlier for a simple constant pressure and constant volume combustion systems. The plot for constant enthalpy, constant pressure combustion is followed by the corresponding plot for the constant internal energy, constant volume combustion.

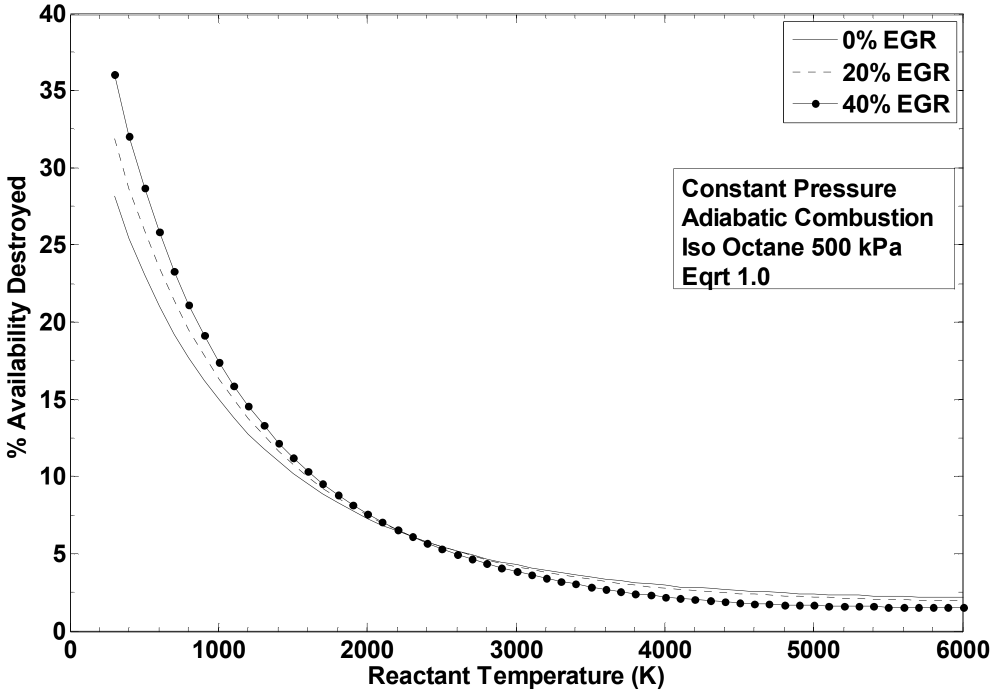

Fig 2. Percentage availability destroyed for different ‘Cooled’ EGR fractions as a function of reactant temperature for constant pressure combustion of iso octane.

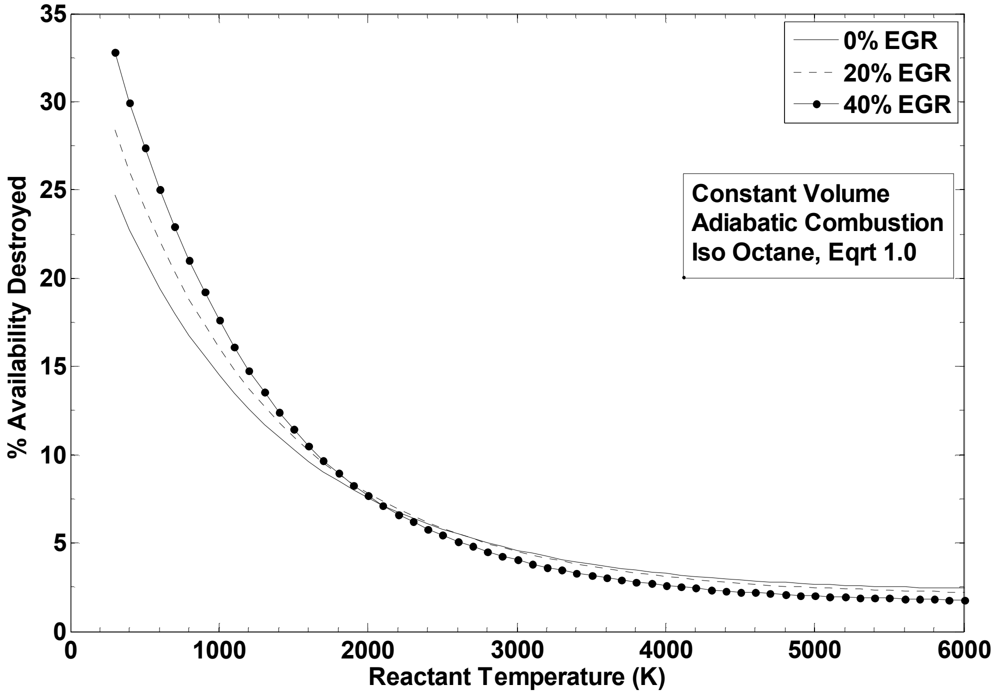

Fig 3. Percentage availability destroyed for different ‘Cooled’ EGR fractions as a function of reactant temperature for constant volume combustion of iso octane, reactant pressure of 500 kPa.

.

Figures 2 and 3 indicate the variation of the percentage of the availability destroyed with reactant temperature. The above cases were for non dissociated reactants with a frozen EGR composition. At lower temperatures the percentage of availability destroyed increases with increasing percentages of EGR. This is due to the fact that product temperatures obtained are correspondingly lower for higher EGR percentages which results in a higher destruction of availability. As far as practical application of the EGR goes, the temperature range of interest is below 1500 K and within this range the availability destroyed is the highest for the highest EGR percentage.

This trend continues until about a reactant temperature of 1700 K after which the curves start coming together. Beyond a reactant temperature of 2500 K, the curves tend to separate with the trend being reversed, i.e. the higher EGR percentages destroy lesser amounts of the original availability. The availability destruction percentages settle down to a value of about 2-3% at the very high temperatures. The trend reversal and the convergence of the curves at similar temperatures is described next.

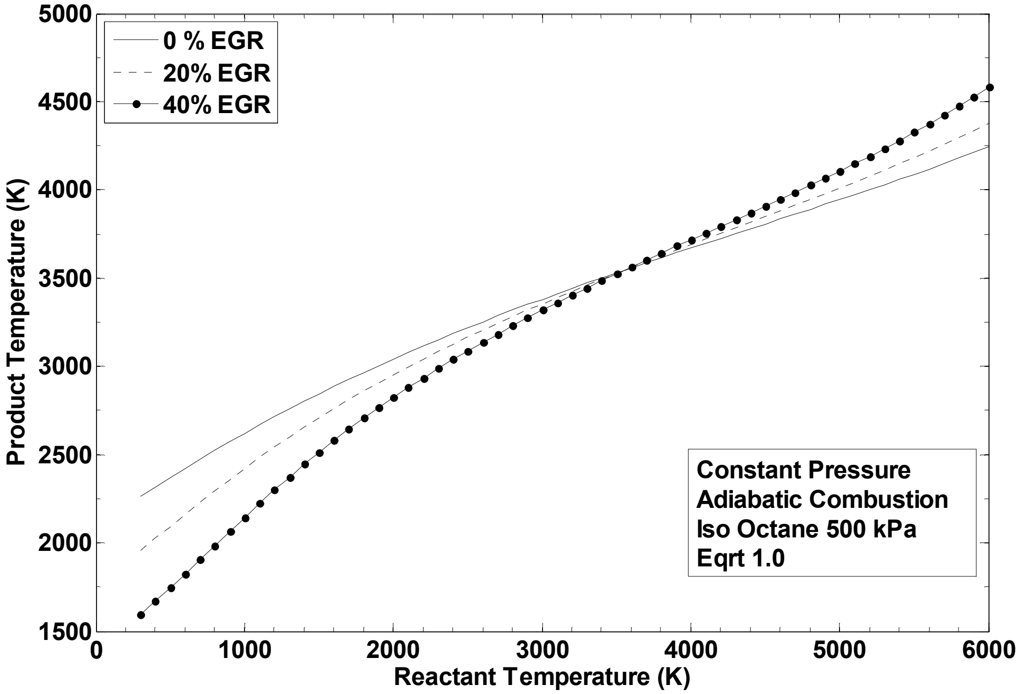

Fig 4. Product temperature for different 'Cooled' EGR fractions as a function of reactant temperature for constant pressure combustion of iso octane.

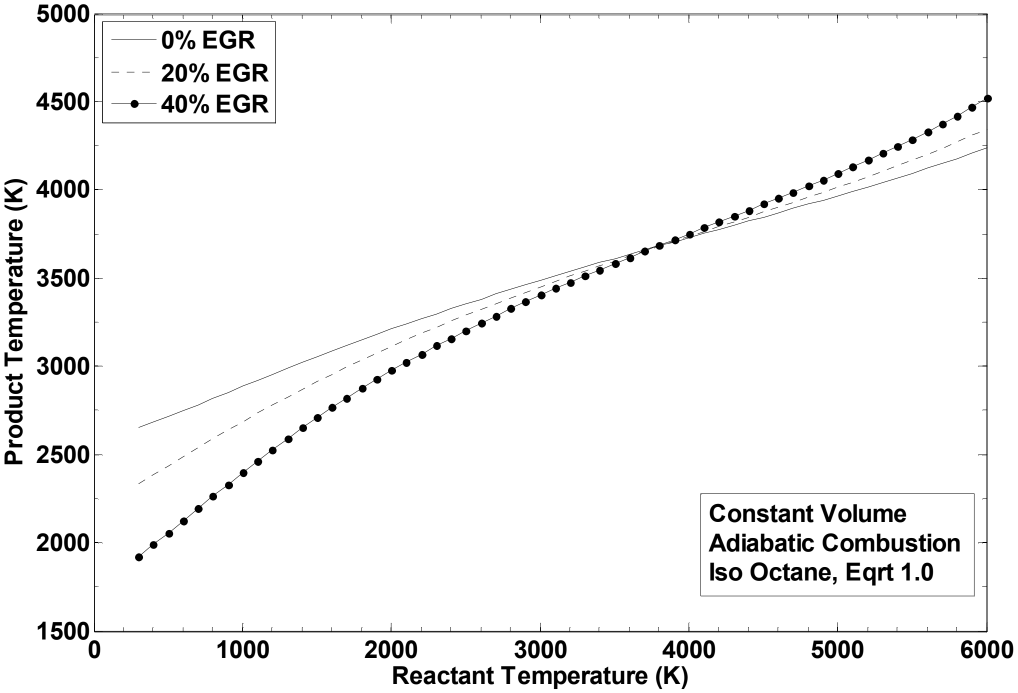

Fig 5. Product temperature for different 'Cooled' EGR fractions as a function of reactant temperature for constant volume combustion of iso octane, reactant pressure of 500 kPa.

Figures 4 and 5 depict the variation of the product temperature with respect to the reactant temperature. The role played by the product temperature is very crucial at the lower reactant temperatures. The difference in the product temperatures between the 3 EGR cases is the greatest at the lower reactant temperatures. This explains the fact that the higher EGR percentages destroy a much greater amount of availability at these lower temperatures. The product temperatures start coming together after a reactant temperature of about 1700 K. The curves cross over at around 3500 K with the higher EGR percentages showing a greater product temperature. The reason for this is that at such high reactant temperatures, a large amount of chemical availability is brought in through the EGR stream and this adds to the fuel chemical availability. This being the non dissociated case, the product temperatures tend to be lower than the reactant temperatures beyond reactant temperatures past about 3500 K. Hence the products have to be heated up to the reactant temperature and this also increases the incoming EGR stream availability. Hence combustion of the high reactive chemical availability species in the EGR stream causes the product temperature to be higher for the higher EGR percentage case when compared the lower ones.

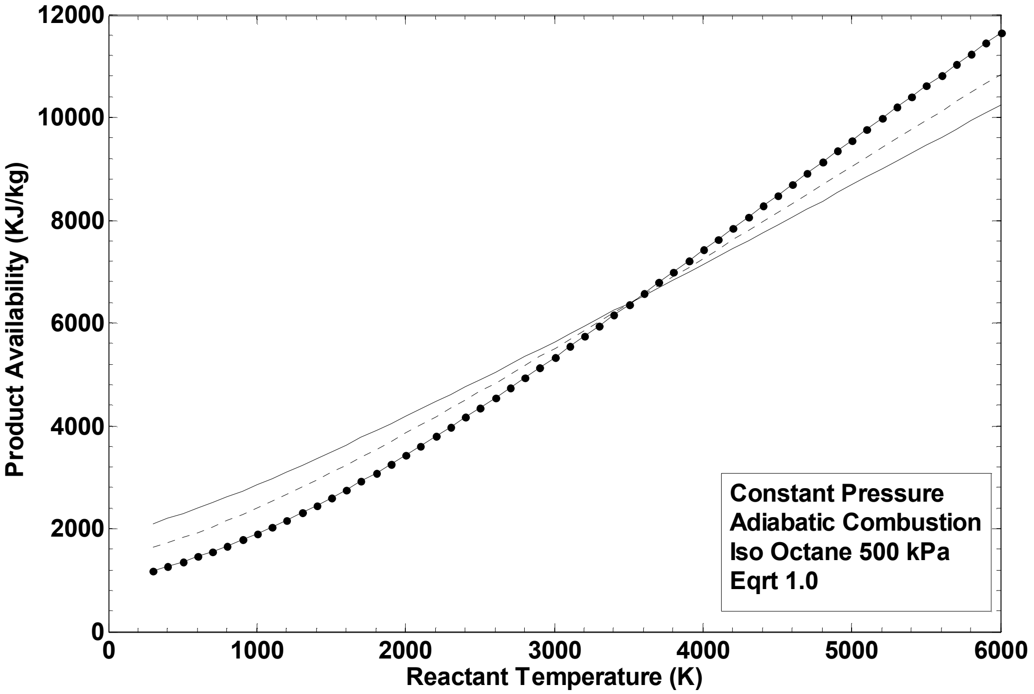

Fig 6. Product availability for different 'Cooled' EGR fractions as a function of reactant temperature for constant pressure combustion of iso octane.

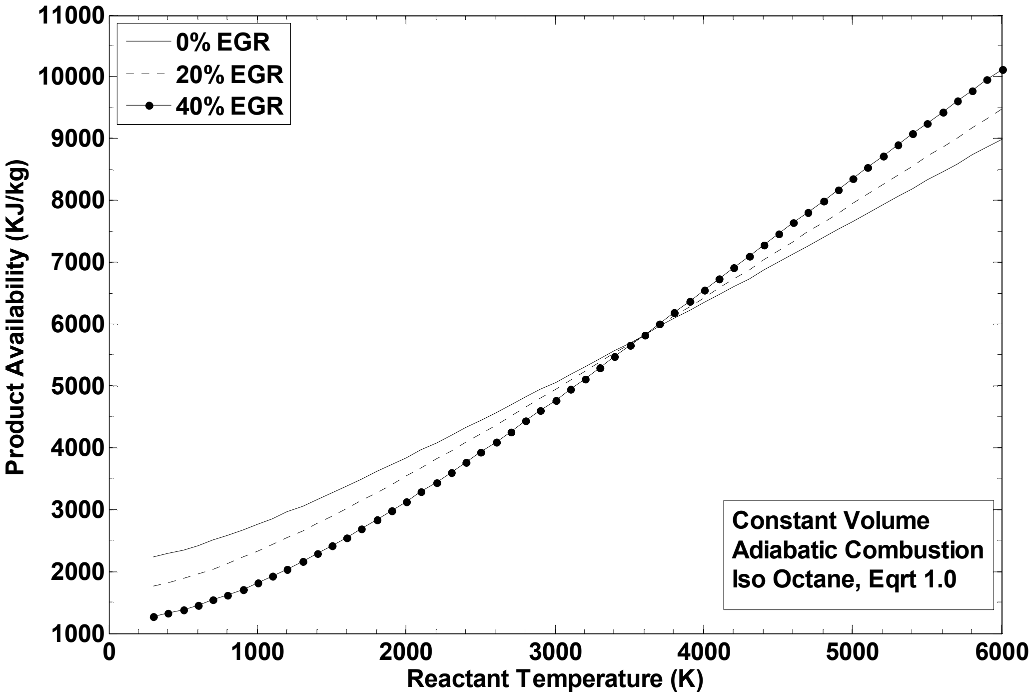

Fig 7. Product availability for different 'Cooled' EGR fractions as a function of reactant temperature for constant volume combustion of iso octane, reactant pressure of 500 kPa.

Figures 6 and 7 indicate the variation of the product availability with reactant temperature for the 3 EGR cases. Again, the differences between the product availabilities are the greatest at the lower reactant temperatures due to the low product temperatures and they start coming closer after about 1700 K owing to the decrease in the difference between the reactant and product temperatures. The rate of increase of the product availability is faster for the higher EGR percentages.

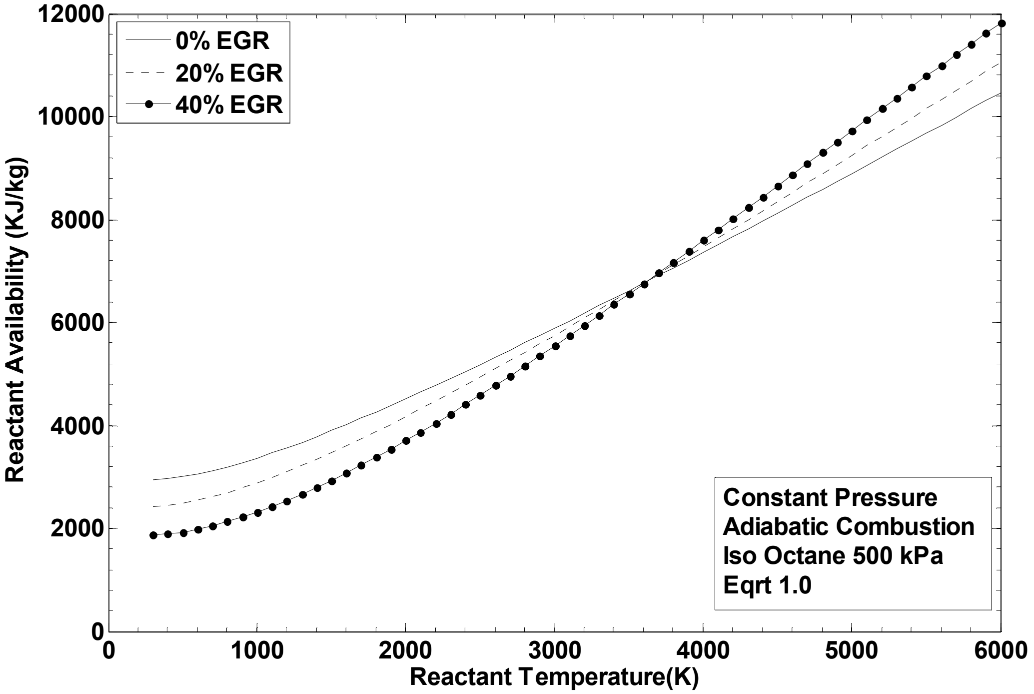

Fig 8. Reactant availability for different 'Cooled' EGR fractions as a function of reactant temperature for constant pressure combustion of iso octane.

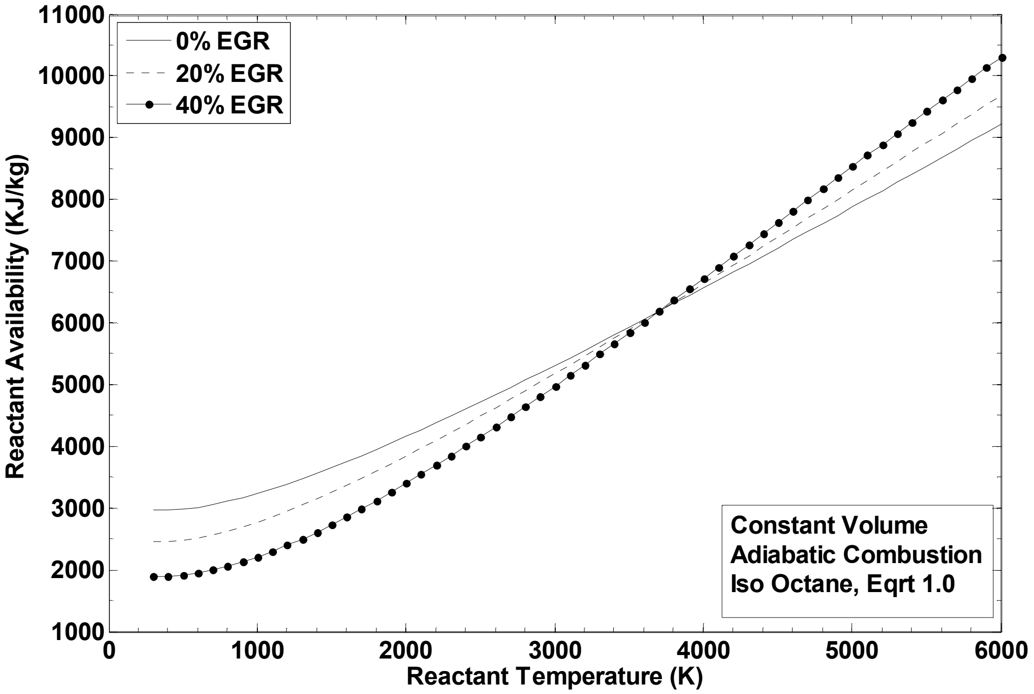

Fig 9. Reactant availability for different 'Cooled' EGR fractions as a function of reactant temperature for constant volume combustion of iso octane, reactant pressure of 500 kPa.

Figures 8 and 9 indicate the variation of the reactant availability with reactant temperature for the 3 EGR cases. Again it is seen that the reactant availabilities start to come together after a temperature of about 1700 K. This is due to the fact that a larger amount reactive chemical availability is added to the higher EGR percentages which bring the curves together. The curves again cross over at around 3500 K beyond which the reactive chemical availability added to the inlet stream for the higher EGR percentages is high enough to compensate for the lower fuel availability in the higher EGR cases thus causing the net reactant availability to be greater in the higher EGR percentage cases at those higher temperatures. The fact that the products need to be heated up to the reactant temperature, beyond reactant temperatures past 3500 K also increases the incoming EGR stream availability thus causing the crossover. The rate of increase of the reactant availability is faster for the higher EGR percentages.

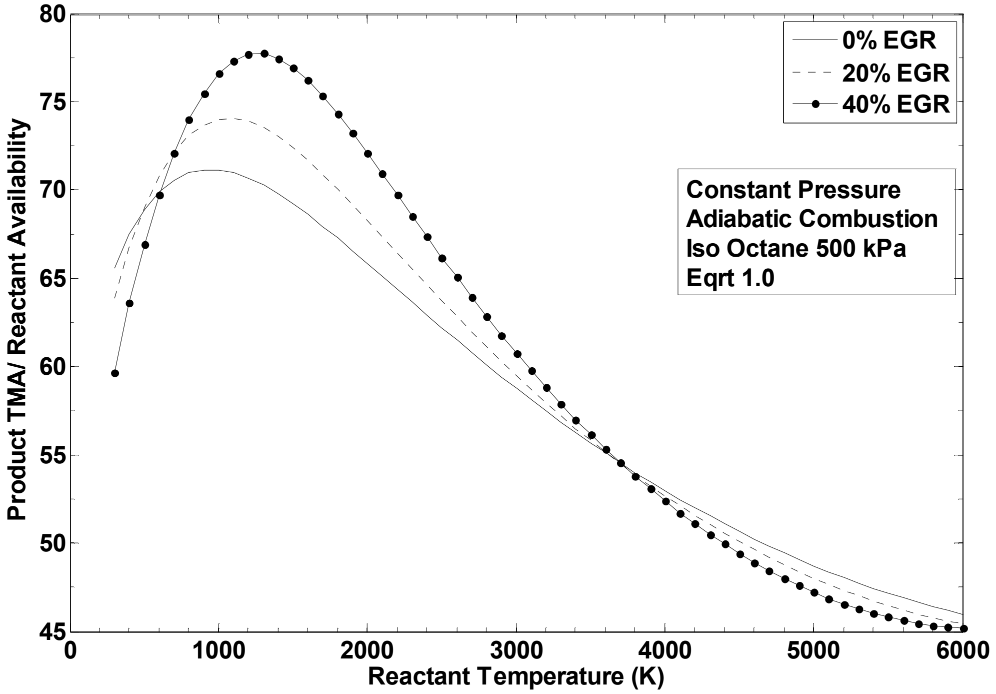

Fig 10. Percentage of reactant availability converted into product thermo-mechanical availability for different 'Cooled' EGR fractions as a function of reactant temperature for constant pressure combustion of iso octane.

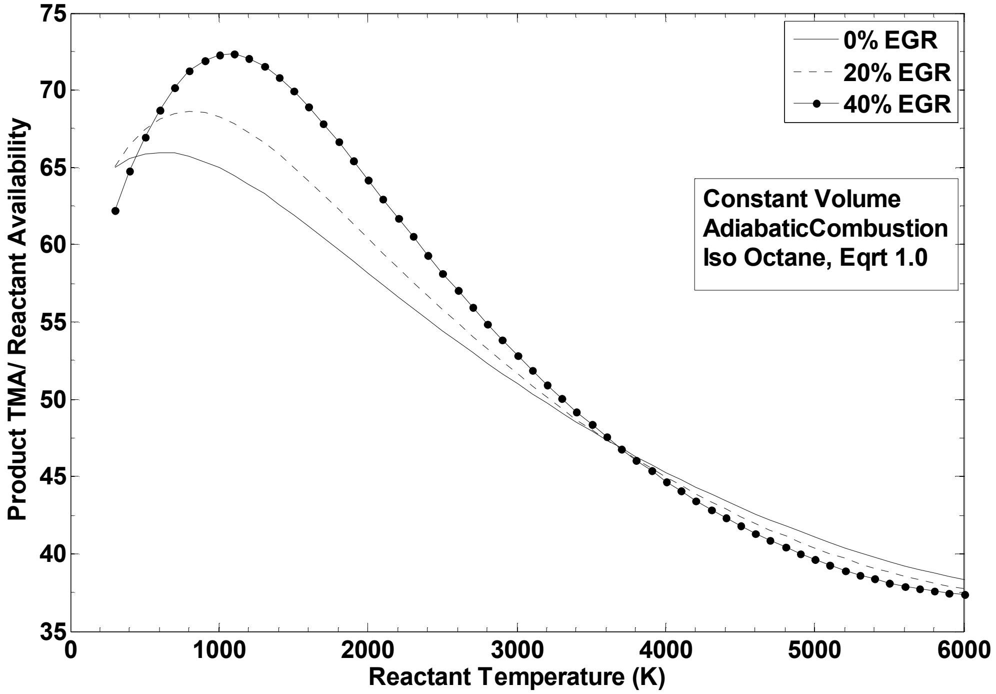

Fig 11. Percentage of reactant availability converted into product thermo-mechanical availability for different 'Cooled' EGR fractions as a function of reactant temperature for constant volume combustion of iso octane, reactant pressure of 500 kPa.

Figures 10 and 11 indicate the variation of the percentage of the original reactant availability that is converted to product thermo-mechanical availability. The rate at which the destruction curve drops off is directly related to the rate at which the original reactant availability is converted into product thermo-mechanical availability. The higher EGR fractions have a faster rate of conversion as seen from the slope of the curves associated with the higher EGR fractions. This effect can also be gauged from figures 4 and 5 where the rate of increase of the product temperature is a lot faster for the curves associated with the higher EGR fractions. The curves in figures 10 and 11 reaches a peak and then starts falling indicating that the amount of the original reactant availability converted to product thermo-mechanical availability now decreases and more and more of the original reactant availability is now being retained in the chemical form in the products. The point of inflection also shifts to the right for the higher EGR fractions and this is expected because of the higher reactant temperatures that are needed for the reactive chemical availability in the products to become significant. As more and more of the original reactant availability is retained in the chemical form in the products, the destruction curves tend to flatten out. Preserving the availability in the chemical form leads to lesser alteration in the value of the availability destroyed.

Hence, the faster rate of conversion of the original reactant availability into product thermo-mechanical availability in the cases with a higher EGR fraction leads to a faster drop in the destruction curve with increase in reactant temperature. Beyond a certain reactant temperature, the higher EGR fractions tend to destroy lesser amounts of availability.

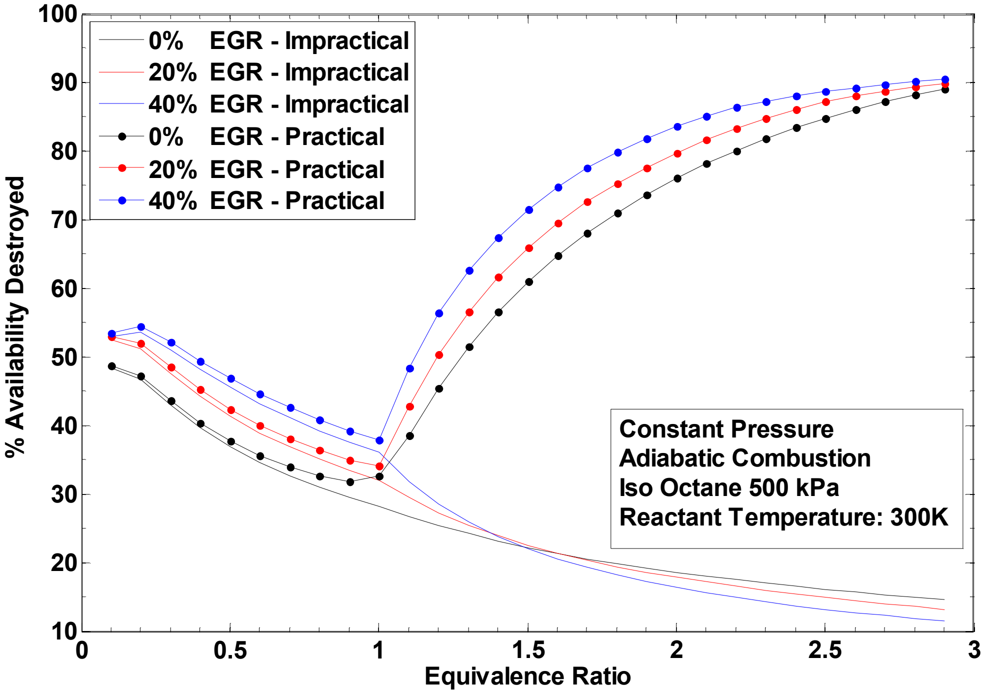

Fig 12. Percentage availability destroyed for different 'Cooled' EGR fractions as a function of equivalence ratio for constant pressure combustion of iso octane, reactant temperature of 300 K.

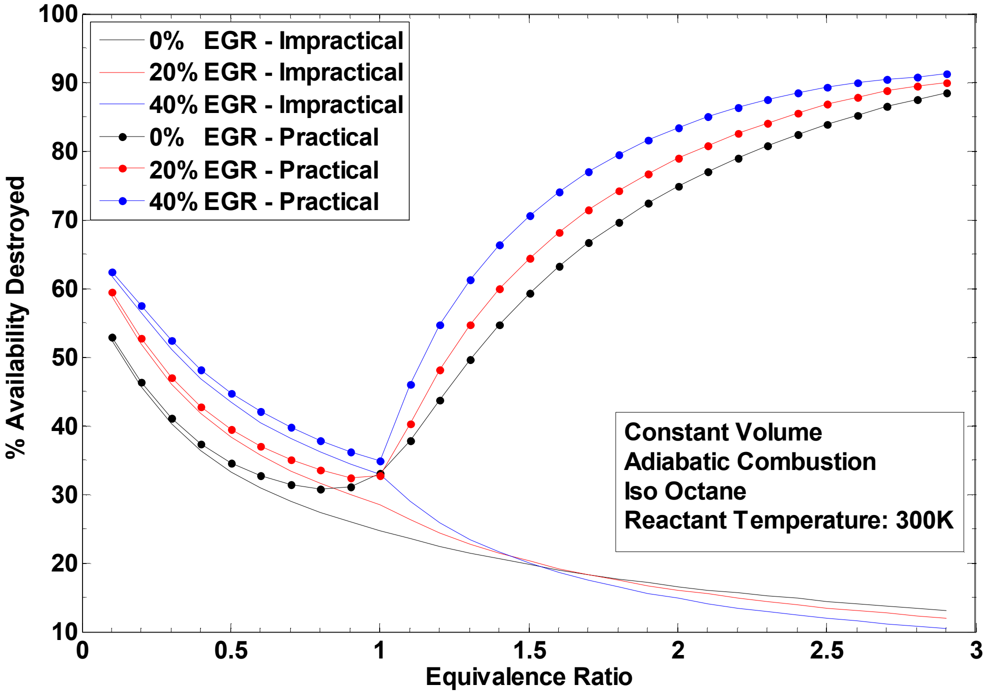

Fig 13. Percentage availability destroyed for different 'Cooled' EGR fractions as a function of equivalence ratio for constant volume combustion of iso octane, reactant pressure of 500 kPa and reactant temperature of 300 K.

Figures 12 and 13 indicate the variation of the destruction of availability with equivalence ratio at a reactant temperature of 300 K for both “practical” and “impractical” cases with 0, 20 and 40% EGR fractions. The “impractical” scenario refers to the case wherein the chemical availability in the products is considered as useful availability that can be extracted and the “practical” case refers to the scenario wherein the chemical availability in the products is left out completely while calculating the availability destruction. In the practical approach, the main point of interest is the equivalence ratio that causes the least destruction of availability for a given EGR percentage.

The availability destroyed curve for both the practical and impractical cases increases as the mixture gets leaner. Leaner mixtures result in lower product temperatures, and hence, the availability destroyed is more as the equivalence ratio decreases. Within this range, the higher EGR percentage destroys a greater amount of availability. This is because the higher EGR percentage acts as a secondary source that reduces the product temperature in addition to the leaner mixture which is the primary source for product temperature reduction.

A noticeable fact is that even in the lean range where the reactive chemical availability in the products is low, the practical curves for a given EGR percentage is always above the corresponding curves for the impractical case. This is due to the fact the impractical case has the diffusive reactant chemical availability in the denominator of the availability destroyed term whereas the practical case ignores this term. Hence the practical case destroys a higher percentage of availability even in the leaner range.

The value of the availability destroyed decreases as an equivalence ratio of 1.0 is approached. This is due to the fact that a greater amount of fuel is supplied which results higher product temperatures. Again, the higher EGR percentage destroys a greater amount of availability as the EGR stream acts as a diluent thus decreasing product temperature.

Deviations start to happen as an equivalence ratio of 1.0 is approached in the practical curves. It is seen that the 0% EGR curve starts to rise at an equivalence ratio of about 0.8. The reason for the practical curves to rise is due to the fact that a large amount of the reactive chemical availability and a small amount of the diffusive chemical availability in the products is being neglected and hence the net product availability is just the thermo-mechanical availability. Hence the curves rise in the richer zones. In the rich zone, the excess fuel present remains in the unburned form and it accounts for the reactive chemical availability that is rejected (and considered “destroyed”). The excess fuel also lowers the product temperature which again results in poor combustion and a greater destruction of availability. Again here the higher EGR percentage destroys a greater percent of availability as the EGR acts as a secondary source of product temperature reduction. The noticeable point is that the point of inflection of the curves shifts towards slightly richer equivalence ratio as the EGR percentage increases.

The 0% EGR curve ("practical") starts to rise first followed by the 20% and lastly by the 40% EGR curve. In the 0% EGR case, the product temperatures are high enough at an equivalence ratio of about 0.8 to form enough products of combustion of high availability (incomplete products). Hence, the value of the product reactive chemical availability starts to become significant. Since this is being neglected, the curve starts to rise. With the increase in the EGR percentage, the equivalence ratio at which the product temperature is high enough to produce enough products of high availability such that the reactive chemical availability term becomes significant if shifted to the right, a slightly richer mixture. This is because a slightly excess amount of fuel needs to be supplied to increase the product temperature to a value where the reactive chemical availability of the products starts to become significant.

The 40% EGR case ("practical") is a special one. For this case, the curve starts to rise exactly at an equivalence ratio of 1.0 and the rise is pretty sharp. This is because of the fact that the product temperatures are never high enough for the reactive availability in the products to be significant. The only time when this value becomes significant is in the rich zone, where the excess fuel contributes to this value and causes the curve to rise up.

From a practical point of view, the equivalence ratio at which the value of availability destroyed is a minimum is important. This value is not fixed and constantly changes with the percent of EGR. It is sensitive to the EGR percent only when the EGR percentages are low (0-20%) and the higher EGR fractions have no effect on this point of inflection.

The curves for the impractical case in figures 12 and 13 continue to decrease even in the rich zone as the reactive chemical availability in the products is considered as useful. But beyond a certain equivalence ratio the trend reverses with the higher EGR percentage destroying a lesser amount of availability.

It is seen from figures 12 and 13 that the curve for the 40% EGR case starts to drop sharply beyond the equivalence ratio of 1.0 finally reversing the trend at an equivalence ratio of about 1.5. In the rich zone with the increase in the EGR percentage and equivalence ratio, more and more of the original availability is retained in the chemical form rather than the thermo-mechanical form. Retaining the original reactant availability in this chemical form destroys a lesser fraction of availability than when it is converted into thermo-mechanical form. Since the higher EGR fractions tends to retain a greater amount of the original reactant availability in the chemical form, which is still considered as useful here, it preserves a larger amount of the original reactant availability. Since this is considered as useful availability, the fraction of the original reactant availability converted into product availability increases with higher EGR percentages there-by leading to a sharper drop in the curve corresponding to 40% EGR, and finally, to the trend reversal.

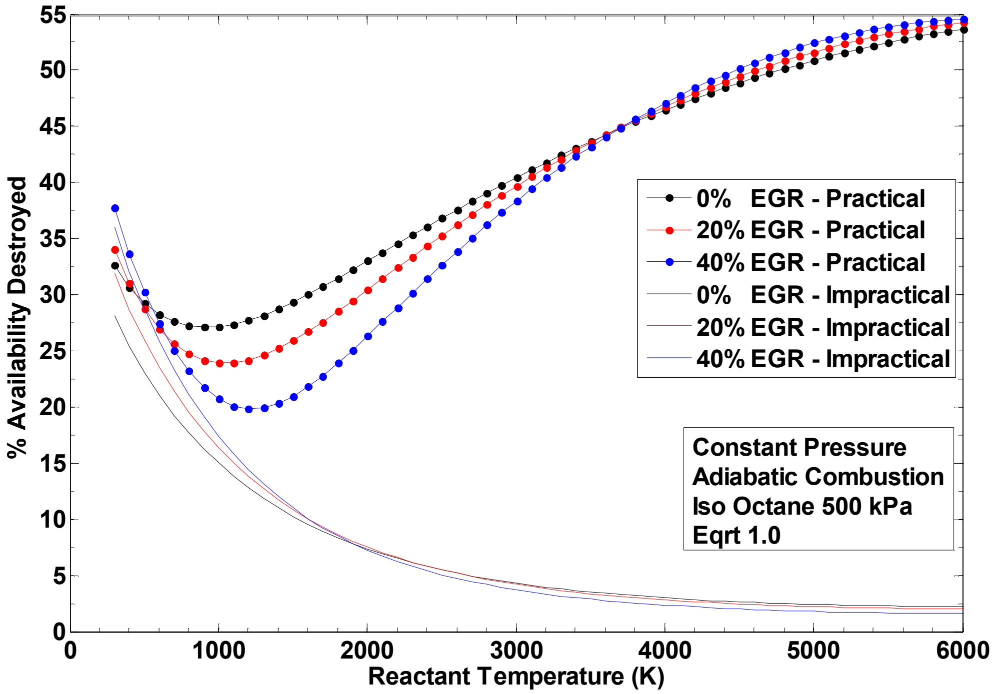

Fig 14. Percentage availability destroyed for different 'Cooled' EGR fractions as a function of reactant temperature for constant pressure combustion of iso octane.

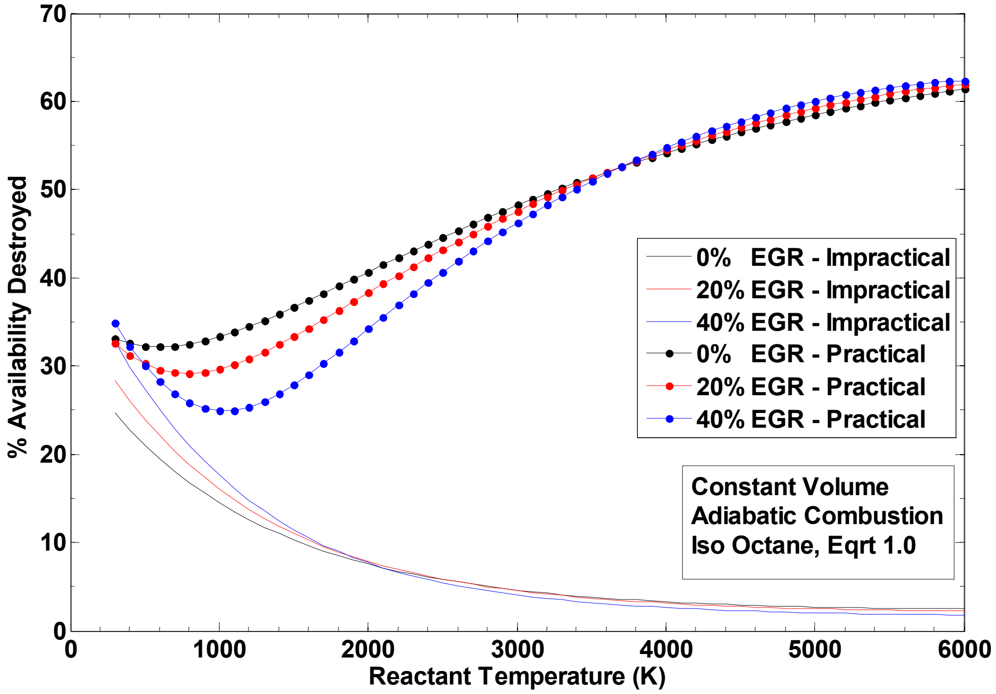

Fig 15. Percentage availability destroyed for different 'Cooled' EGR fractions as a function of reactant temperature for constant volume combustion of iso octane, reactant pressure of 500 kPa.

Figures 14 and 15 indicate the variation in the availability destroyed with reactant temperature for the “practical” and “impractical” scenarios at various EGR fractions. The two curves are expected to overlap at low reactant temperatures which do not happen. This is primarily due to the fact that even though the reactive chemical availability at these low reactant temperatures is negligible when compared to the thermo-mechanical availability, the diffusive chemical availability remains a constant at all temperatures. This value is the same for the reactant side and the product side. This value is neglected in the practical case whereas it is a part of the availability destruction formula in the impractical scenario and hence the curves do not overlap even at the low reactant temperatures.

As expected the availability destroyed value in the practical case decreases up to a certain reactant temperature before it starts to climb again. The reason for the curves to climb up is because at the higher reactant temperatures, a larger fraction of the original reactant availability is now being retained in the chemical form (evident from the falling thermo-mechanical conversion percentage from figures 10 and 11) which is now being disregarded. Again the point of inflection shifts to the right with increase in the EGR fraction since the higher EGR fractions need a correspondingly higher reactant temperature for the reactive chemical availability in the products to be significant.

For low reactant temperatures, the higher EGR fractions destroy a larger amount of availability. The destruction curve tends to drop off at a much faster rate for the higher EGR fractions as explained for figures 2 and 3. At the very high temperatures, the higher EGR fractions, again, tended to destroy a higher amount of availability. This is again evident from figures 10 and 11. After a reactant temperature of about 3800 K, the curves cross over with the curve corresponding to the higher EGR fraction converting a lesser amount of its original reactant availability into product thermo-mechanical availability. The rest is preserved in the chemical form and since this is disregarded in the practical case in figures 14 and 15, the higher EGR fraction now destroys a larger amount of availability.

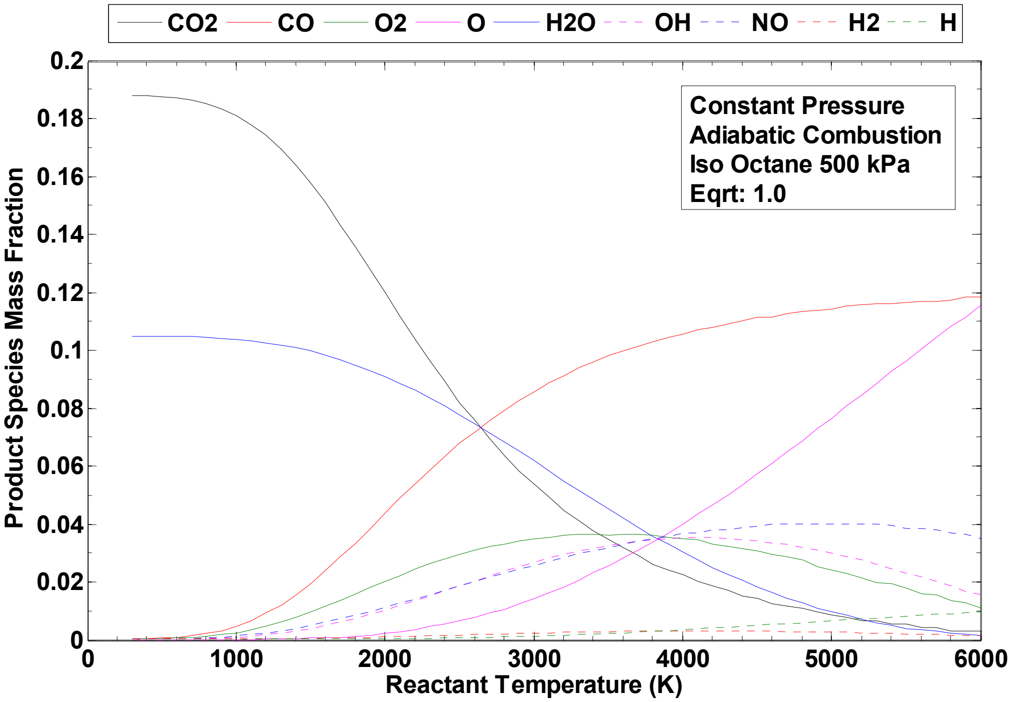

Fig 16. Product species mass fraction for a 40% 'Cooled' EGR fraction as a function of reactant temperature for constant pressure combustion of iso octane.

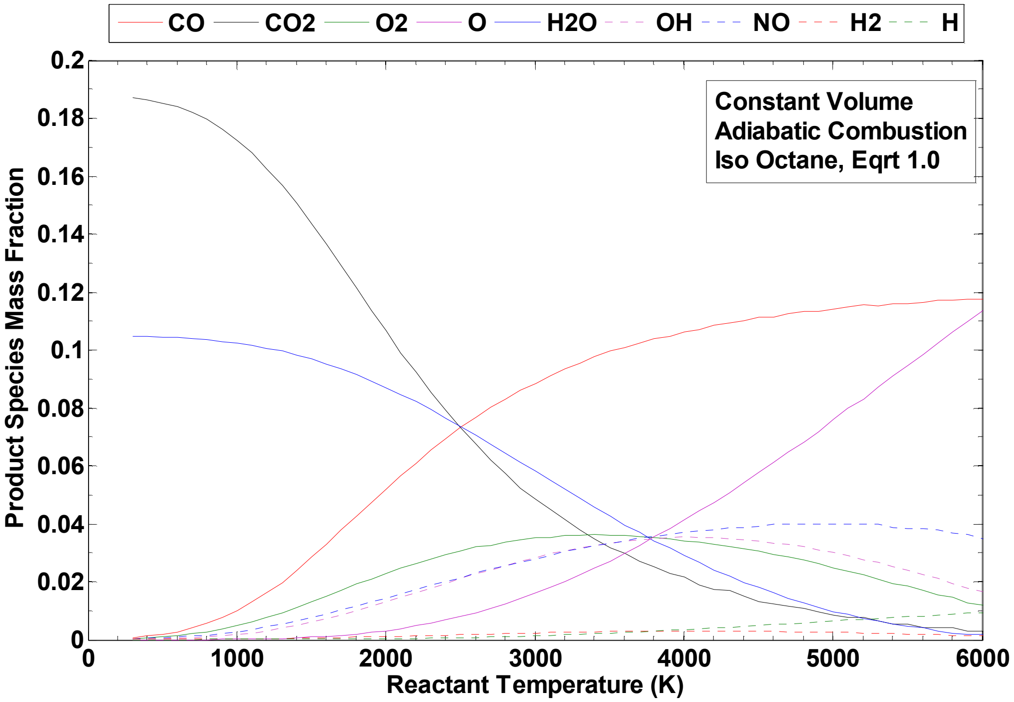

Fig 17. Product species mass fraction for a 40% 'Cooled' EGR fraction as a function of reactant temperature for constant volume combustion of iso octane, reactant pressure of 500 kPa.

Figures 16 and 17 depict the product species mass fraction for the 40% EGR case. This helps in explaining the reason for the rise in the availability destruction curves after a reactant temperature of about 1000 K in figures 14 and 15. Only the dominant product species have been depicted in the figures. Even at the lower reactant temperatures, the equilibrium does predict a high amount of CO mass fraction in the products which has a high amount of reactive chemical availability associated with it which is now being disregarded in the practical cases in figures 14 and 15. This along with the presence of other species whose reactive chemical availability is now being disregarded is the reason for the rise in the availability destruction curves in figures 14 and 15.

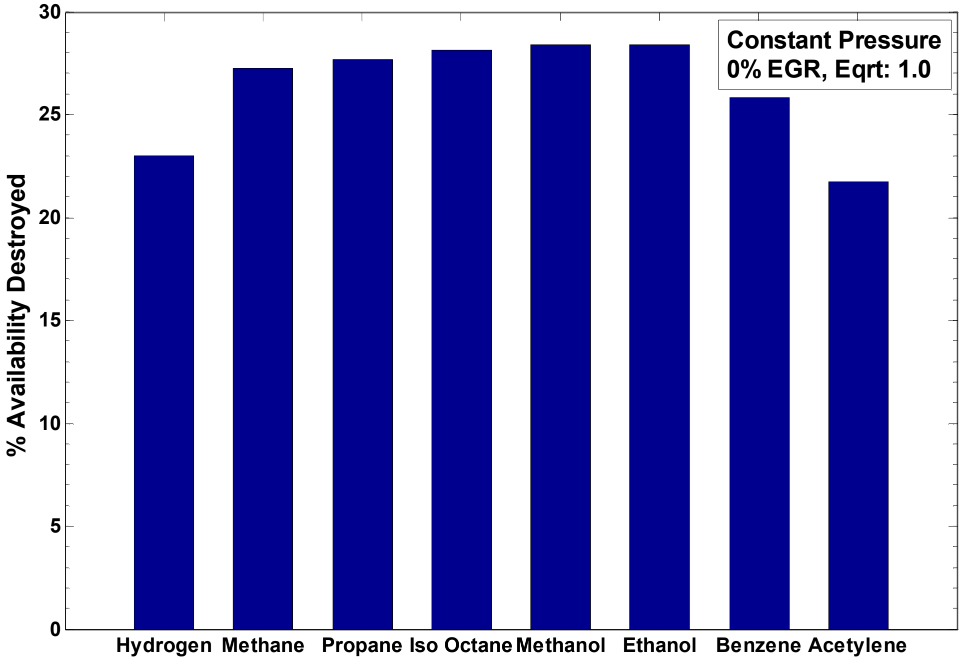

Fig 18. Percentage availability destroyed for 0% 'Cooled' EGR fraction for different fuels for constant pressure combustion of iso octane, reactant pressure of 500 kPa and reactant temperature of 300 K.

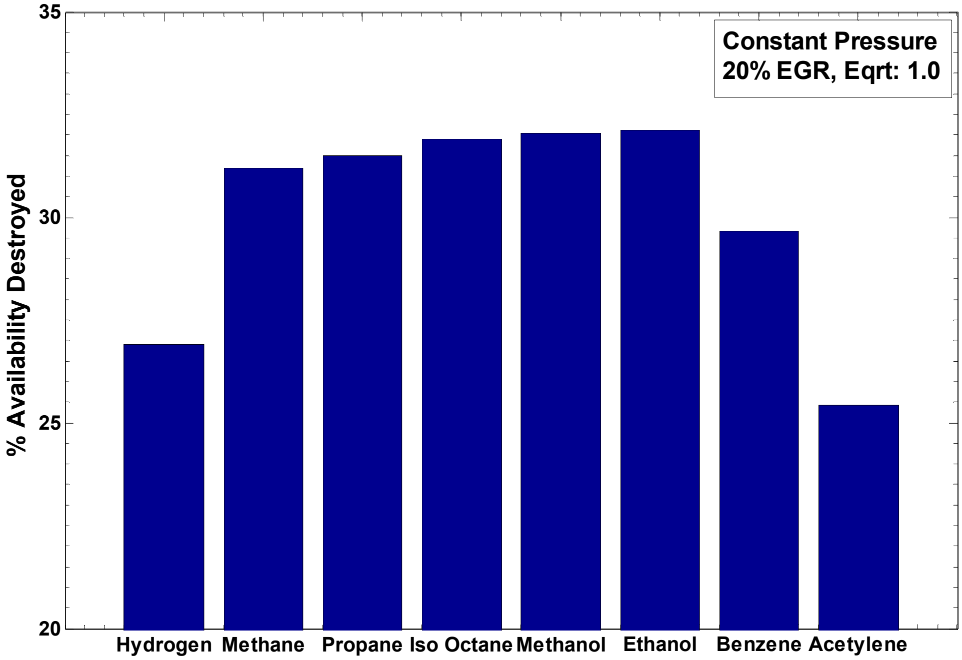

Fig 19. Percentage availability destroyed for 20% ‘Cooled’ EGR fraction for different fuels for constant pressure combustion of iso octane, reactant pressure of 500 kPa and reactant temperature of 300 K.

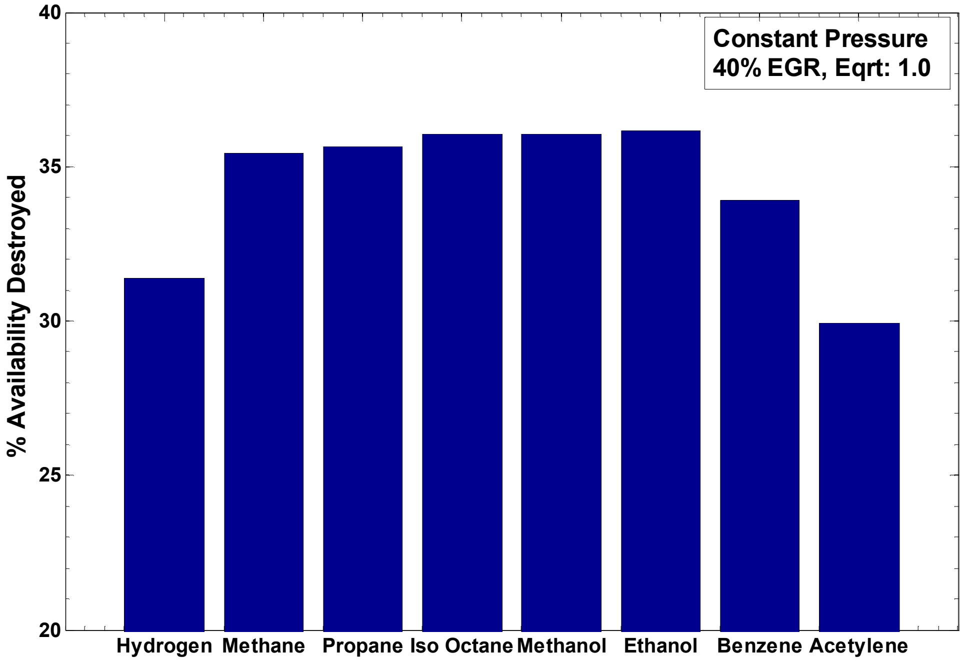

Fig 20. Percentage availability destroyed for 40% ‘Cooled’ EGR fraction for different fuels for constant pressure combustion of iso octane, reactant pressure of 500 kPa and reactant temperature of 300 K.

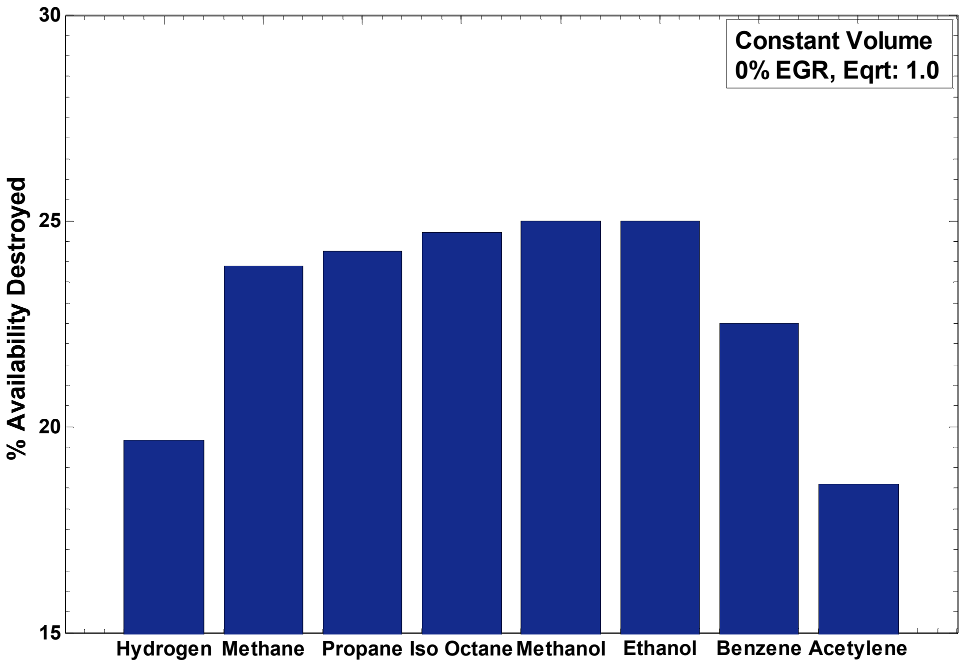

Fig 21. Percentage availability destroyed for 0% 'Cooled' EGR fraction for different fuels for constant volume combustion of iso octane, reactant pressure of 500 kPa and reactant temperature of 300 K.

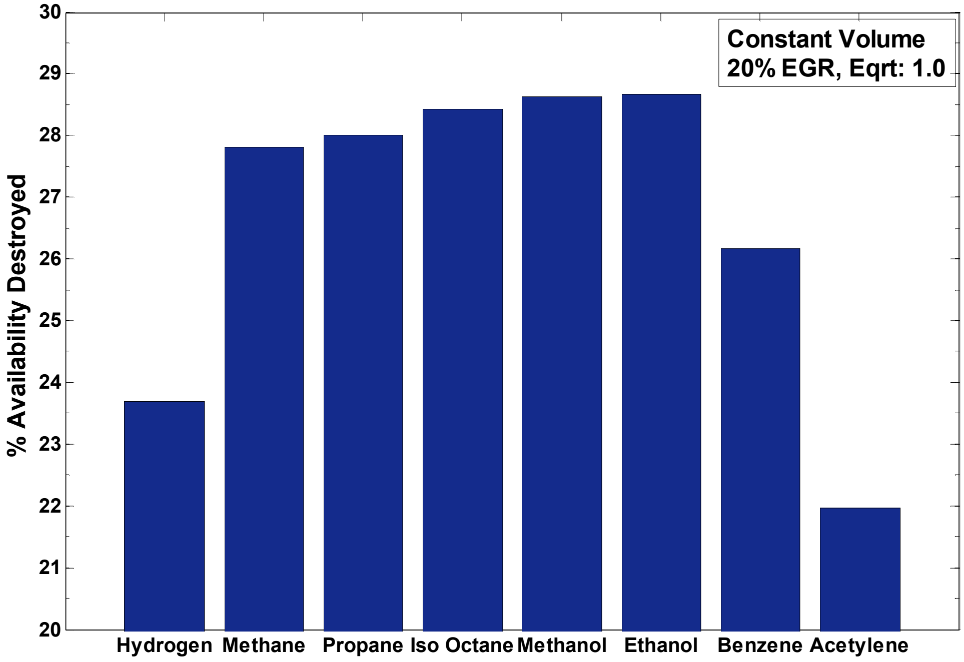

Fig 22. Percentage availability destroyed for 20% 'Cooled' EGR fraction for different fuels for constant volume combustion of iso octane, reactant pressure of 500 kPa and reactant temperature of 300 K.

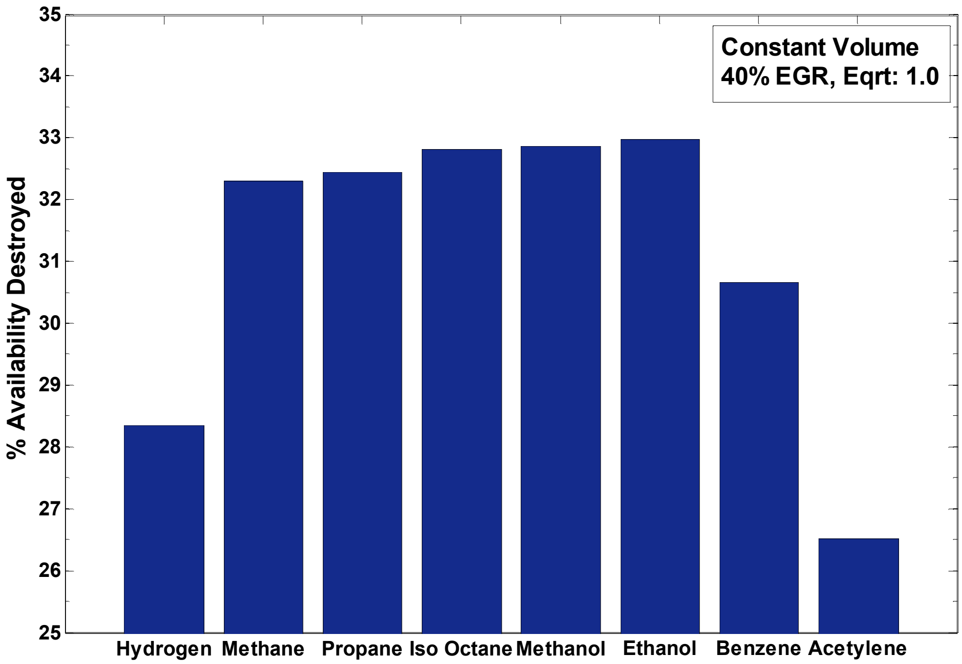

Fig 23. Percentage availability destroyed for 40% ‘Cooled’ EGR fraction for different fuels for constant volume combustion of iso octane, reactant pressure of 500 kPa and reactant temperature of 300 K.

Figures 18 through to 23 shows for both the HP and UV combustion processes, the percentage of availability destroyed for various fuels at 300 K for the 3 different EGR fractions. For both the HP and UV combustion processes, hydrogen destroys the least availability at 300 K. This is an important insight from a practical point of view with regards to the combustion of hydrogen from a second law perspective. The availability destruction increases with increase in the complexity amongst the linear hydrocarbons, i.e. iso octane destroying a fraction more availability than propane which destroys a fraction more than methane. The alcohols destroy the highest percentage of availability. The presence of oxygen in the fuel and the lower product temperatures causes a slightly higher destruction of availability.

As expected the percentage availability destroyed increases with increase in EGR fraction. The benzene case has the most significant rise amongst all the fuels. Hydrogen still results in the least availability destruction even at 40% EGR. The fact that most of the hydrocarbon fuels seems to destroy similar amounts of availability at higher EGR percentages indicates that the reduced temperature plays a bigger role in determining the availability destruction than the nature of the fuel.

Water Injection

The following section deals with the injection of water in the gaseous form into the inlet along with the fuel/air charge. The injected water fraction is again defined on a mass basis as in the case of EGR. Only constant enthalpy and constant pressure combustion case has been analyzed here.

The main effect of the injection of the above species into the inlet is the corresponding reduction in the product temperature. This is because the injected species tend to dilute the incoming fuel/air charge leading to lower product temperatures and greater destruction of availability. In the subsequent section, a comparison is made between cooled EGR and water/nitrogen/carbon dioxide injection. In a practical application, one advantage of reducing product temperatures is the corresponding reduction in the NOx levels. But there is a fine line between reducing the NOx levels and compromising the efficiency of combustion.

Figure 24 shows the variation of the percentage of the availability destroyed with reactant temperature for the case with water injection. The percentage of availability destroyed increases with increase in the water injection in the lower reactant temperature ranges and the trend reverses after around 1100 K.

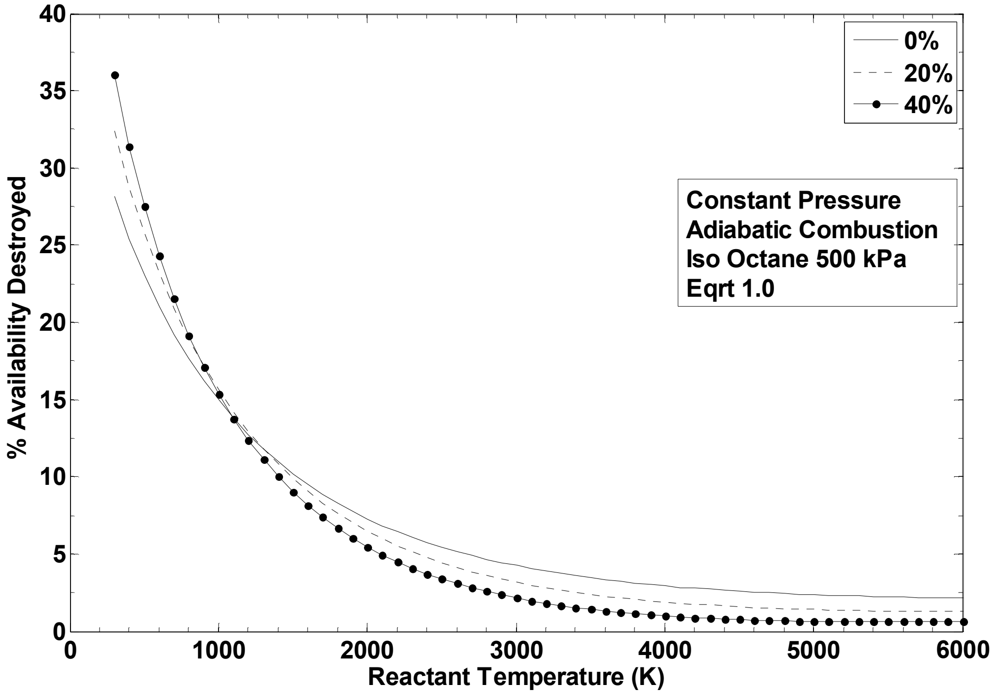

Fig 24. Percentage availability destroyed for different fractions of injected water as a function of reactant temperature for constant pressure combustion of iso octane.

The rate at which the destruction of availability decreases is directly proportional to the rate of conversion of the reactant availability into product thermo-mechanical availability. In other words, the faster the reactant availability is converted into product thermo-mechanical availability, the faster is the rate at which the destruction of availability curve drops. This is the reason for the cross over of the availability destruction curves in figure 24. Preserving the original reactant availability in the chemical form in the products does not alter the availability destruction curve significantly. This is the reason for the curves to flatten out at the higher reactant temperatures as more and more of the original reactant availability is now retained in the chemical form in the products which as mentioned before does not alter the availability destruction curve significantly.

Another point to notice in figure 24 is that the curves corresponding to lower fractions of injected water tend to flatten out quicker. This is due to the fact that the lower fraction of water leads to higher product temperatures at a much lower reactant temperature. This higher product temperature results in the formation of more and more equilibrium species of combustion rather than complete products. These incomplete species have a much higher reactive chemical availability associated with them. As mentioned before, the larger the fraction of the reactant availability that is preserved in the chemical form in the products, the lesser it effects the availability destruction curve. The curves corresponding to higher injected water fractions tend to flatten out at slightly higher reactant temperatures as it needs that slightly higher reactant temperature to have a sufficiently high product temperature to form incomplete species of combustion having a high reactive chemical availability.

Figure 25 depicts the variation of the product temperature with reactant temperature for the three different fractions of injected water for the constant HP combustion process. As expected the product temperature is correspondingly lower for the higher injected fractions of water.

Figure 26 shows the percentage of the original reactant availability that is converted into product thermo-mechanical availability. As mentioned before, the rate at which the reactant availability is converted into product thermo-mechanical availability is higher for the curves corresponding to higher fractions of injected water which is evident from the sharper slopes for the curves with higher injected water fractions. The percentage of the reactant availability that is converted into product thermo-mechanical availability increases with increase in reactant temperature up to a certain limit after which it decreases. The decrease is due to the fact that more and more of the reactant availability is now being preserved in the chemical form in the products.

It is also evident that the point of inflection shifts to the right with increase in the injected water fraction. This is because the higher water fractions need a correspondingly higher reactant temperature to form incomplete species of higher availability in the products which preserves the reactant availability in the chemical form.

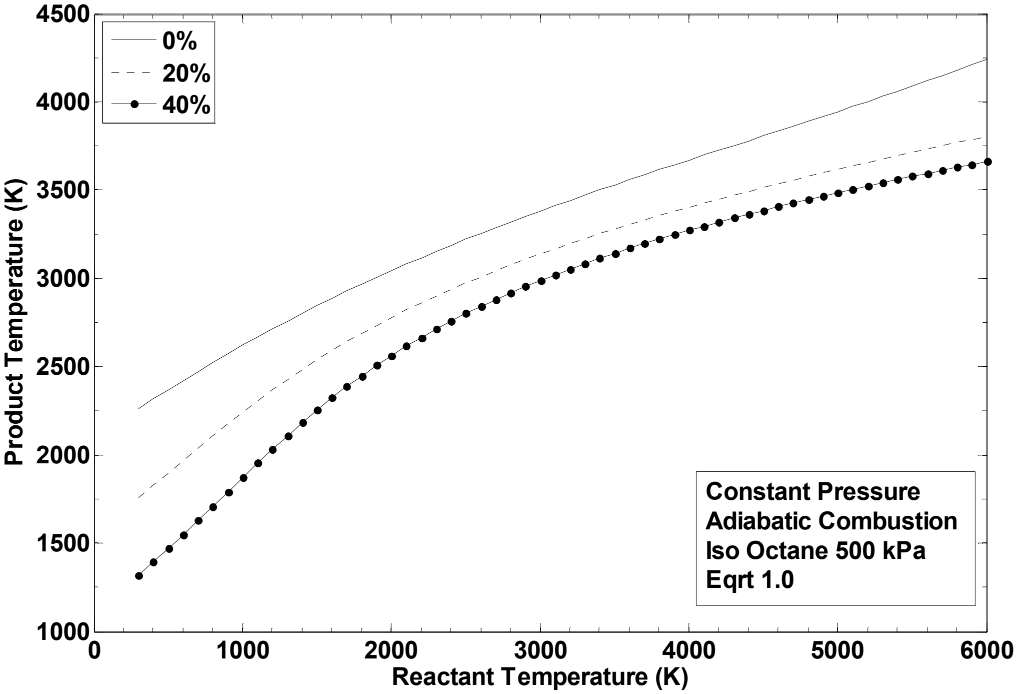

Fig 25. Product temperature for different fractions of injected water as a function of reactant temperature for a constant pressure combustion of iso octane.

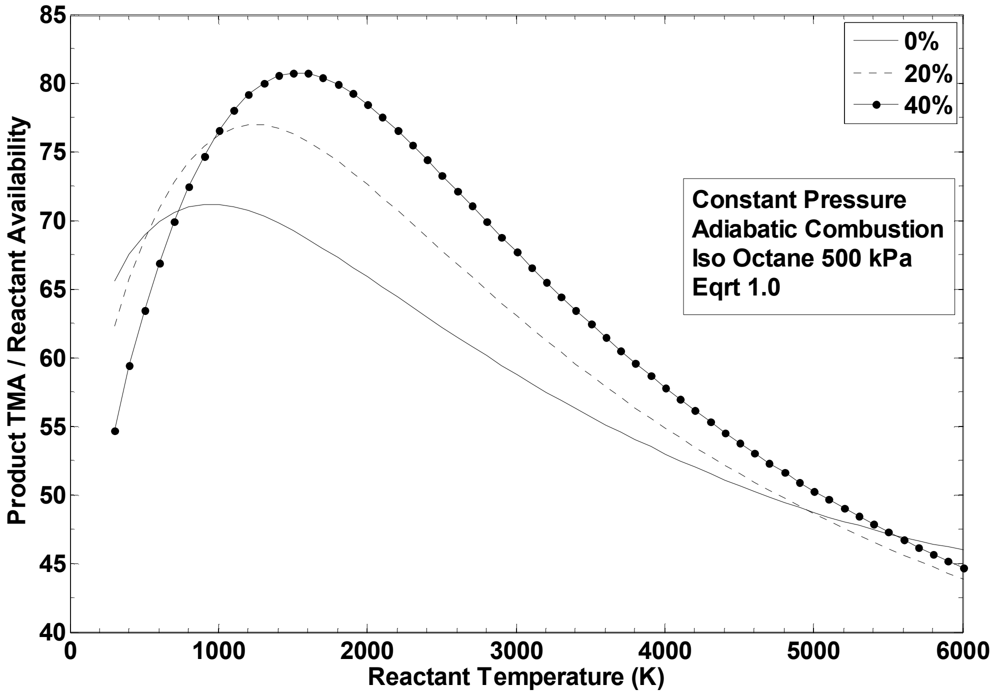

Fig 26. Percentage of reactant availability converted into product thermo-mechanical availability for different fractions of water injected as a function of reactant temperature for constant pressure combustion of iso octane.

Another reason for the sharper decrease in the availability destruction for the curves corresponding to higher injected water fractions is the higher diffusive availability associated with the higher injected water fractions. In the EGR setup, the diffusive availability was independent of the EGR fraction as the species were recycled and hence the number of atoms of each element stayed the same and hence the diffusive availability stayed the same whereas here the diffusive availability changes as more and more water is injected into the inlet. There is no recycling of species that take place here during the water injection process.

Figure 27 depicts the variation of the product temperature with the injected water fraction. As expected the final product temperature decreases with increase in the water fraction. The plot shown is for a reactant temperature of 300 K and depicts a constant enthalpy pressure process.

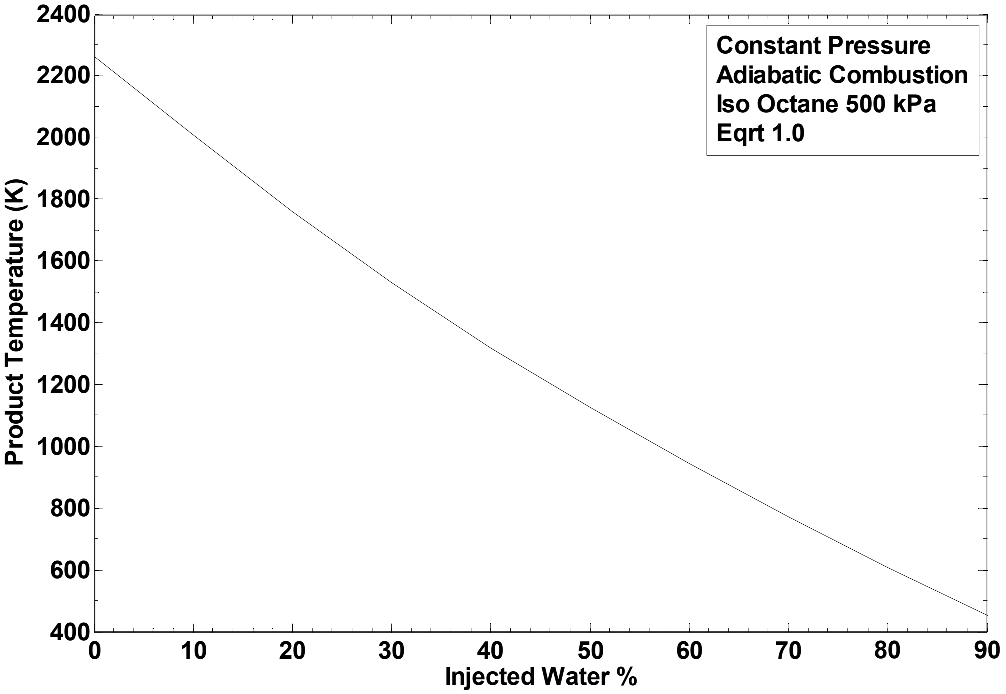

Fig 27. Product as a function of fraction of injected water for constant pressure combustion of iso octane, reactant temperature of 300 K.

Comparison of Cooled EGR / Water / N_2 / CO_2 Injection

Figures 28 and 29 show the availability destroyed at a reactant temperature of 300 K for the various kinds of species that are injected in the inlet for 20% and 40% injection fractions respectively. EGR (cooled) is also compared with the nitrogen, water and carbon dioxide injection cases. The 'Cooled EGR' process is different from the remaining three processes as it involves a recycling aspect that is absent in the others. All the 4 cases do not show significant differences at the lower reactant temperature of 300 K which is of interest from a practical point of view.

In the 20% case, the water injection technique destroys the maximum availability with the carbon dioxide injection destroying the least availability. In the 40% case, the availability destroyed increases for all 4 cases with the water injection and the EGR (cooled) destroying almost identical amounts of availability. The carbon dioxide injection still destroyed the least availability. A point to notice is that the product temperature for the CO_2 injection case is lower than the N_2 injection case but still the carbon dioxide case destroys a lesser amount of availability. The reason for this is the higher diffusive availability associated with carbon dioxide when compared to nitrogen.

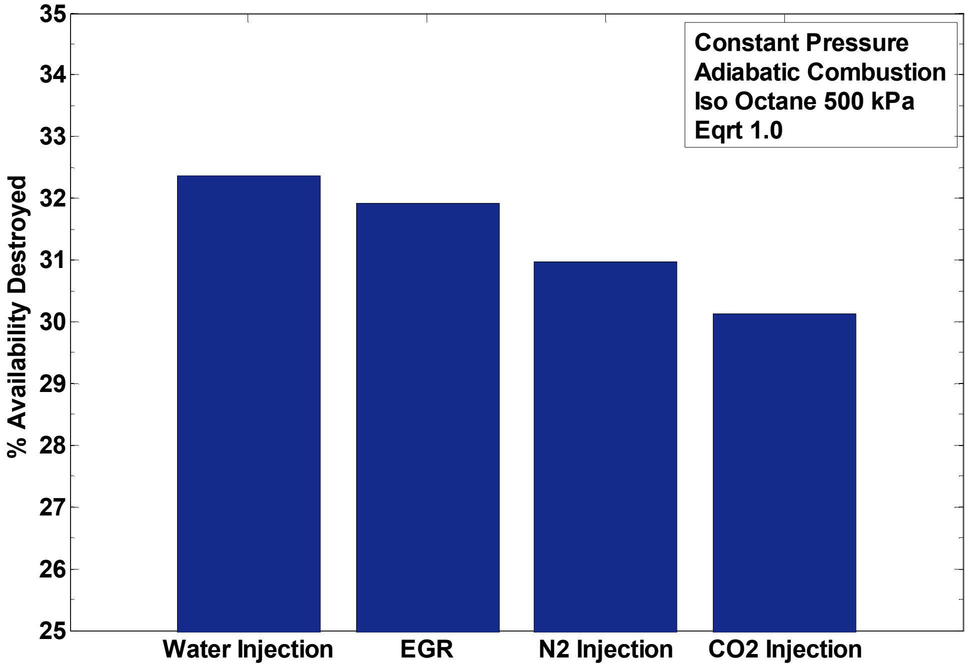

Fig 28. Percentage availability destroyed for 4 injected species (20% injected fraction) for constant pressure combustion with iso octane, reactant temperature of 300 K.

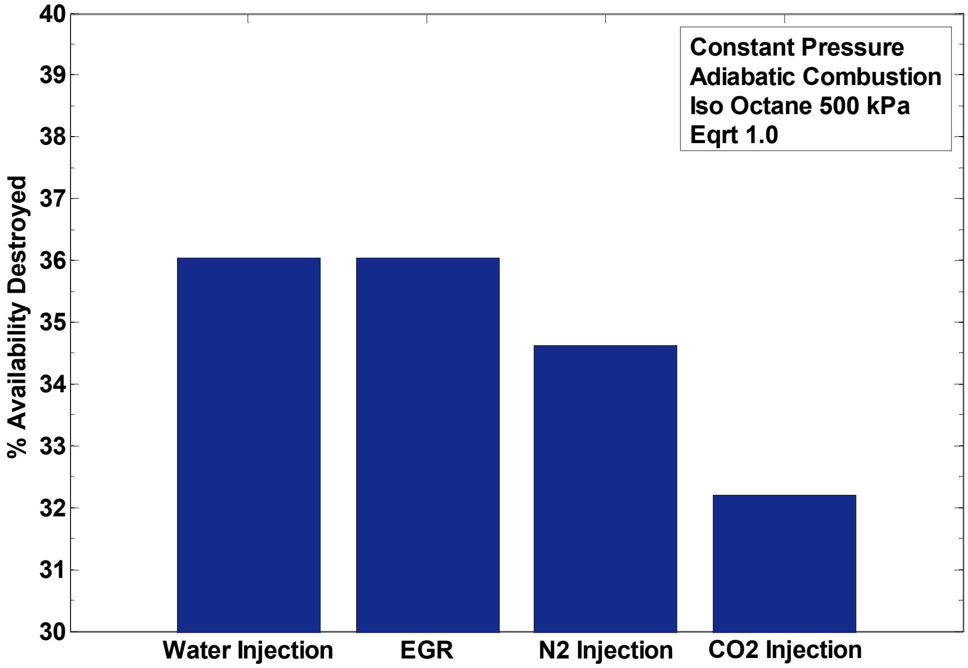

Fig 29. Percentage availability destroyed for 4 injected species (40% injected fraction) for constant pressure combustion with iso octane, reactant temperature of 300 K.

Figure 30 compares the percentage of availability destroyed for the four different techniques with variation in the reactant temperature for a constant enthalpy pressure process with a 40% injection fraction. At a reactant temperature of 300 K, the availability destroyed for the 4 techniques are depicted in figure 29. With increase in the reactant temperature, the water injection curve tends to drop the fastest and ends up destroying the least availability at the higher reactant temperatures. The curves for the remaining 3 injection techniques sticks to a pattern with the EGR (Cooled) destroying the greatest amount of availability followed by the nitrogen injection process and the carbon dioxide injection destroying the least amount of availability. These three curves tend to converge at the very high reactant temperatures.

The reason for the much sharper drop in the availability destruction curve for water injection is due the combination of several factors that are explained using the subsequent figures.

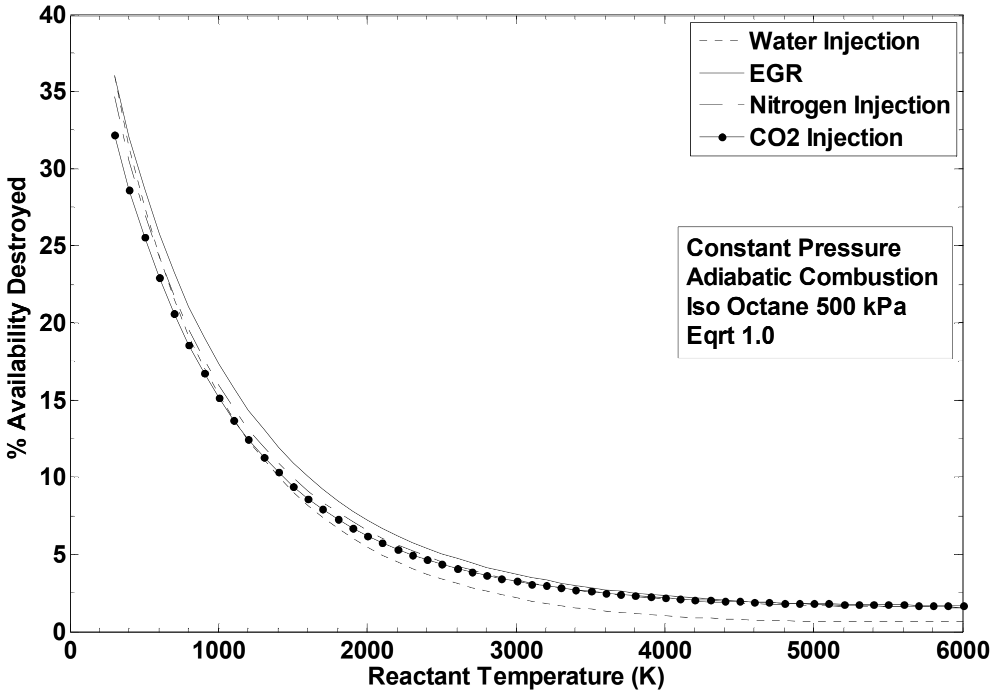

Fig 30. Percentage availability destroyed for the 4 injected species with a 40% injection fraction for constant pressure combustion with iso octane.

Figure 31 indicates the variation of the product temperature with the reactant temperature for the four techniques. The water injection technique tends to have the lowest product temperature for the entire reactant temperature range. At the very low reactant temperatures the nitrogen injection leads to the highest product temperature followed closely by carbon dioxide injection and the EGR. As mentioned before, the carbon dioxide injection still tends to destroy a lesser amount of availability at the very low reactant temperature when compared to the nitrogen injection technique due to its higher diffusive chemical availability.

With increase in the reactant temperature, the product temperature curves tend to separate. The water injection has the lowest product temperatures for the entire reactant temperature range. A sharp drop is noticed in the carbon dioxide injection curve with increase in the reactant temperature and it settles very close but above the water injection curve. The EGR and the nitrogen injection techniques lead to significantly higher product temperatures with the EGR process leading to higher product temperatures at the very high reactant temperatures.

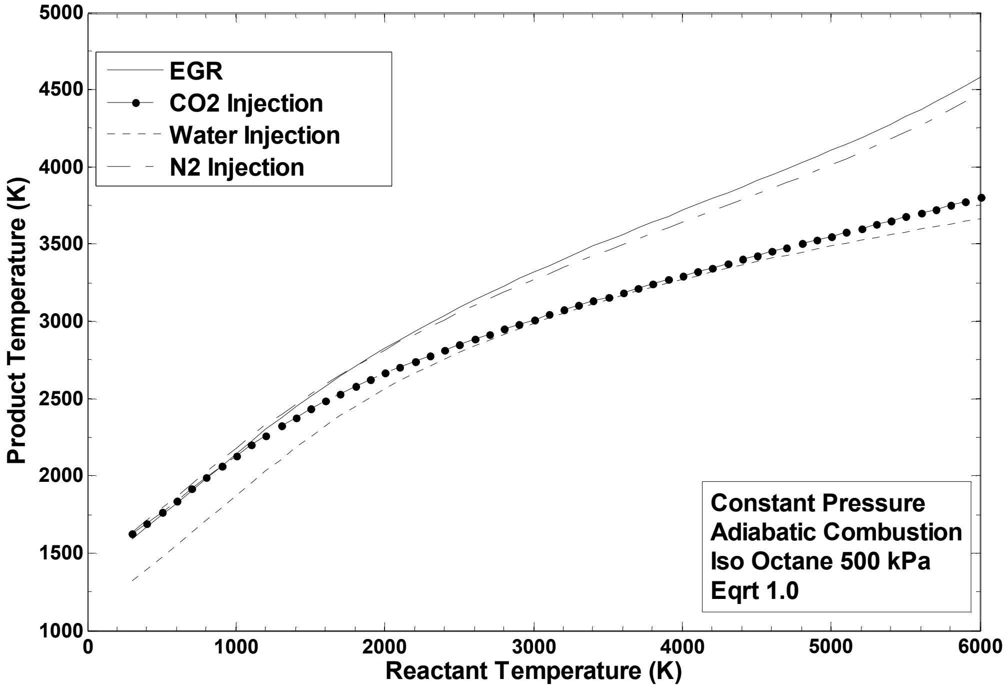

Fig 31. Product temperature for the 4 injected species with a 40% injection fraction for constant pressure combustion with iso octane.

Even though the EGR curve tends to have the highest product temperature for most of the reactant temperature range, it destroys the highest amount of availability as shown in figure 30. The main reason for this is the much lower diffusive chemical availability associated with the EGR process.

Figures 32 and 33 limit the reactant temperature range in figures 30 and 31 to 3000 K. Most of the trend changes occur within this reactant temperature range and the curves tend to converge beyond this temperature range. This helps the interpretation of the results.

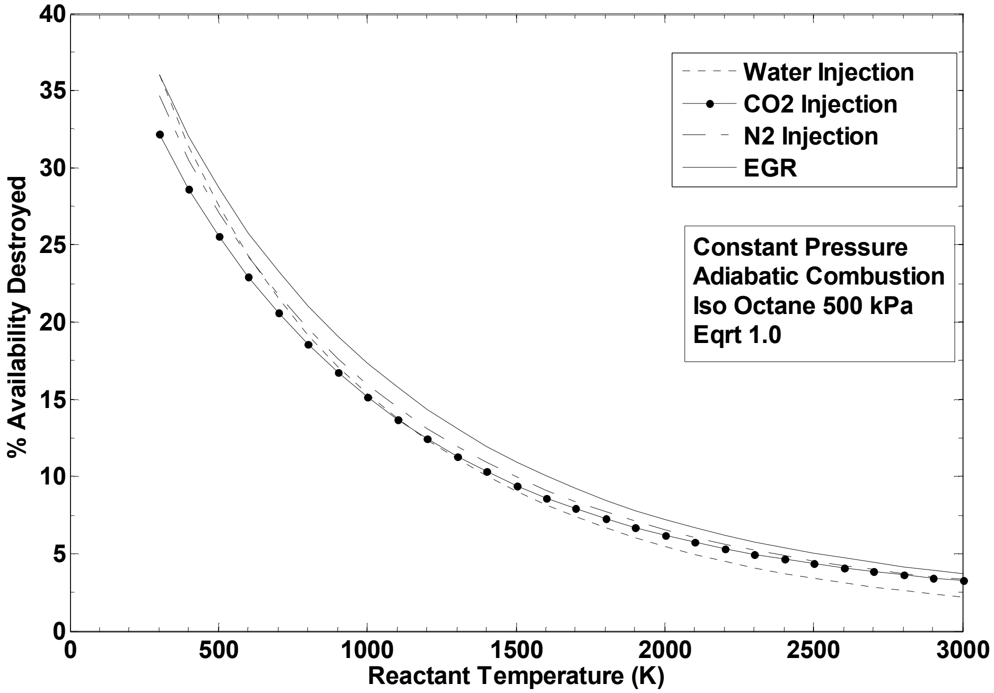

Fig 32. Percentage availability destroyed for the 4 injected species with a 40% injection fraction for constant pressure combustion with iso octane.

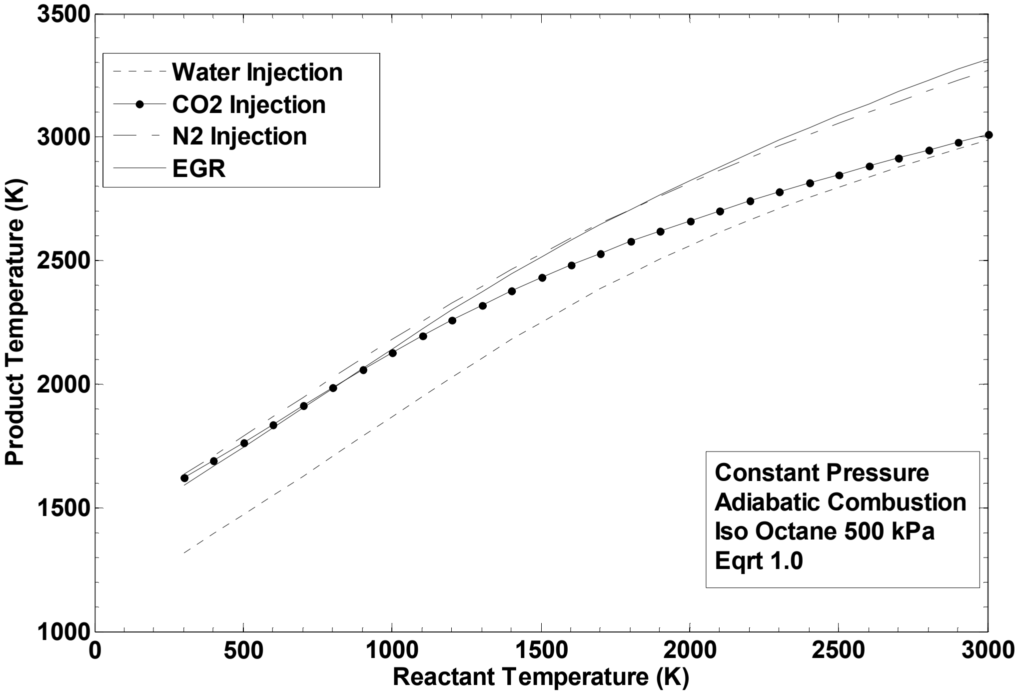

Fig 33. Product temperature for the 4 injected species with a 40% injection fraction for constant pressure combustion with iso octane.

Figures 34 and 35 depict the reactant and product thermo-mechanical availabilities for the four techniques. The thermo-mechanical availability for the EGR process is higher than the nitrogen and the carbon dioxide injection cases for the majority of the reactant temperature range. Only the water injection technique has higher thermo-mechanical availability in both the figures.

Figure 36 shows the reactive chemical availability in the products for the four cases. Here again the EGR process has a higher availability than the nitrogen and the carbon dioxide cases for the most part of the reactant temperature range. The water injection tends to cross over at the very high reactant temperatures. The incoming fuel chemical availability stays the same for the four cases since the injection fractions are the same.

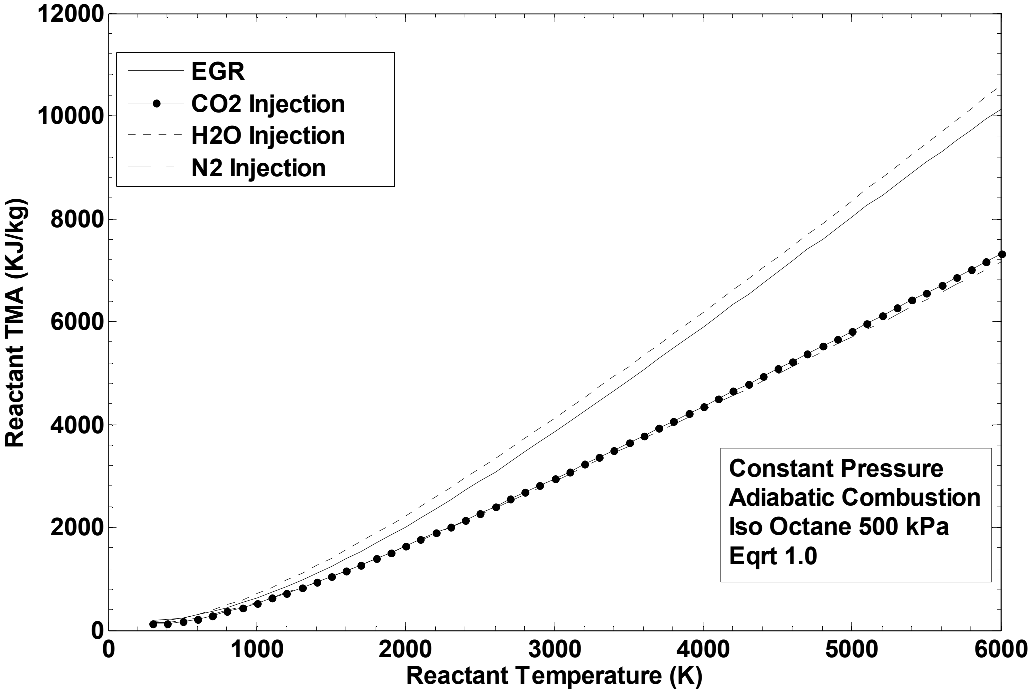

Fig 34. Reactant thermo-mechanical availability for the 4 injected species with a 40% injection fraction as a function of reactant temperature for a constant pressure combustion of iso octane.

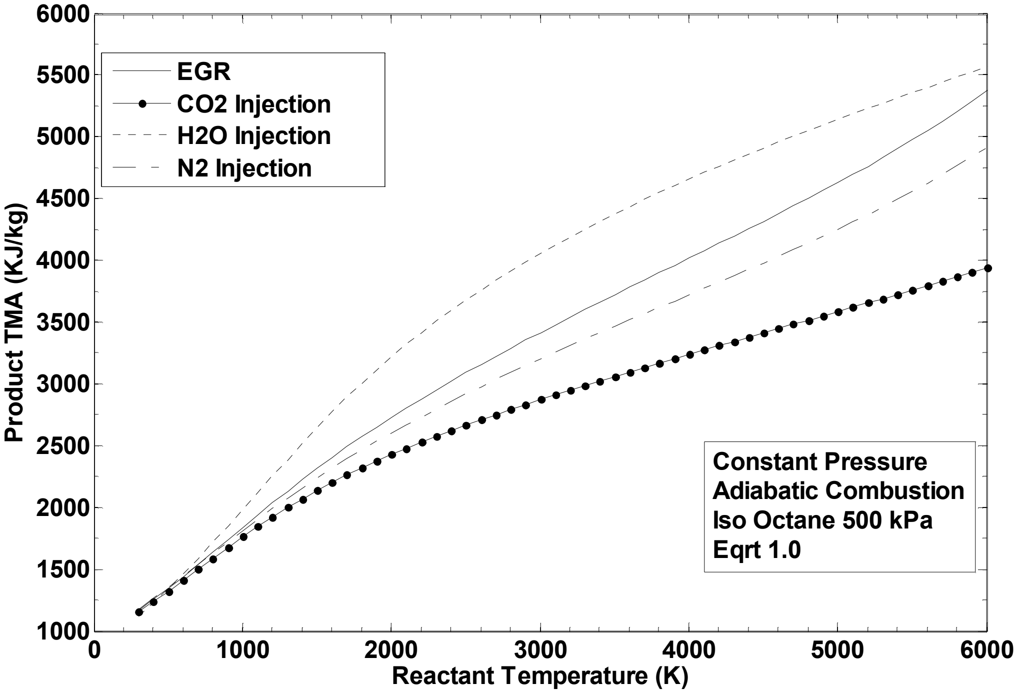

Fig 35. Product thermo-mechanical availability for the 4 injected species with a 40% injection fraction as a function of reactant temperature for a constant pressure combustion of iso octane.

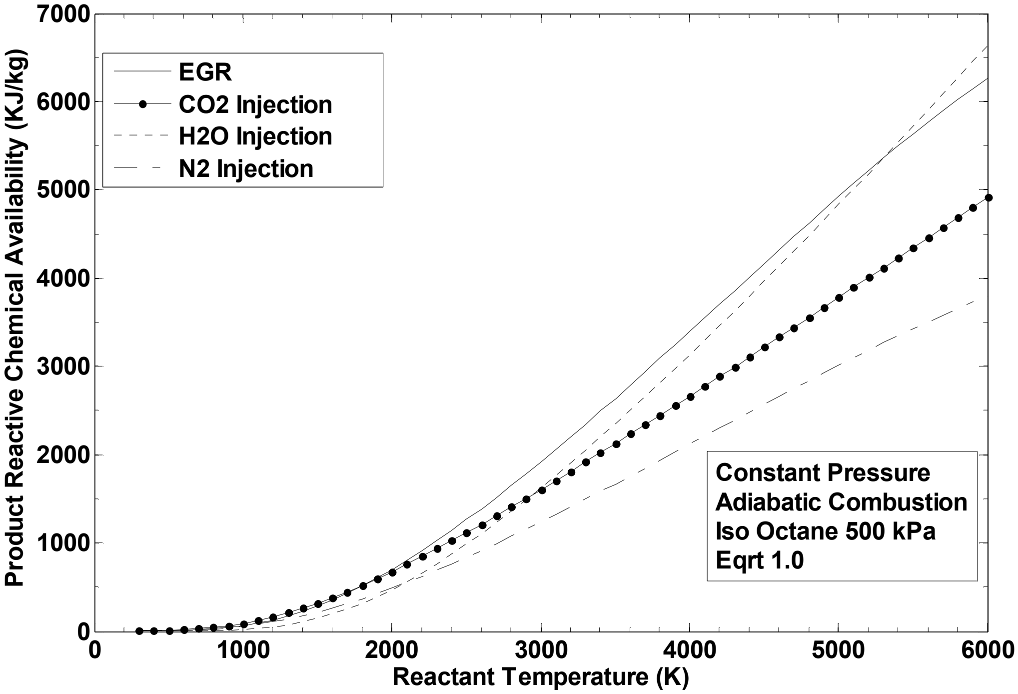

Fig 36. Product reactive chemical availability for the 4 injected species with a 40% injection fraction as a function of reactant temperature for a constant pressure combustion of iso octane.

From figures 34, 35 and 36 it appears that the EGR process should have been a lot more efficient and should have destroyed a lesser amount of availability. The higher reactant and product thermo-mechanical availabilities, the higher reactive product chemical availability points to towards a lesser destruction of availability. The reason for the EGR process to still destroy the highest amount of availability is due to two reasons. The first being the much lower diffusive chemical availability when compared to the water and the carbon dioxide injection processes. The second reason (and the significant reason) is due to the fact that the EGR process involves bringing in availability in the chemical form through the EGR stream. The exhaust gases possess a high degree of reactive chemical availability which is added to the reactant availability thus leading to a greater destruction of availability in the EGR process. The recycling aspect is not involved in the remaining three techniques.

Figure 37 shows the diffusive chemical availabilities for the four cases. The value of the diffusive chemical availability stays the same over the entire temperature range on a per kilogram basis.

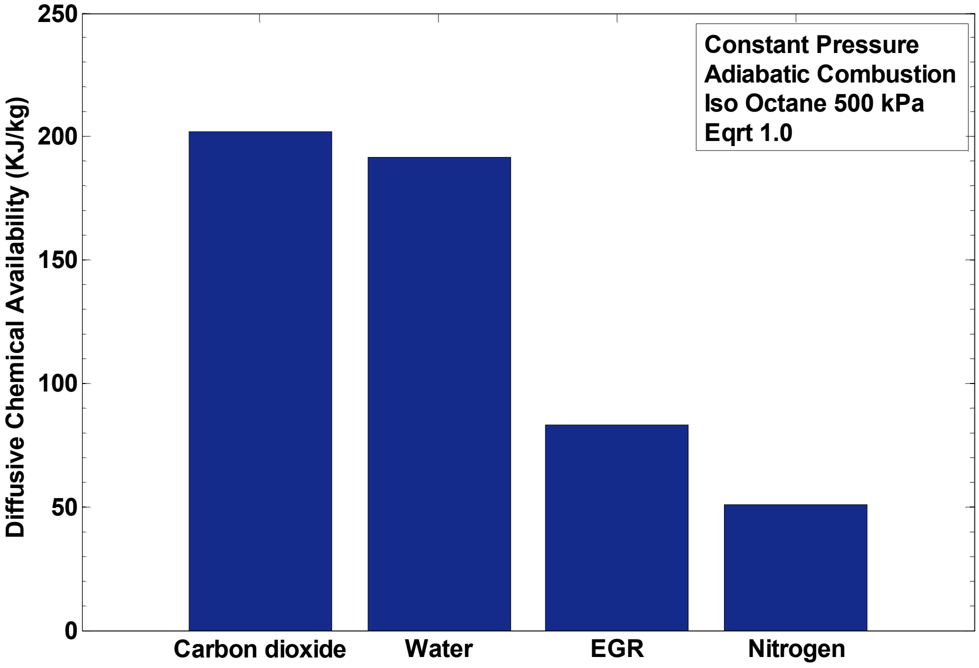

Fig 37. Diffusive chemical availability for the 4 injected species with a 40% injection fraction for a constant pressure combustion of iso octane.

It is clearly seen that the diffusive chemical availabilities associated with the carbon dioxide and water injection processes are a lot higher when compared to the EGR and the nitrogen injection processes. The low EGR diffusive chemical availability has already been sighted as a reason for the higher destruction of availability associated with the EGR process.

Another point to be noticed in figure 30 is that the carbon dioxide injection leads to a lesser availability destruction when compared to nitrogen injection. But figure 31 clearly shows that the product temperature associated with the nitrogen injection is significantly higher than the carbon dioxide injection case. This leads to much higher product thermo-mechanical availability for the nitrogen injection case as shown in figure 35. The reactant thermo-mechanical availabilities for both the cases are pretty similar as shown in figure 34.

Hence it appears that the nitrogen injection should have destroyed a significantly lesser amount of availability when compared to the carbon dioxide injection case. But this is not so due to a couple of reasons. The higher product thermo-mechanical availability associated with the nitrogen injection when compared to the carbon dioxide injection is countered by a significantly higher product reactive chemical availability for the carbon dioxide injection case when compared to the nitrogen injection case as shown in figure 36. Also, the significantly higher diffusive chemical availability associated with the carbon dioxide injection plays a role in destroying a lesser amount of availability when compared to the nitrogen injection case.

The final point to be addressed in figure 30 is the reason behind the much sharper fall in the availability destruction curve associated with water injection. At first glance it appears that the water injection should have destroyed the highest amount of availability since it tends to have the lowest product temperature which is evident from figure 31. Yet figure 35 shows that the water injection case tends to have the highest product thermo-mechanical availability even though it leads to the lowest product temperatures.

Figure 38 shows the product reference thermo-mechanical availability associated with the four cases. Here it is clearly shown that the species predicted by the equilibrium code for the water injection technique has the lowest thermo-mechanical availability at the reference state. This leads to net higher product thermo-mechanical availability for the water injection case as shown in figure 35.

Also, from figure 36, it is clearly seen that the reactive chemical availability associated with the products in the case of water injection rises at a much a much faster rate when compared to the other three cases and is the highest at the very high reactant temperatures. It is also noticeable that when the product thermo-mechanical curve associated with the water injection case starts to flatten out in figure 35 at the very high reactant temperatures, the corresponding curve associated with the product reactive chemical availability in figure 36 starts to rise higher and crosses over. The availabilities seem be getting transformed from one form to the other.

Another reason for the much sharper fall in the availability destruction associated with the water injection case is the much higher diffusive chemical availability associated with the water injection case when compared to the EGR and the nitrogen injection case which is evident from figure 37.

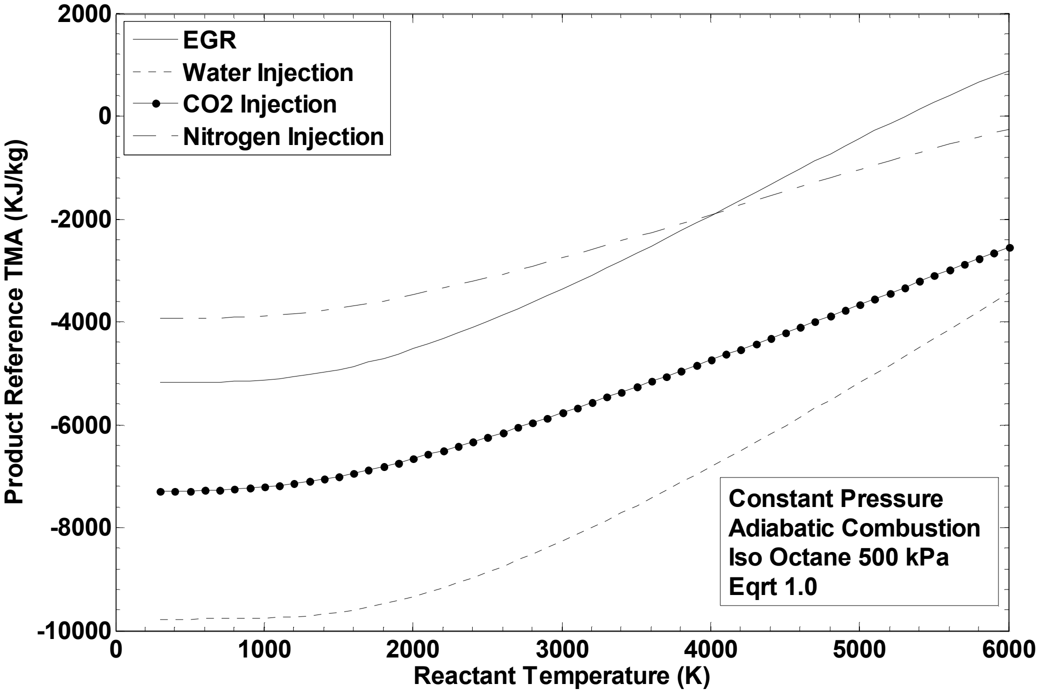

Fig 38. Product reference thermo-mechanical availability for the 4 injected species with a 40% injection fraction as a function of the reactant temperature for constant pressure combustion of iso octane.

Constant Pressure vs. Constant Volume Combustion

In this section, the constant pressure and the constant volume combustion cases have been compared. All the cases mentioned here involve non dissociated reactants and a 0% EGR fraction. Two different operating pressures of 50 kPa and 5000 kPa have been used to compare the two different forms of combustion. The constant pressure and constant volume combustion cases have also been compared at an operating pressure of 500 kPa at three different reactant temperatures for various fuels.

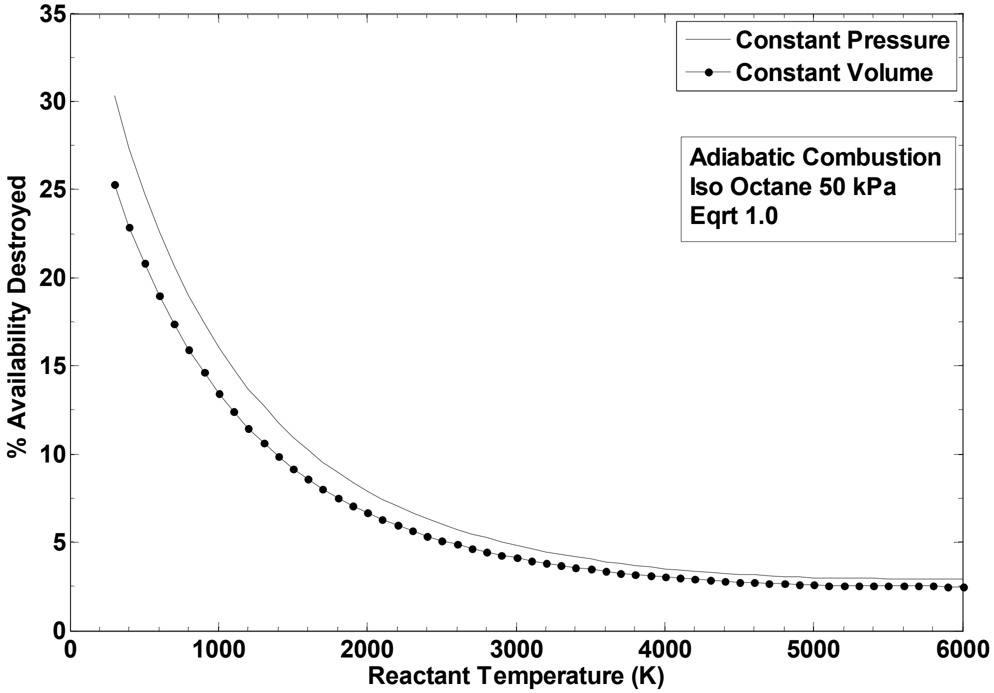

Fig 39. Percentage availability destroyed as a function of reactant temperature for constant pressure and constant volume combustion systems with iso octane, reactant pressure of 50 kPa.

Figure 39 indicates the variation of the destruction of availability with reactant temperature for constant volume and constant pressure combustion processes with iso octane as a fuel for the combustion reaction occurring at a pressure of 50 kPa and an equivalence ratio of 1.0. The constant volume combustion process proves to be more efficient for the entire reactant temperature range. The main reason behind this is that the product availability for the constant pressure process is lower than the constant volume case. The very low pressure of 50 kPa means that the pressure difference between the reactant pressure and the ambient pressure is very low in the constant pressure combustion case. The constant volume combustion results in much higher product pressures and hence there is a much bigger window as far as the pressure difference is concerned between the product pressure and the ambient pressure. The higher product pressures also results in higher product temperatures in the constant volume case for the large part of the reactant temperature range and this also contributes to a lower destruction of availability.

Figure 40 indicates the variation of the product pressure with reactant temperature for the constant pressure and constant volume combustion cases. As explained previously, the constant volume combustion process results in significantly higher product pressures which contributes to the lower destruction values. With increase in reactant temperature, the final product pressure falls and hence the two destruction curves starts to come together at the higher reactant temperatures.

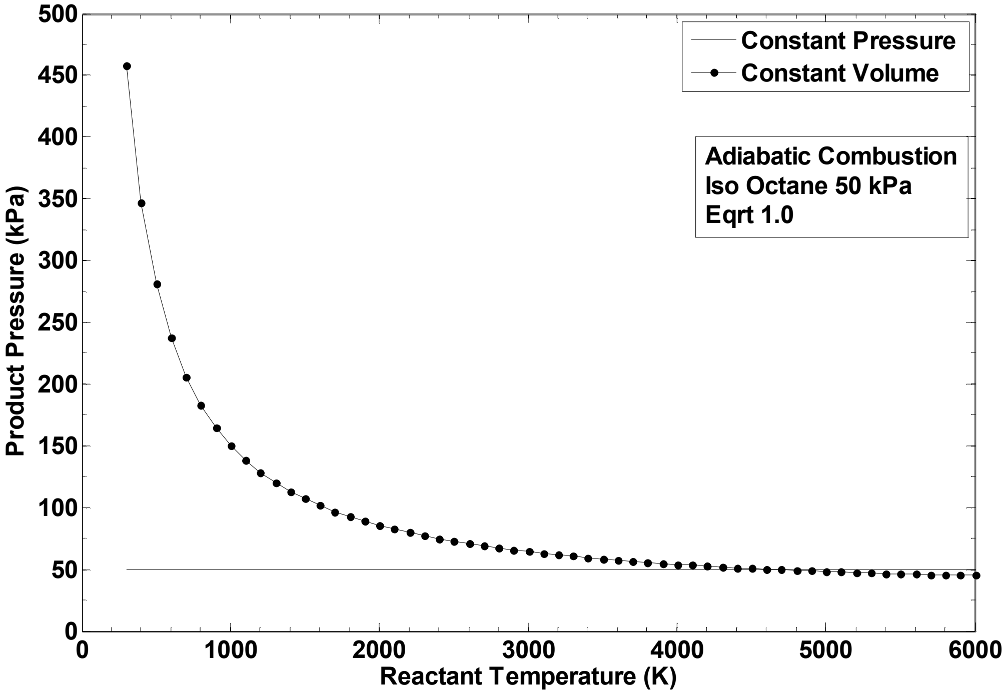

Fig 40. Product pressure as a function of reactant temperature for constant pressure and constant volume combustion systems with iso octane, reactant pressure of 50 kPa.

The two curves tend to cross over at around 4500 K and this corresponds to the reactant temperature at which the product temperature curves in figure 41 crosses over. Even though the product temperature and pressure for the constant pressure combustion case is higher when compared to the constant volume case, the constant volume still continues to destroy a lesser amount of availability. This is because the cross over happens at the higher reactant temperatures and by this point most of the original reactant availability is being preserved as product chemical availability in both the cases and hence there is not much change in the availability destruction values.

Figure 41 indicates the variation of the product temperatures with reactant temperature in both the cases. As stated before, the product temperature in the constant volume case is higher than the constant pressure for most part of the reactant temperature range and crosses over beyond 4500 K corresponding to the crossover point in figure 40.

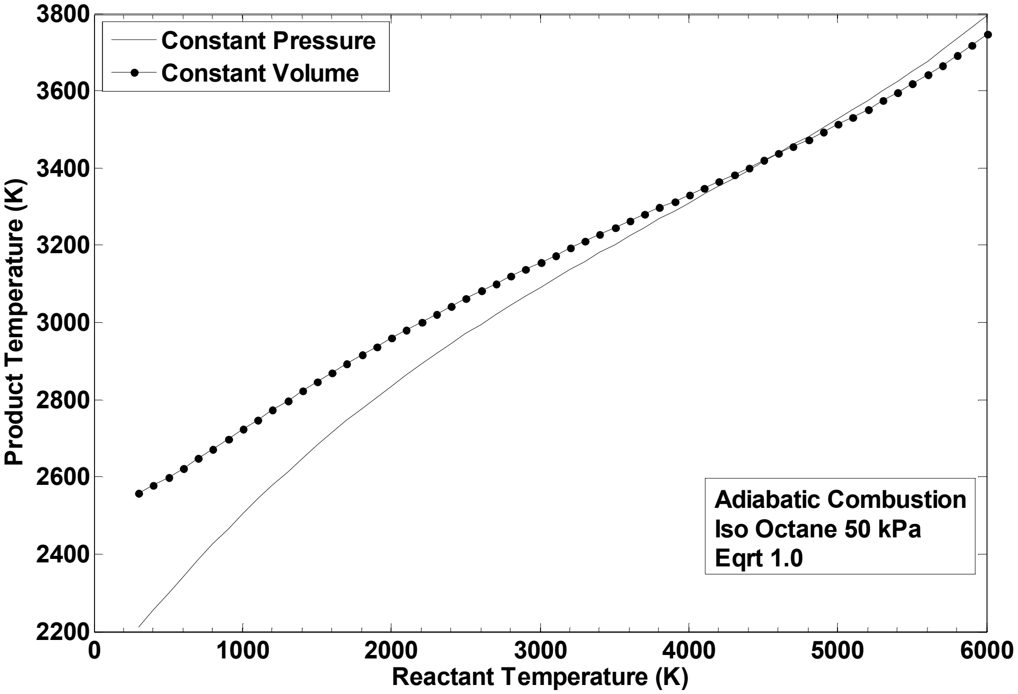

Fig 41. Product temperature as a function of reactant temperature for constant pressure and constant volume combustion systems with iso octane, reactant pressure of 50 kPa.

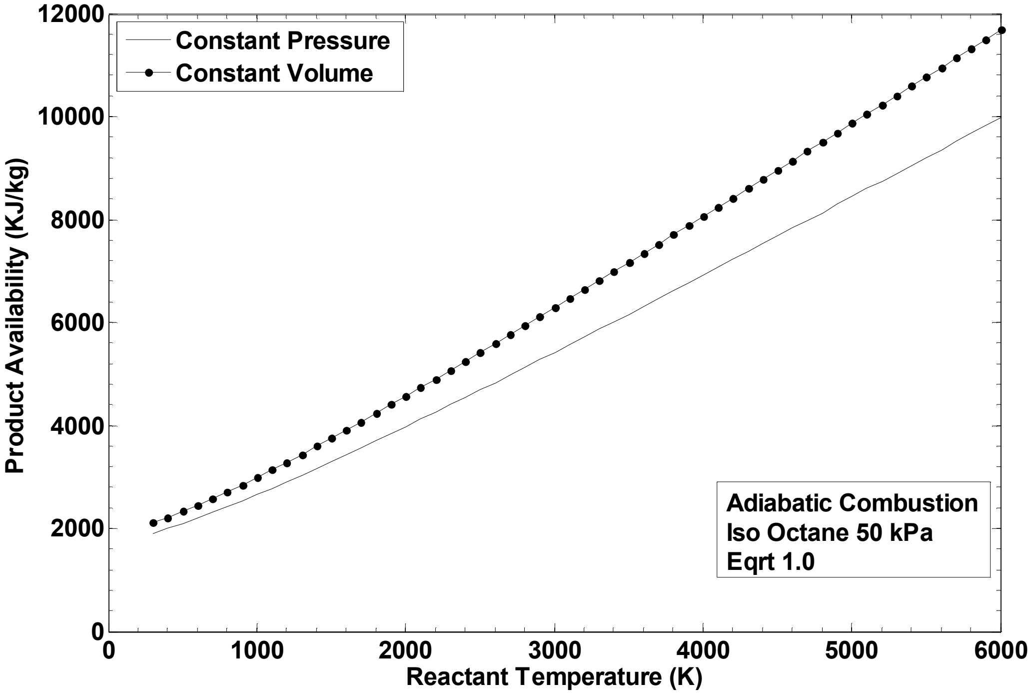

Fig 42. Product availability as a function of reactant temperature for constant pressure and constant volume combustion systems with iso octane, reactant pressure of 50 kPa.

Figure 42 shows the variation of the total product availability with reactant temperature for the two cases. As stated before, the higher pressures and temperatures for the constant volume case results in higher product availabilities which lead to lower values of destruction in figure 39.

Figures 43, 44, 45 and 46 show the variation of the same variables as in figures 39 through to 42 but at a reactant pressure of 5000 kPa. It is seen that the destruction curves cross each other at around 1200 K in figure 43. The constant volume case is more efficient below this temperature. One of the main reasons that aids in the crossover is the much higher reactant pressure of 5000 kPa. The pressure difference between the reactant pressure and the ambient is much higher when compared to the 50 kPa case and this is a part of the thermo-mechanical availability that can be exploited. This is especially significant in the constant pressure case. It makes the constant pressure process a lot more efficient as the operating pressure is much higher than the ambient pressure.

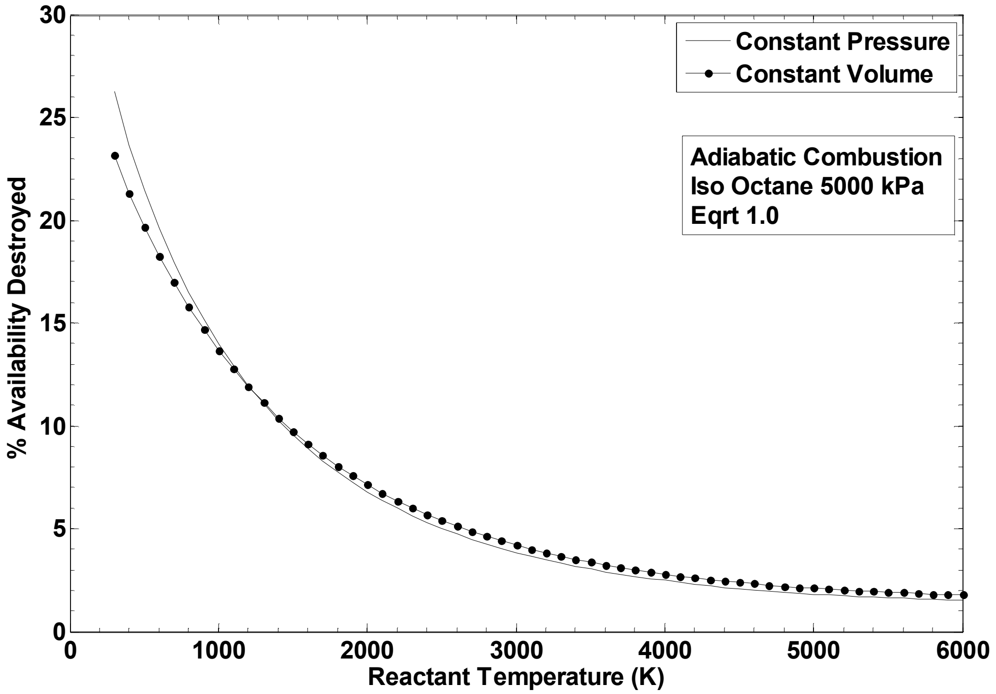

Fig 43. Percentage availability destroyed as a function of reactant temperature for constant pressure and constant volume combustion systems with iso octane, reactant pressure of 5000 kPa.

Figure 44 shows the variation of the product pressure with the reactant temperature for both the case. In this case, the product pressure curve for the constant volume case is always above the constant pressure curve and hence the corresponding product temperature curves in figure 45 also never cross each other. The constant volume process is expected to be more efficient from figures 44 and 45. But the reason for the cross over is due to two main factors. One being, as mentioned before, the much higher reactant pressure of 5000 kPa which helps the constant pressure process to be a lot more efficient. The second reason is that the product mixture at the higher temperatures and pressures in the constant volume process requires a larger volume (V_0) under the ambient conditions which reduces the product availability. This is not the case at a reactant pressure of 50 kPa. At 50 kPa, the product mixture requires a smaller volume (V_0) under the ambient conditions which increases the product availability.

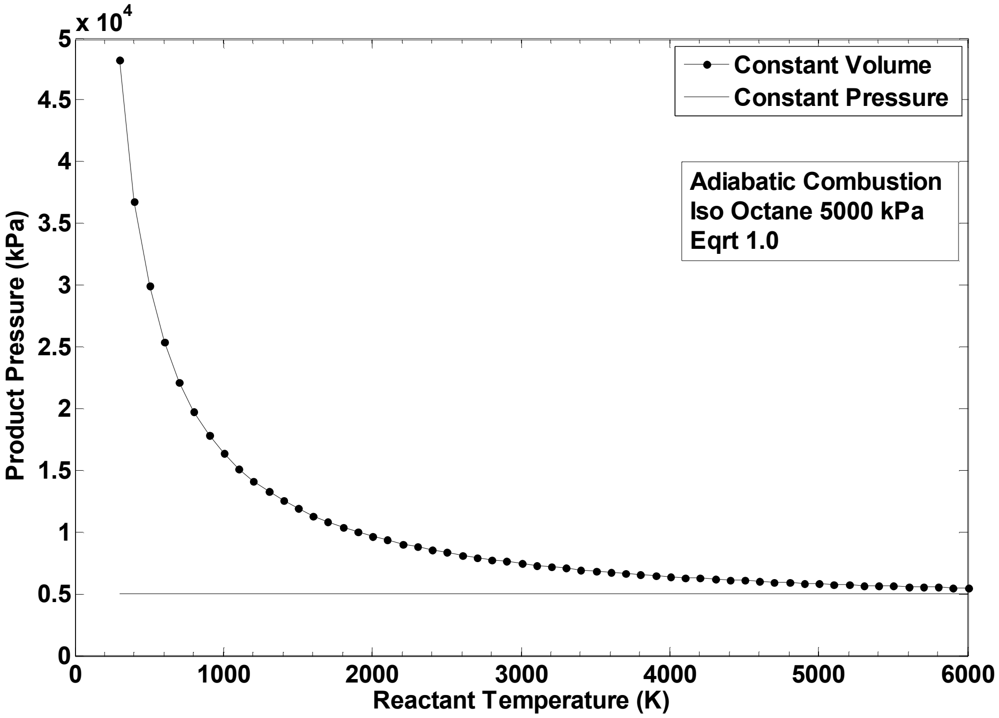

Fig 44. Product pressure as a function of reactant temperature for constant pressure and constant volume combustion systems with iso octane, reactant pressure of 5000 kPa.

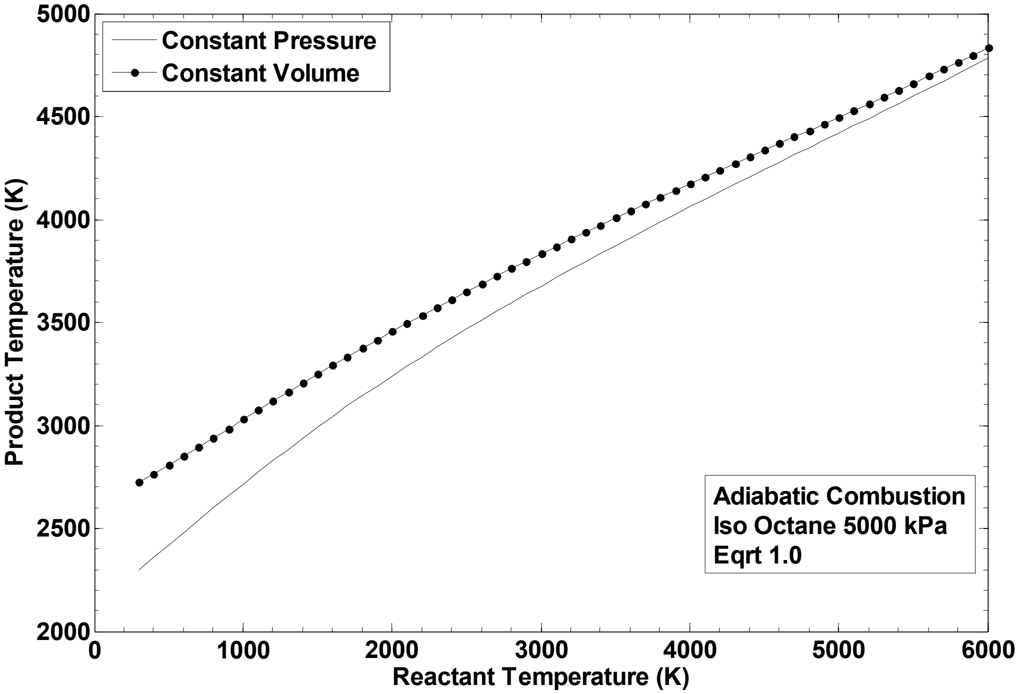

Fig 45. Product temperature as a function of reactant temperature for constant pressure and constant volume combustion systems with iso octane, reactant pressure of 5000 kPa.

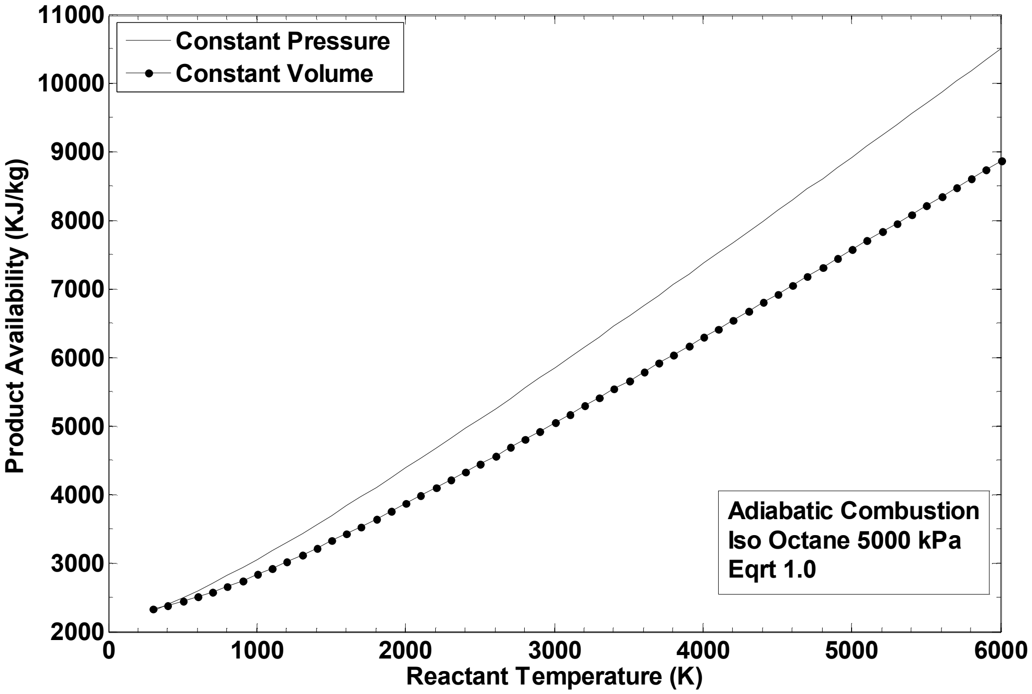

Fig 46. Product availability as a function of reactant temperature for constant pressure and constant volume combustion systems with iso octane, reactant pressure of 5000 kPa.

Figure 46 shows the variation of the total product availability with reactant temperature for the two cases. As stated before, the constant pressure case has a much higher availability when compared to the constant volume one. This is due to the larger reference volume in the constant volume case coupled with the greater product availability associated with the higher reactant pressure of 5000 kPa in the constant pressure case.

In all, it is seen that the availability destroyed values are lower at the higher pressures and this is mainly due to the higher product temperatures associated with the higher reactant pressures.

Figure 47 shows the variation of the availability destroyed with reactant temperature for the constant pressure and constant volume cases for a reactant pressure of 500 kPa. Similar to the 5000 kPa case, the curves cross over beyond a certain reactant temperature and the explanation for it has already been provided.

Figures 48, 49 and 50 shows the values of the availability destroyed at reactant temperatures of 1000 K, 3000 K and 5000 K for a reactant pressure of 500 kPa for constant pressure and constant volume cases for various fuels. As expected, the constant volume case is more efficient at the 1000 K reactant temperatures and this is evident figure 47. The 3000 K and the 5000 K cases indicate that the constant pressure case is more efficient and corresponds to the cross over that occurs in figure 47. The actual values of availability destroyed for various fuels follows the same trend as before with the alkanes destroying more availability with increasing complexity, i.e. iso octane destroying more than propane and methane destroying the least. The alcohols tend to destroy the most availability as seen previously. Hydrogen destroys the least availability followed by acetylene and benzene.

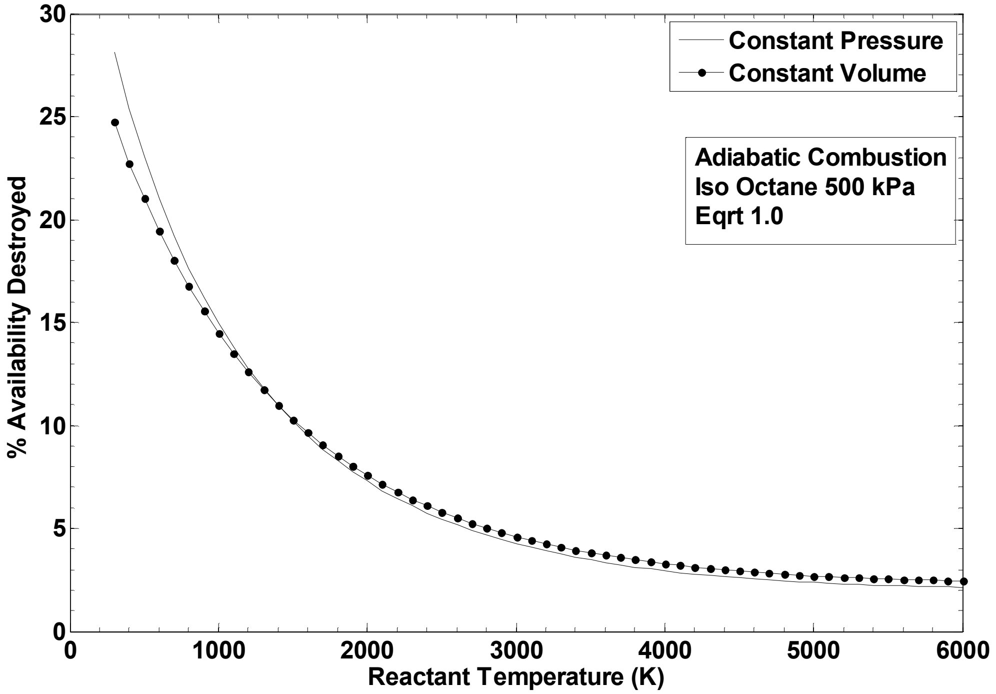

Fig 47. Percentage availability destroyed as a function of reactant temperature for constant pressure and constant volume combustion systems with iso octane, reactant pressure of 500 kPa.

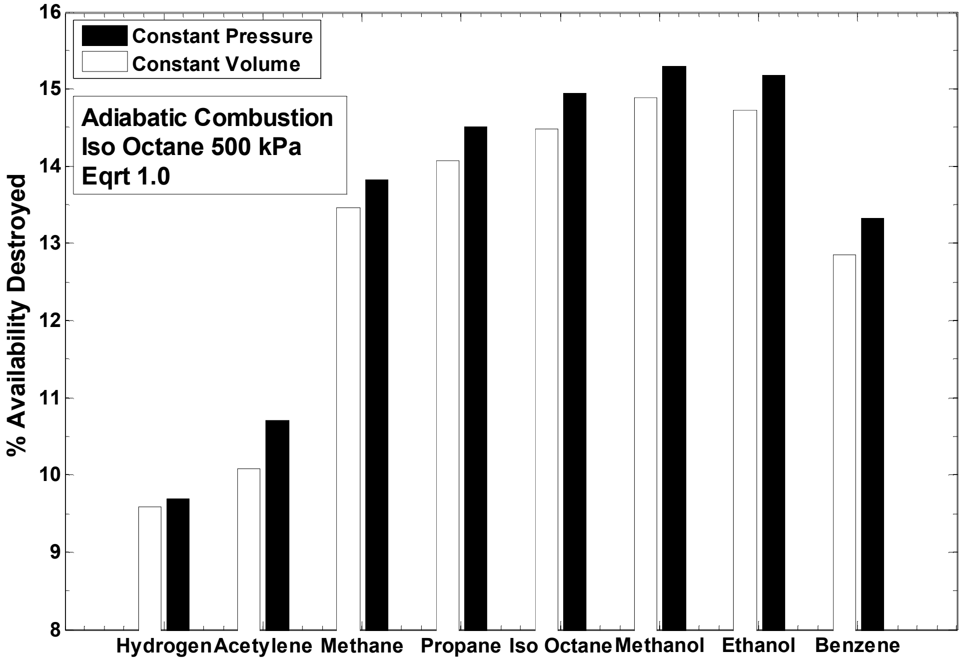

Fig 48. Percentage availability destroyed for different fuels for constant pressure and constant volume combustion systems with iso octane, reactant pressure of 500 kPa and reactant temperature of 1000 K.

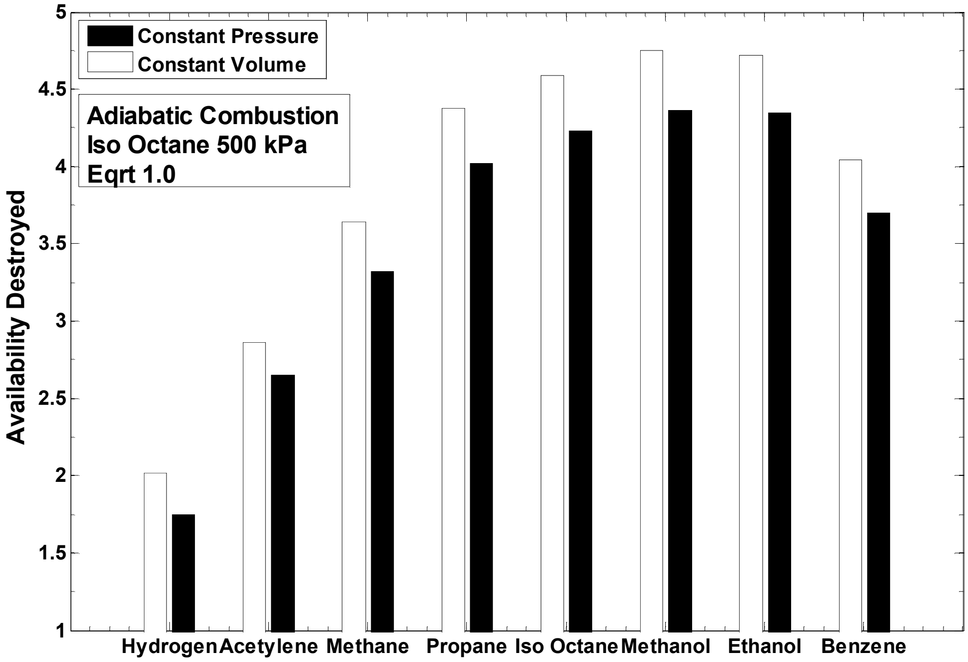

Fig 49. Percentage availability destroyed for different fuels for constant pressure and constant volume combustion systems with iso octane, reactant pressure of 500 kPa and reactant temperature of 3000 K.

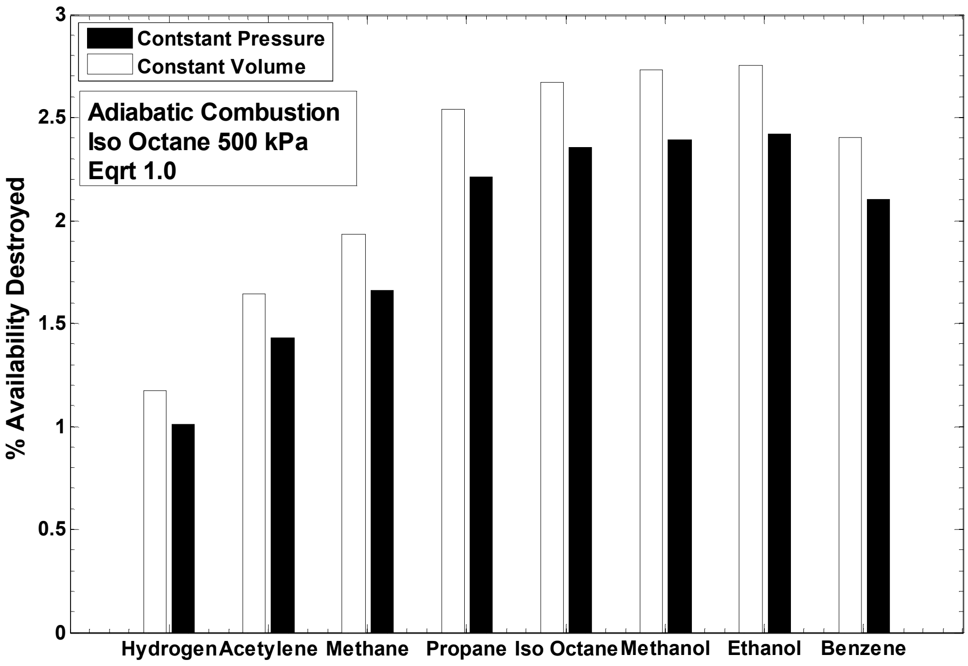

Fig 50. Percentage availability destroyed for different fuels for constant pressure and constant volume combustion systems with iso octane, reactant pressure of 500 kPa and reactant temperature of 5000 K.

V. SUMMARY

The effect of EGR, water/N_2/CO_2 injection and oxygen enrichment on the availability destroyed due to combustion was studied for a range of conditions and fuels for constant pressure and constant volume systems.

Cooled EGR

- Percentage availability destroyed ranged from 36% to 1.5% and 33% to 2% depending on the EGR fraction for a reactant temperature range of 300 K to 6000 K for constant pressure and constant volume combustion systems, respectively.
- Higher EGR fractions lead to greater destruction of availability at the lower reactant temperatures with the trend reversed at the higher temperatures due to lesser percentage of reactant availability converted to product thermo-mechanical availability.
- A ‘Practical’ case showed that the equivalence ratio which corresponded to the lowest amount of availability destroyed at a reactant temperature of 300 K, varied from 0.8 to 1.0 and the reactant temperature that corresponded to the lowest destruction ranged from 800 K to 1300 K for the different EGR fractions.
- Availability destroyed increased with increase in the complexity of the hydrocarbon fuels with acetylene destroying the least and the alcohols destroying the highest amounts of availability at a reactant temperature of 300 K.
- Availability destroyed was sensitive to the lower product temperatures at the higher EGR fractions and not to the structure of the fuel being analyzed.

Water Injection

- Percentage availability destroyed ranged from 36% to 0.5% with a 40% injected fraction for a reactant temperature range of 300 K to 6000 K for constant pressure combustion.
- Higher injected fractions lead to greater destruction of availability at the lower reactant temperatures with the trend reversed at the higher temperatures due to lesser percentage of reactant availability converted to product thermo-mechanical availability.
- Product temperature ranged from 2300 K to 450 K at a reactant temperature of 300 K for injected fractions varying from 0% to 90%.

Comparison Between the Cooled EGR/Water/CO_2/N_2 Injections

- Water injection and cooled EGR resulted in the greatest destruction of availability (36%) for a 40% fraction at a reactant temperature of 300 K with the CO_2 injection lead to the least destruction of about 32%.

Constant Pressure vs. Constant Volume

- Constant volume combustion was more efficient at the lower reactant pressures (50 kPa).
- Constant pressure combustion was more efficient at the higher reactant temperatures (past 1000 K) for higher reactant pressures (5000 kPa).
- Constant volume combustion was more efficient for the different fuels at a reactant temperature of 1000 K with constant pressure combustion being more efficient at reactant temperatures of 3000 K and 5000 K, for a reactant pressure of 500 kPa.

Frozen vs. Non-Frozen ‘Cooled’ EGR

- Analysis of the cooled EGR using a frozen and non-frozen EGR composition showed marginal differences in the availability destroyed.

Adiabatic EGR

- Percentage of availability destroyed decreased with increase in the EGR fraction (14% availability destruction for a 40% EGR fraction).
- Constant volume combustion lead to higher product temperatures and higher mix temperatures than the constant pressure combustion.
- 100 % EGR rate represented an adiabatic flow tube with the exhaust gases looping around.

Oxygen Enrichment

- Percentage availability destroyed dropped sharply to about 25% and the product temperature increased to about 2900 K for 40% oxygen in the inlet, at a reactant temperature of 300 K for constant pressure combustion.

Condensed Species Equilibrium

- Solid carbon is a part of the products at equivalence ratios richer than 3.0 and reactant temperatures lesser than 3000 K.
- Alcohols, being non sooting fuels showed no deviation in the availability destroyed with and without solid carbon.
- Overall effect of the condensed species on availability destroyed was found to be negligible.

REFERENCES

[1] Caton, J.A. A Review of Investigations Using the Second Law of Thermodynamics to Study Internal Combustion Engines. In: SAE Paper no. 2000-01-1081. Society of Automotive Engineers, 2000.

[2] Rakopoulos, C.D., Giakoumis, E.G. Second Law Analysis Applied to Internal Combustion Engines Operation. Progress in Energy and Combustion Science 2005; 1 – 46.

[3] Van Gerpen, J.H., Shapiro, H.N. Second Law Analysis of Diesel Engine Combustion. Journal of Engineering for Gas Turbines and Power 1990; 112: 129 – 137.

[4] Van Gerpen, J.H., Shapiro, H.N. Two Zone Combustion Models for Second Law Analysis of Internal Combustion Engines. In: SAE Paper no. 0148-7191/89/0227-0823. Society of Automotive Engineers, 1989.

[5] Daw, S., Chakravarthy, K., Conklin, J., Graves, R. Refining Understanding of Combustion Irreversibility. In: Proceedings of the 2004 Technical Meeting of the Central States Section of the Combustion Institute, 2004, March 21 – 23; Austin, Texas.

[6] Dunbar, W.R. Lior, N. Sources of Combustion Irreversibility. Combustion Science and Technology 1994; 103: 41-61.

[7] Caton, J.A. On the Destruction of Availability (Exergy) Due to Combustion Processes – with Specific Application to Internal Combustion Engines. Energy 2002; 25: 1097-1117.

[8] Chavannavar, P.S. Parametric Examination of the Destruction of Availability due to Combustion for a Range of Conditions and Fuels. Masters thesis, Department of Mechanical Engineering, Texas A&M University, College Station, Texas, 2005.

[9] Rakopoulos, C.D., Kyritsis, D. Hydrogen Enrichment Effects on the Second Law Analysis of Natural and Landfill Gas Combustion in Engine Cylinders. International Journal of Hydrogen Energy 2005;11.002.

[10] Rakopoulos, C.D., Kyritsis, D. Comparative Second Law Analysis of Internal Combustion Engine Operation for Methane, Methanol, and Dodecane fuels. Energy 2001; 26: 705 – 722.

[11] Mitchell, D.L., Pinson, J.A., Litzinger, T.A. The Effects of Simulated EGR via Intake Air Dilution on Combustion in an Optically Accessible DI Diesel Engine. In: SAE Paper no. 932798. Society of Automotive Engineers, 1993.

[12] Ladommatos, N., Abdelhalim, S.M., Zhao, H., Hu, Z. Effects of EGR on Heat Release in Diesel Combustion. In: SAE Paper no. 980184. Society of Automotive Engineers, 1988.

[13] Jacobs, T., Assanis, D., Philpis, Z. The Impact of Exhaust Gas Recirculation on Performance and Emissions of a Heavy Duty Diesel Engine. In: SAE Paper no. 2003-01-1068. Society of Automotive Engineers, 2003.

[14] Caton, J.A. The Effect of Exhaust Gas Recirculation for Spark Ignition Engine: A Second Law Analysis. Central States Section of the Combustion Institute. 2006 Spring Technical Conference, Combustion Fundamentals and Applications, Cleveland, Ohio.

[15] Zehe, M.J., Gordon, S., McBride, B.J. CAP: A Computer Code for Generating Tabular Thermodynamic Functions from NASA Lewis Coefficients. Report no. NASA/TP – 2001 – 210959/REV1, National Aeronautics and Space Administration, Glenn Research Center, Cleveland, Ohio 2001.

[16] Chemical Equilibrium with Applications, Thermodynamic Properties. http://cea.grc.nasa.gov (Accessed February, 2006)

[17] Gordon, S. McBride, B.J. Computer Program for Calculation of Complex Chemical Equilibrium Compositions and Applications. Reference Publication 1311, National Aeronautics and Space Administration, Lewis Research Center, Cleveland, Ohio 1994.

[18] Moran, M.J. Shapiro, H.N. Fundamentals of Engineering Thermodynamics. 4th ed. Wiley: New York, 2004.

[19] Annamalai, K. Puri. Advanced Thermodynamics Engineering, CRC Press: Boca Raton, Florida, 2003.

APPENDIX I

Frozen vs. Non-Frozen EGR (Cooled)

The recirculated species may be assumed to have a “frozen” or a “non-frozen” composition. The frozen EGR case assumes that the EGR species remain unchanged as these are brought to the reactant temperature from the product temperature. On the other hand the continuous temperature change during the cooling/heating process may cause the EGR composition to be altered. Hence, the non-frozen case presents a more practical picture and it is useful to study the two cases. In the non-frozen case, the EGR species are allowed to attain a new equilibrium composition at the reactant temperature. Hence, these two cases bracket the possible compositions of the EGR gases when they are bought to the reactor inlet.

Figure 51 compares the frozen and non-frozen EGR cases with a 40% EGR fraction and tracks the percentage availability destroyed with change in reactant temperature. Only the 40% EGR case has been depicted here as it showed the maximum deviation from the frozen case. The curves overlap at the lower temperatures, and then separate out in the middle with the frozen EGR case destroying fractionally lesser amount availability before reversing the trend again at the very high temperatures with the non-frozen EGR now destroying fractionally lesser amount of availability. Since most practical applications fall in the lower temperature range, the choice of either model in the EGR simulation does not make a difference as far as tracking the availability destruction goes.

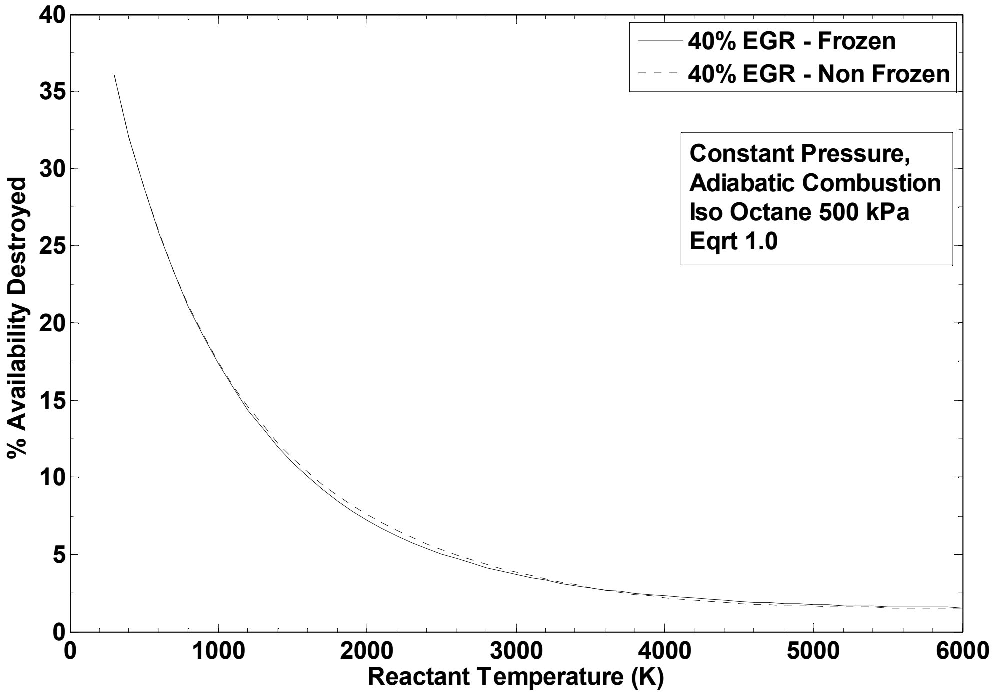

Fig 51. Percentage availability destroyed for frozen and non-frozen 'Cooled EGR' cases as a function of reactant temperature for constant pressure combustion of iso octane.

In the lower temperature ranges, the product temperatures are not high enough to form too many incomplete species after combustion. The majority of the products in this temperature range are in the form of complete products of combustion. Hence even when it is recycled in the frozen state, it does not alter the inlet composition significantly when compared to the non-frozen case. In the non-frozen case, the new equilibrium composition attained at the reactant temperature is not very different from the frozen case as the product temperatures are pretty low and majority of the species exists in its complete form. Hence the two curves overlap.

As the reactant temperature increases, beyond 1000 K, the product temperatures are now high enough such that a larger amount of species in the products exist in incomplete forms. Now when this composition is recycled in a non-frozen manner, the new equilibrium composition at the reactant temperature will force most of these incomplete species to be converted to complete species thus lowering the incoming EGR stream reactive chemical availability.

In the frozen case, since the EGR composition is maintained fixed, the EGR stream reactive chemical availability coming in is much higher due to the incomplete species of higher availability. These act as an additional source of chemical energy in addition to the fuel chemical energy. This results in a slightly higher product temperature in the frozen EGR case as the chemical energy in the EGR species also contributes to the heat released during combustion. This causes the frozen EGR curve to dip slightly below the non-frozen EGR curve in the middle temperature range.

At the higher reactant temperatures past about 3000 K, the trend reverses. The reason for this is due to the fact that the product temperature falls below the reactant temperature at the higher reactant temperatures. Now when the EGR species are recycled in the non-frozen case, the new equilibrium composition is attained at the reactant temperature that is higher than the product temperature. This results in the formation of a greater amount of incomplete species in the non-frozen case and the higher reactive chemical availability contributed by it leads to a higher product temperature in the non-frozen case thus leading to a slightly lesser destruction of availability when compared to the frozen case at these high reactant temperatures.

Figure 52 shows the product temperature variation with the reactant temperature for the 2 cases. As explained, in the lower reactant temperature range, the two curves overlap indicating that the two cases give the same value of availability destruction. Past 1000 K, the curves move away from each other with the frozen EGR case having a higher product temperature and this trend reverses past about 3000 K. This is again due to the fact that at those higher reactant temperatures, the product temperatures are lesser than the corresponding reactant temperatures. Hence in the non-frozen EGR case the EGR stream has to be heated to the higher reactant temperature and this causes the final product temperature for the non-frozen EGR case to be higher.

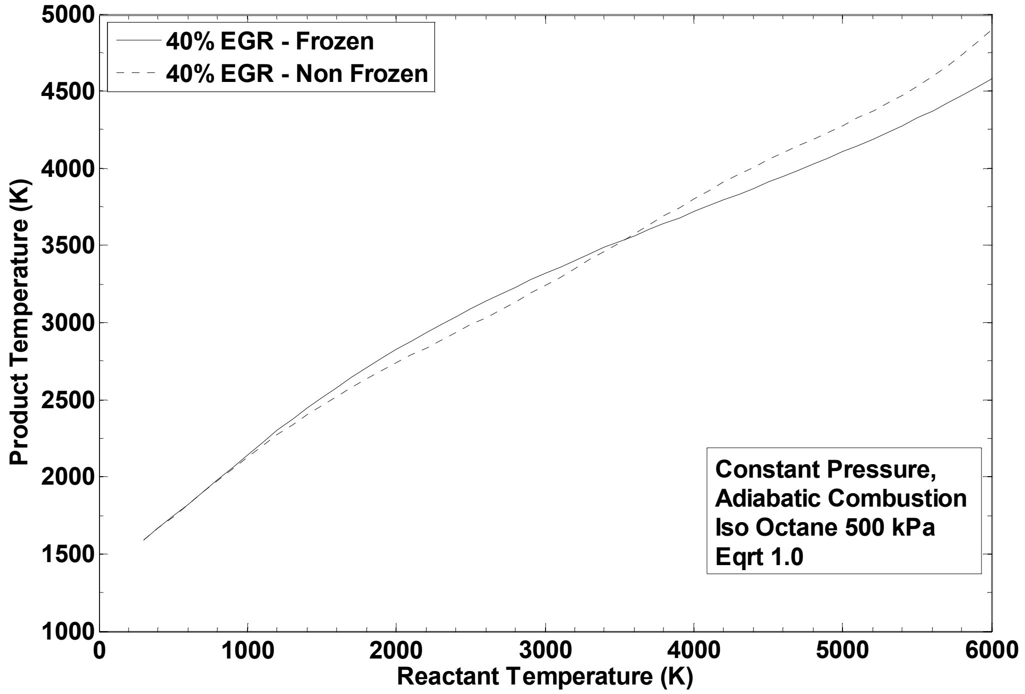

Fig 52. Product temperature for frozen and non-frozen 'Cooled EGR' cases as a function of reactant temperature for constant pressure combustion of iso octane.

Similar trends are noticed in figures 53 and 54 which indicate the variation of the product and reactant availabilities with reactant temperature and the reasons for the crossover is the same as explained for figure 52. The cross points in figure 53 and 54 matches with the cross over point in figure 51.

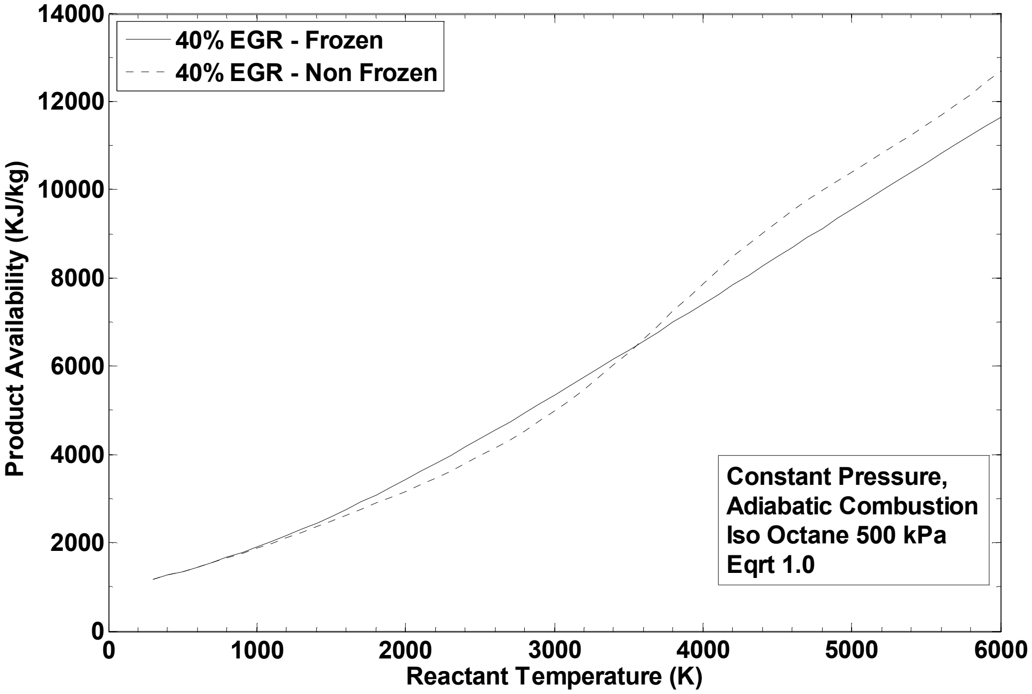

Fig 53. Product availability for frozen and non-frozen 'Cooled EGR' cases as a function of reactant temperature for constant pressure combustion of iso octane.

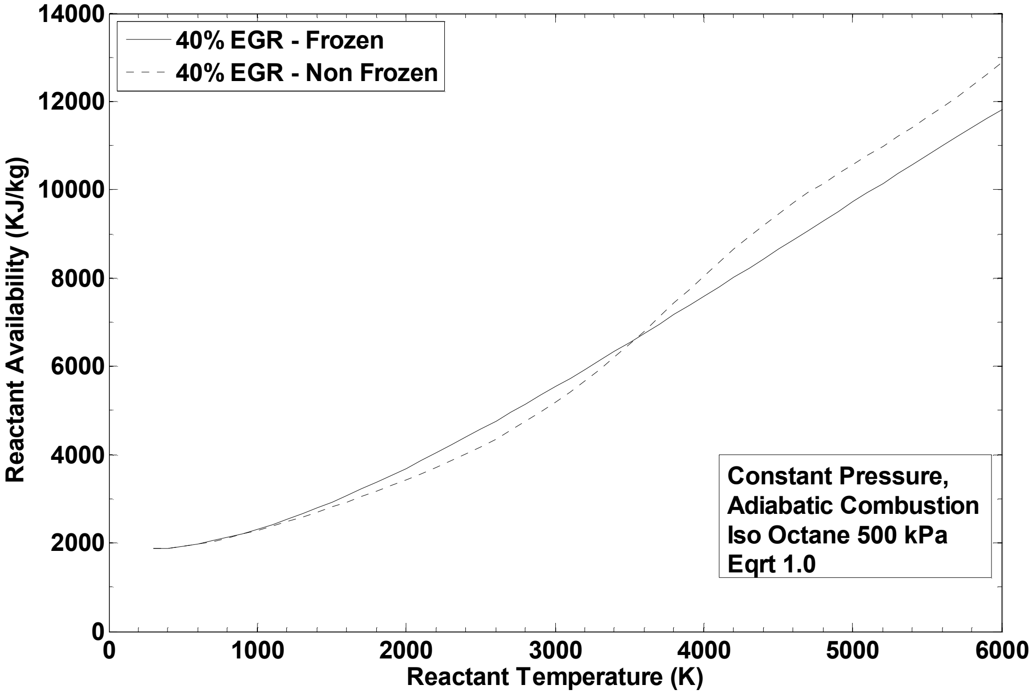

Fig 54. Reactant availability for frozen and non-frozen 'Cooled EGR' cases as a function of reactant temperature for constant pressure combustion of iso octane.

Figure 55 gives a better picture in distinguishing between the two cases. It shows the EGR stream reactive chemical availability varying with reactant temperature. It clearly shows that at low reactant temperatures, the two cases yield the same results with deviation starting to happen beyond 1000 K which corresponds to the start of the deviation in figure 51.

It can also be seen that it is only past 2000 K or so that the EGR stream availability in the non-frozen case starts becoming significant indicating that the new equilibrium composition at the reactant temperature results in a majority of complete products till about a temperature of 2000 K. Again it is seen that the EGR stream availability in the non-frozen stream crosses over at reactant temperatures past 3000 K leading to the fractionally lower destruction of availability in the non-frozen EGR case at the higher reactant temperatures.

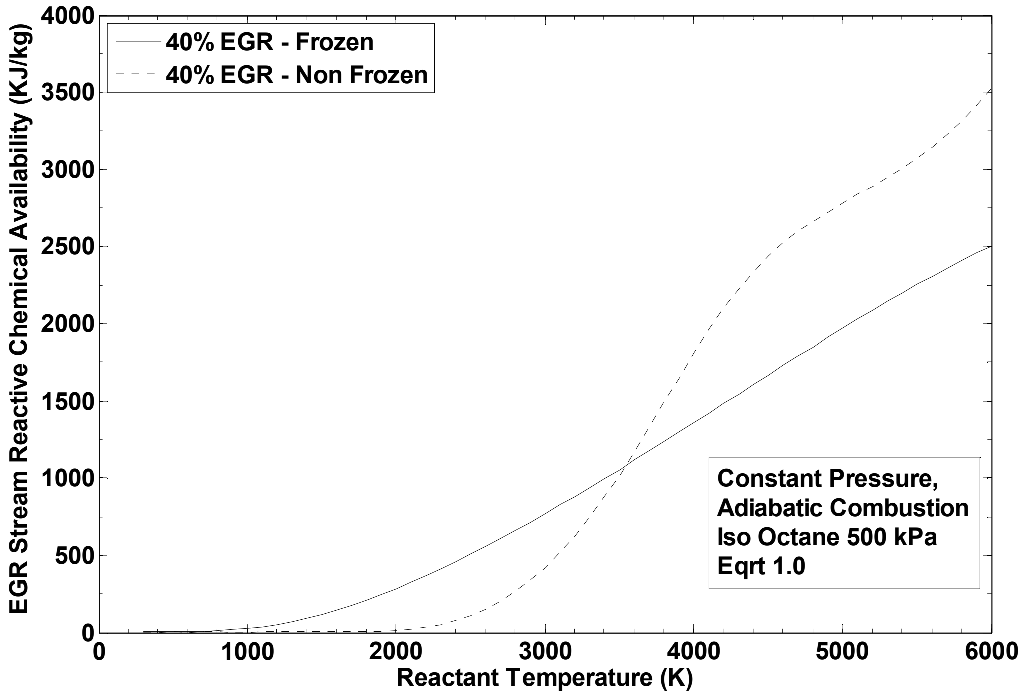

Fig 55. EGR reactive chemical availability for frozen and non-frozen ‘Cooled EGR’ cases as a function of reactant temperature for constant pressure combustion of iso octane.

Adiabatic EGR

Adiabatic exhaust gas recirculation involves the recycling of a fraction of the exhaust gas adiabatically and mixing it with the inlet fuel and air charge. From a practical point of view, recycling the exhaust gas adiabatically is virtually impossible. The mixing of the exhaust gases at the product temperature with the fuel and air charge at the reactant temperature results in a new 'Mix' temperature. This acts as the new reactant temperature for performing the availability analysis.

The mix temperature is found out by performing a simple energy balance between the exhaust gas stream and the incoming fuel and air stream. In a constant enthalpy-pressure process, an enthalpy balance is done whereas as in a constant internal energy-volume process an internal energy balance is performed to find the mix temperature.

$$(h_{EGR} * m_{EGR}) + (h_{A/F} * m_{A/F}) = (h_{inlet} * m_{inlet}) \qquad \text{(Equation 3.29, Section II)}$$

$$(u_{EGR} * m_{EGR}) + (u_{A/F} * m_{A/F}) = (u_{inlet} * m_{inlet}) \qquad \text{(Equation 3.30, Section II)}$$

From the above energy balance, the specific enthalpy/internal energy (h_{inlet} / u_{inlet}) of the mixture is determined and the mix temperature is then found by using an iteration procedure.

A point to notice in the adiabatic EGR process is that the specific enthalpy/internal energy of the mixture that is determined from the above energy balance is always equal to the original reactant mixture enthalpy/internal energy for a given inlet fuel/air temperature. The original reactant mixture refers to the case without an EGR setup (1st Run in an EGR simulation). Due to this, the product temperature remains constant and it is only the reactor inlet temperature that changes as the fuel/air stream mixes with the adiabatic EGR stream resulting in a new mix temperature for a given fuel/air inlet temperature.

Since the product temperature always stays the same, the adiabatic EGR for such simple systems does not represent a practical scenario. With increase in the EGR fraction, the mix temperature essentially approaches the original product temperature and at 100% EGR, the adiabatic case essentially represents an adiabatic flow tube with the exhaust gases looping around continuously.

Figure 56 indicates the variation of the mix temperature with EGR fraction for 3 different EGR cases for an inlet fuel/air temperature of 300 K. As expected, in the cooled EGR case, the exhaust gas is cooled to the inlet temperature and hence the mix temperature stays fixed at

300 K for all EGR fractions. For the adiabatic EGR case, the mix temperature is between the original product temperature and the inlet fuel/air temperature. As the EGR fraction increases, the mix temperature increases. It finally becomes equal to the original product temperature at 100% EGR. The original product temperature for the constant volume combustion case is higher than the constant pressure combustion case, indicating lesser destruction of availability in the constant volume case.

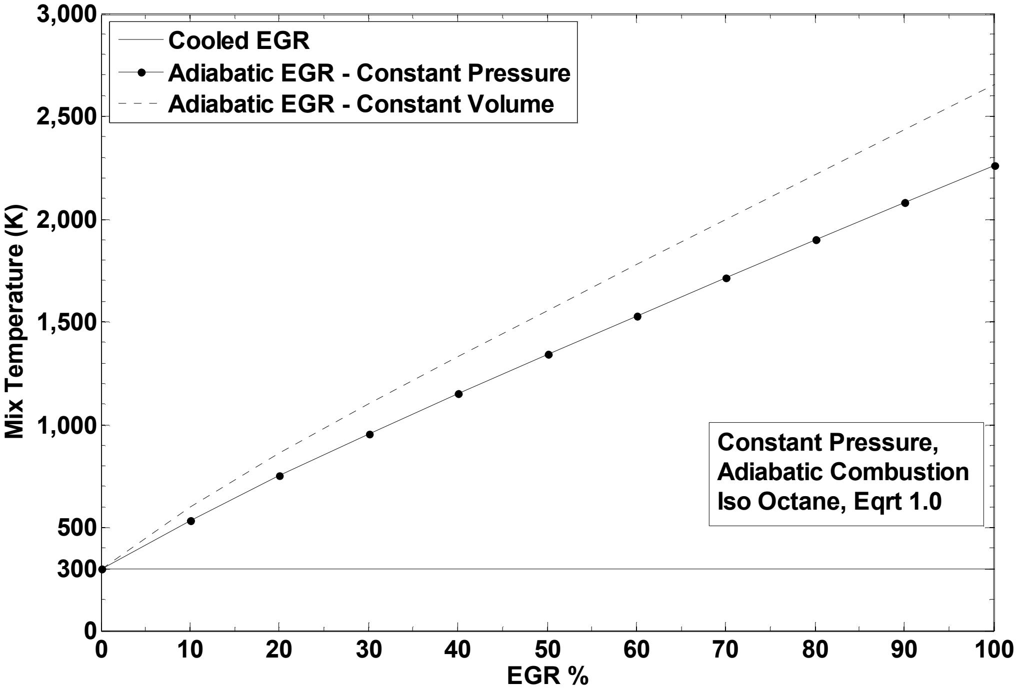

Fig 56. Mix temperature for ‘Cooled’ and ‘Adiabatic’ EGR as a function of EGR % for constant pressure (500 kPa) and constant volume combustion of iso octane, reactant temperature of 300 K.

Figure 57 shows the variation of the availability destroyed with reactant temperature for a constant enthalpy pressure process with an adiabatic EGR setup. It is seen that the availability destroyed decreases with increase in the EGR fraction which is contrary to the cooled EGR case where the availability destroyed increases with increase in EGR fraction.

The reason for this is the peculiar nature of the adiabatic EGR setup for such simple systems. In all EGR processes, the total reactant availability tends to decrease with increase in the EGR fraction. This is primarily due to the fact that a fraction of the fuel chemical availability has been replaced by the EGR charge of lower availability. But in the cooled EGR case, this decrease in the total reactant availability is countered by a corresponding decrease in the total product availability. This is because the product temperature decreases in the cooled EGR case due to the charge dilution by the exhaust gases. In the adiabatic EGR case the product temperature remains constant for a given fuel/air inlet temperature. Hence it is just the total reactant availability that decreases without any change in the product availability. This leads to the reduction in the percentage of the availability destroyed.

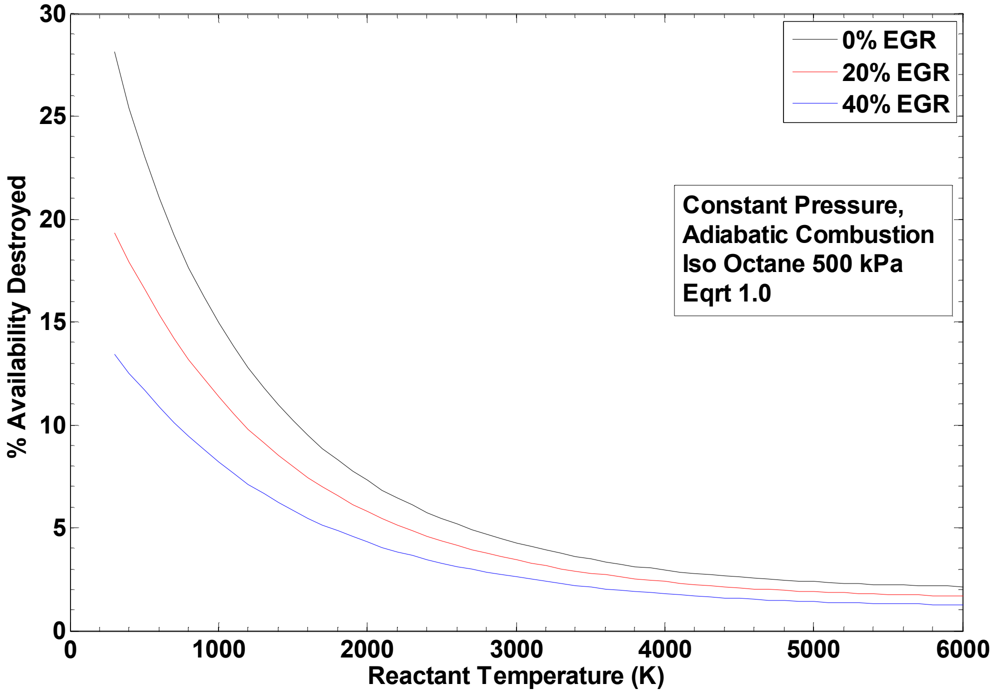

Fig 57. Percentage availability destroyed for different 'Adiabatic' EGR fractions as a function of reactant temperature for constant pressure combustion of iso octane.

Figure 58 compares the cooled and the adiabatic EGR cases for a constant enthalpy pressure process with an EGR fraction of 0.2. As explained, the cooled case destroys a higher percentage of availability for a given EGR fraction and the trends are opposite for the adiabatic and cooled EGR cases with increase in the EGR fraction.

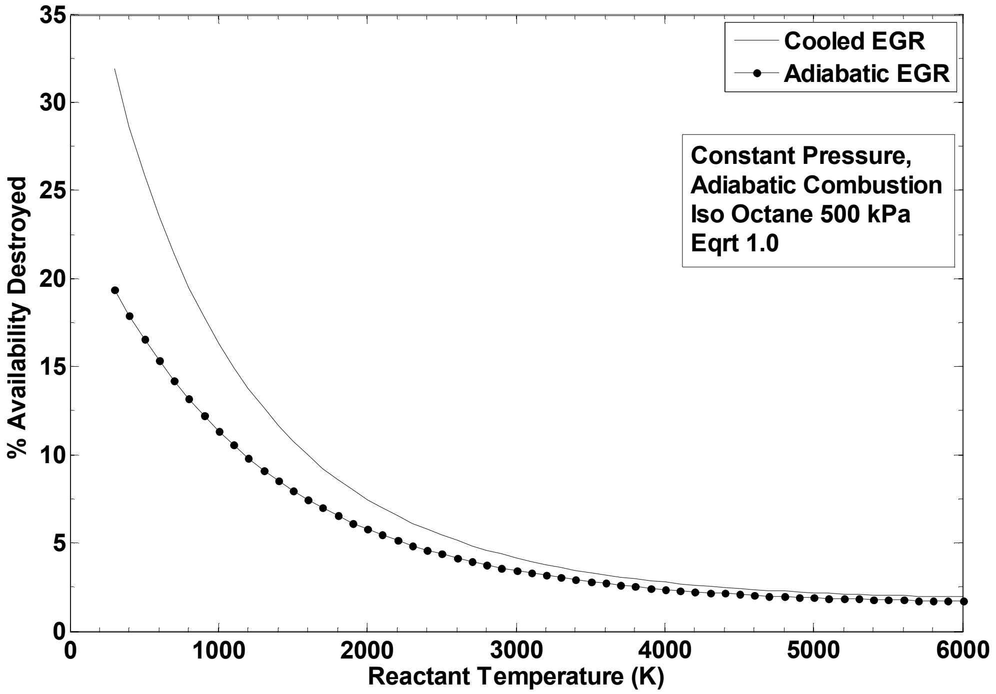

Fig 58. Percentage availability destroyed for a 20% 'Adiabatic' and 'Cooled' EGR fraction as a function of reactant temperature for constant pressure combustion of iso octane.

Oxygen Enrichment

Oxygen enrichment for combustion processes involves increasing the oxygen content in the inlet mixture, thereby ensuring higher temperature, better combustion and lesser destruction of availability. The oxygen enrichment case has been simulated and compared here with a cooled EGR process. The EGR process is essentially opposite to the oxygen enrichment process. During an EGR process, the oxygen content in the inlet mixture essentially decreases as the inlet charge is diluted by the exhaust gases. Although the equivalence ratio stays the same, the net oxygen content in the reactant mixture decreases due to the exhaust gases, resulting in lower temperatures and a higher destruction of availability.

To simulate oxygen enrichment, the oxygen fraction in the incoming air is increased and correspondingly the nitrogen fraction is decreased. The CO_2, Ar and H_2O fractions are kept the same. Since the oxygen fraction in the incoming air increases, the incoming moles of fuel must be changed to keep the equivalence ratio fixed.

Figure 59 shows the percentage of availability destroyed with change in the oxygen percentage by volume in the inlet. The area to the left of the vertical reference line indicates an EGR scenario, and hence, the oxygen percentage in the inlet continuously decreases which leads to greater destruction of availability. The EGR case discussed here is a cooled one and the availability destruction plotted is at an inlet temperature of 300 K for a constant enthalpy pressure process. The vertical reference line indicates the 0% EGR/O_2 Enrichment case. The area to the right of the vertical line indicates the zone in which air with enriched oxygen fraction is supplied for combustion. As expected this decreases the percentage of the availability destroyed.

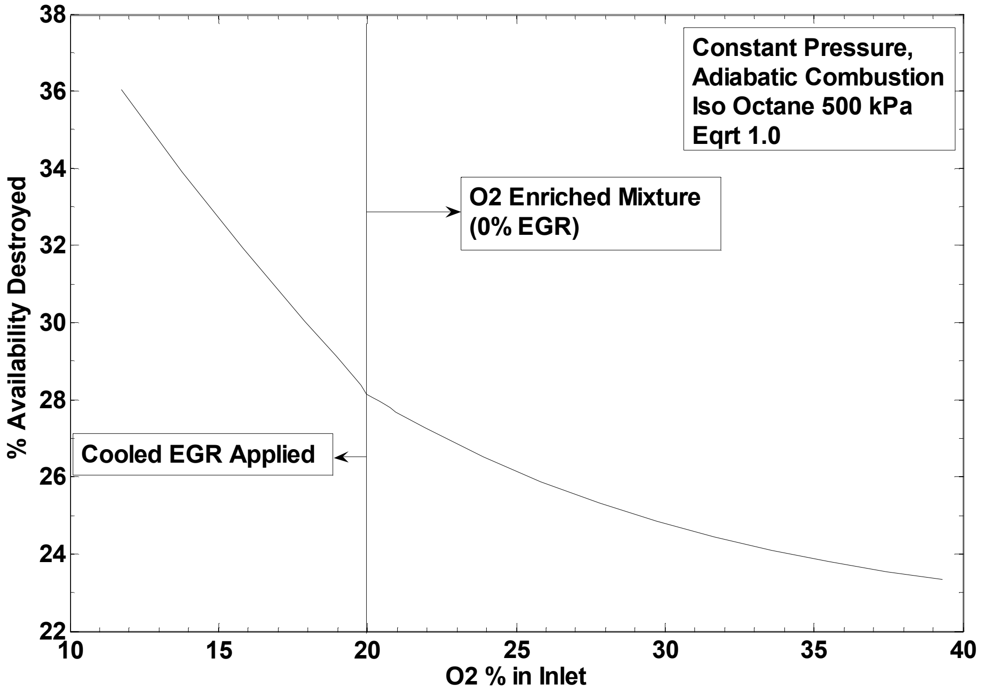

Fig 59. Percentage availability destroyed for 'Cooled' EGR and Oxygen enriched cases as a function of oxygen percentage in inlet for constant pressure combustion of iso octane, reactant temperature of 300 K.

Figure 60 shows the corresponding variation of the product temperature with the oxygen percentage in the inlet. As expected the product temperature decreases with decrease in the oxygen percentage in the inlet. This represents the area to the left of the vertical line, i.e. the area where the cooled EGR is applied. The product temperature increases with increase in the oxygen percentage in the inlet indicating better combustion and lesser destruction of availability as shown in figure 59.

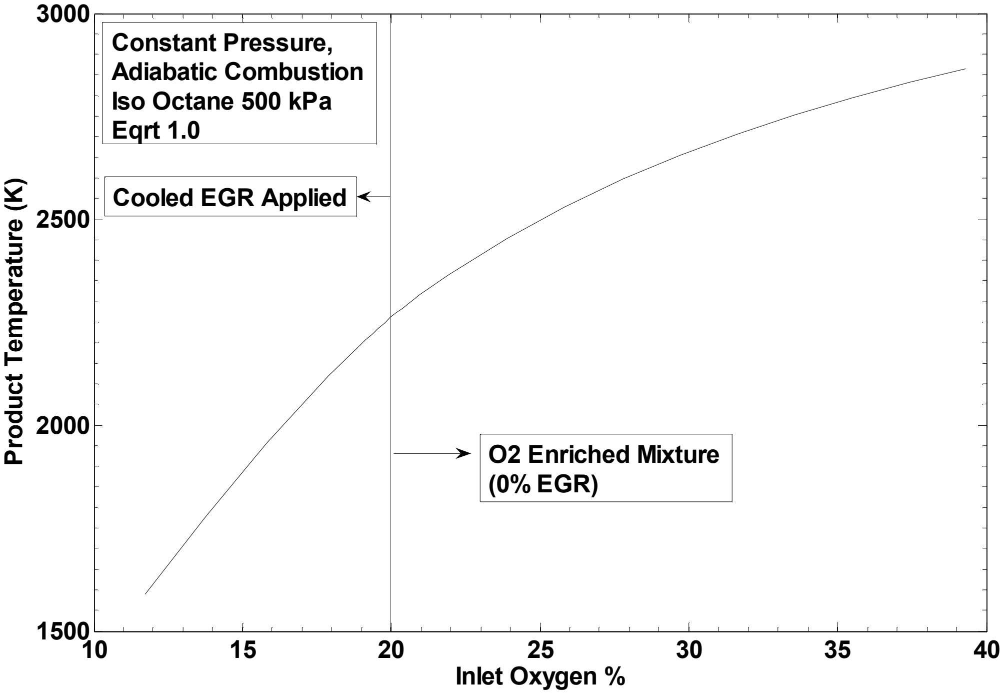

Fig 60. Product temperature for ‘Cooled’ EGR and Oxygen enriched cases as a function of oxygen percentage in inlet for constant pressure combustion of iso octane, reactant temperature of 300 K.

Condensed Species Equilibrium

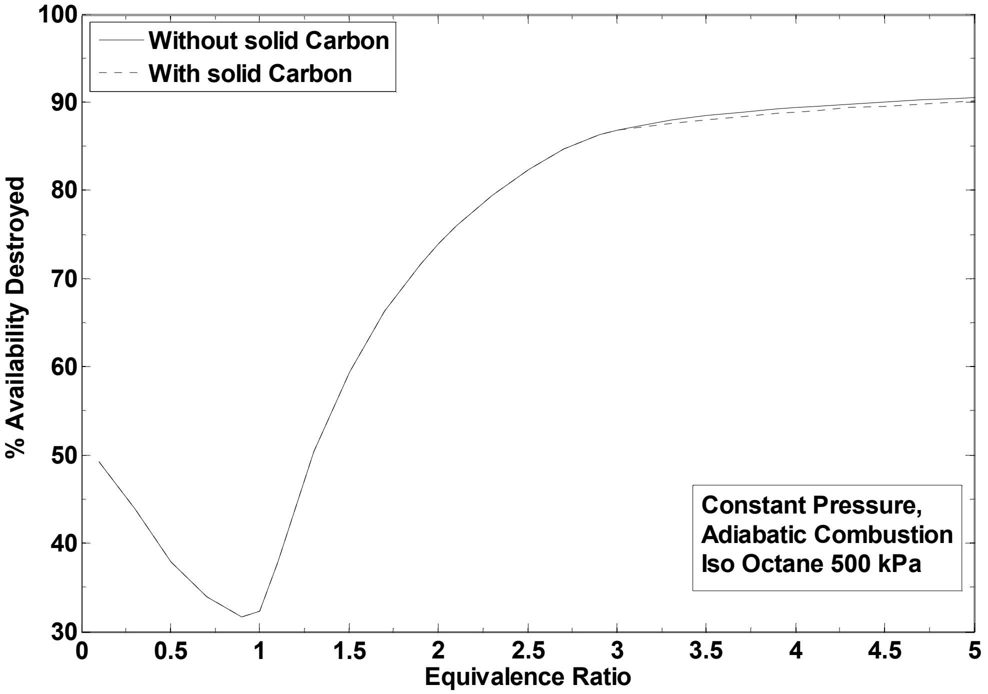

Fig 61. Percentage availability destroyed for 'Practical' cases with and without solid carbon for constant pressure combustion of iso octane, reactant temperature of 300 K.

Figure 61 shows the percentage availability destroyed as a function of the equivalence ratio for cases with and without the presence of solid carbon in the products. A "practical" case is considered here wherein the reactive chemical availability left in the product mixture after the combustion process is not accounted for as useful availability. For equivalence ratios from 0.0 to about 3.0, the two curves overlap as there is no significant solid carbon present at equivalence ratios less than 3.0. At around an equivalence ratio of 3.0, the two curves separate out with the curve corresponding to the inclusion of solid carbon destroying a marginally lesser amount of availability when compared to the one without solid carbon. Here the total reactant availability is the same for both the cases. The case with solid carbon shows marginally higher product thermo-mechanical availability than the one without solid carbon at a reactant temperature of 300 K which is consistent with a higher product temperature in the case involving solid carbon at a reactant temperature of 300 K. Here the reactive chemical availability of the product mixture is not considered as useful. The diffusive chemical availabilities in both the cases are close to the same value. Hence the case with solid carbon corresponds to a lesser percentage of destruction of availability due to the slightly higher product thermo-mechanical availability associated with it. The curves indicate a reduction in the availability destroyed till about an equivalence ratio of about 0.9 after which the availability destroyed increases. This is due to the formation of incomplete products of combustion whose reactive chemical availability is not being accounted for.

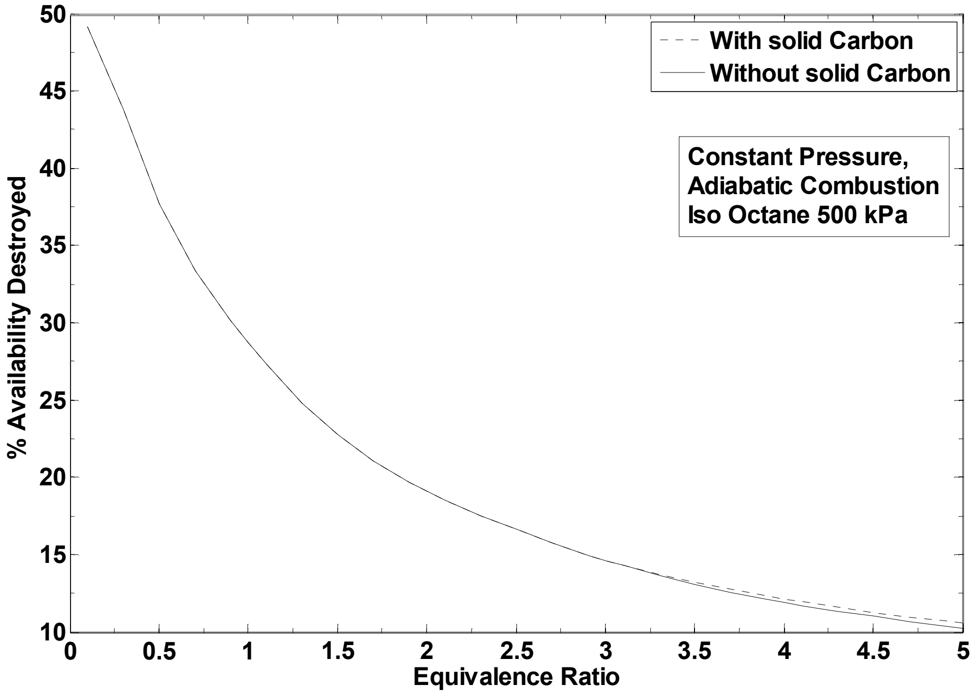

Fig 62. Percentage availability destroyed for 'Impractical' cases with and without solid carbon for constant pressure combustion of iso octane, reactant temperature of 300 K.

Figure 62 indicates the effect of varying the equivalence ratio on the percentage of availability destroyed. An "impractical" case is considered here wherein the reactive chemical availability left in the product mixture after the combustion process is accounted for as useful availability. This leads to a reduction in the availability destroyed with increase in equivalence ratios. Again here, the two curves are together till an equivalence ratio of about 3.0 after which they separate due to the formation of solid carbon. Here the trend is opposite to the one observe in figure 1 in that the case involving solid carbon destroys more availability than the case without solid carbon. This is due to the fact that the reactive chemical availability previously unaccounted for is larger in the case without solid carbon and this dominates the slightly lower product thermo-mechanical availability observed in the case without solid carbon and leads to an overall greater product availability when compared to the case with solid carbon and hence leads to a lesser destruction of availability.

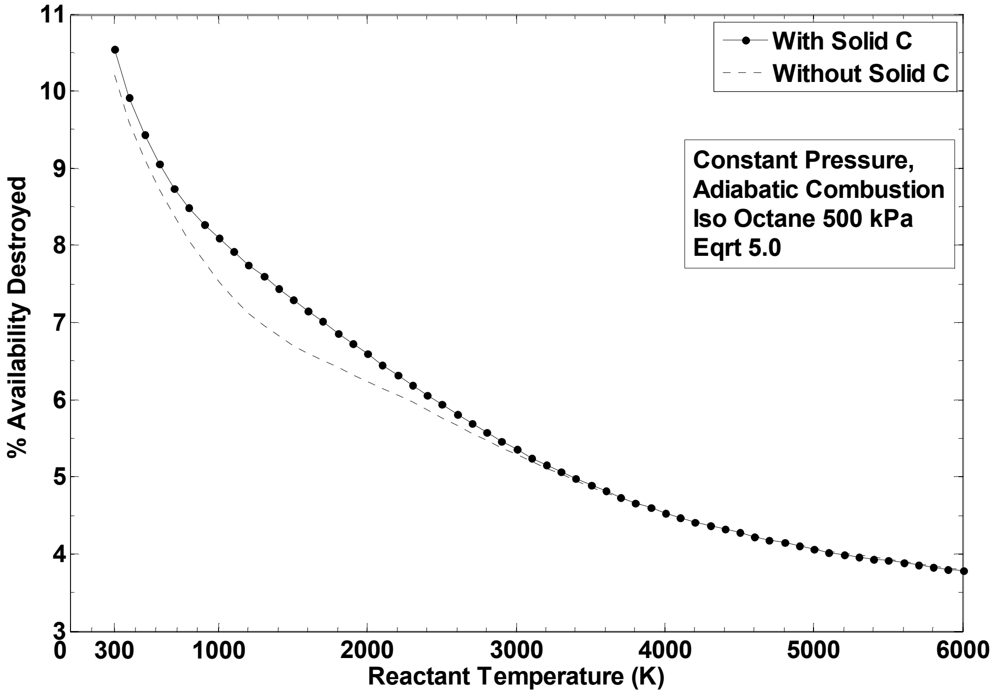

Fig 63. Percentage availability destroyed for cases with and without solid carbon as a function of reactant temperature for constant pressure combustion of iso octane.

Figure 63 shows the percentage of availability destroyed as a function of reactant temperature for an equivalence ratio of 5.0 for cases with and without solid carbon. This is an “impractical” scenario as the reactive chemical availability in the product mixture is being accounted for as useful availability. Here the two curves merge at a reactant temperature of around 3000 K indicating the fact that at this temperature all the solid carbon is converted into various gaseous carbon species. Again, the availability destroyed in the case with solid carbon is more than the case without solid carbon which is consistent with the trend in figure 62. The higher product availability for case without solid carbon is due a higher reactive chemical availability. Even though the product thermo-mechanical availability is higher for the case with solid carbon, the higher reactive chemical availability in the case without solid carbon compensates for this and leads to a lower destruction of availability.

From figures 61, 62 and 63 it is clearly seen that the solid carbon is predicted by the equilibrium in the product species only when the equivalence ratio is grater than 3.0. At an equivalence ratio of 5.0, the solid carbon exists in the product species only up to a reactant temperature of about 3500K. After this temperature, all the solid carbon is converted into various gaseous carbon species. The temperature of 3500K is close to the sublimation temperature of solid carbon too.

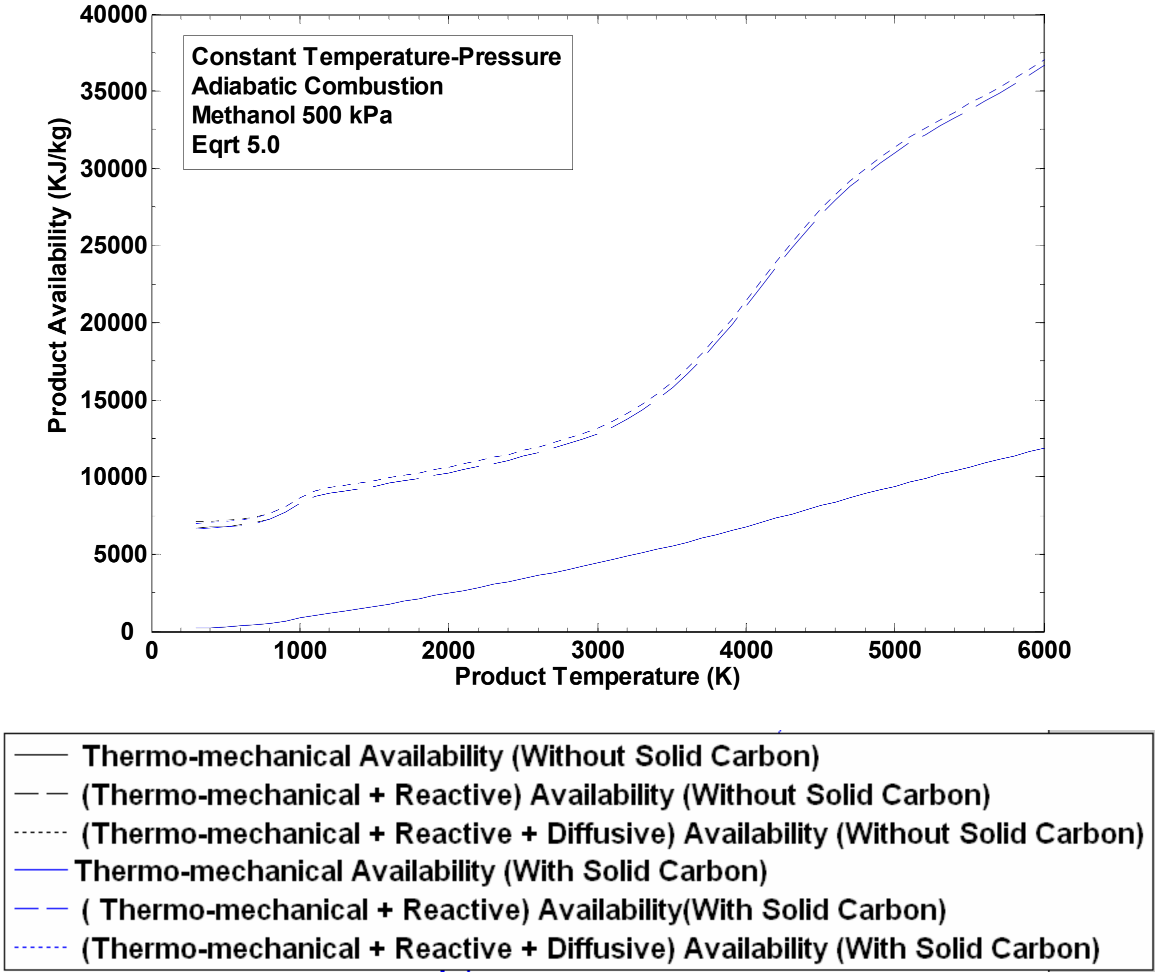

Fig 64. Various components of product availability for cases with and without solid carbon as a function of product temperature for constant temperature and pressure combustion of methanol.

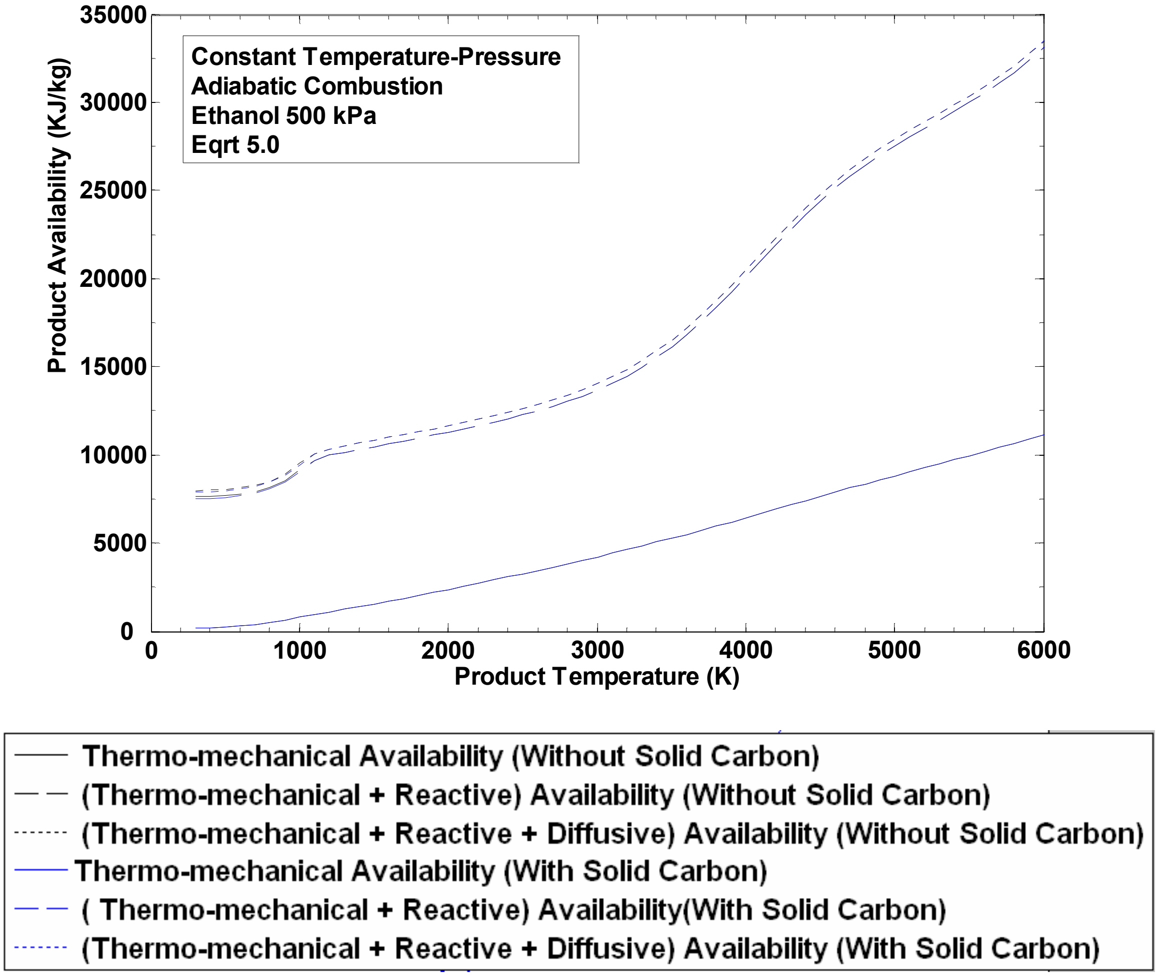

Fig 65. Various components of product availability for cases with and without solid carbon as a function of product temperature for constant temperature and pressure combustion of ethanol.

Figures 64 and 65 depict the product availability as a function of product temperature at an equivalence ratio of 5.0 and a pressure of 500 kPa for a constant temperature and constant pressure combustion of methanol and ethanol. It is seen that there is negligible effect on the thermo-mechanical availability of the products due to the inclusion of solid carbon in the products. The diffusive availabilities also remain constant in both the cases. The oxygenated fuels methanol and ethanol shows negligible variations in the reactive availabilities in the both the cases. The solid carbon disappears at much lower temperatures in the case of oxygenated fuels which again lead to negligible variations in the product availabilities in both the cases. Although equilibrium predicts that solid carbon will be a part of the products at such rich equivalence ratios for the oxygenated fuels, the fact that it disappears at much lower temperatures when compared to other hydrocarbon fuels and the identical trends shown in both cases for the product availabilities agrees with the notion that the oxygenated fuels are generally regarded as non sooting fuels.

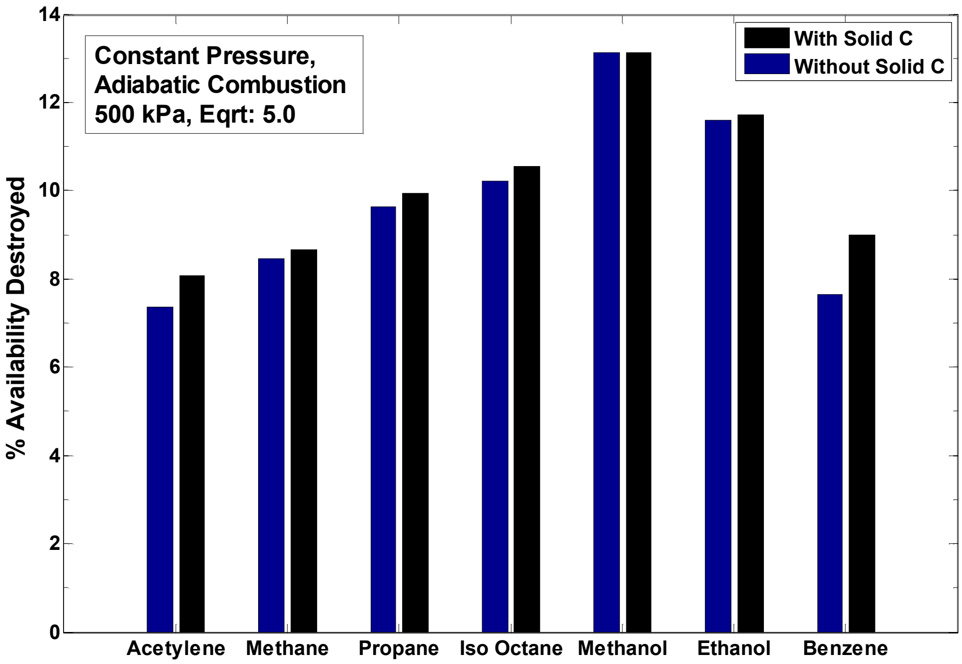

Fig 66. Percentage availability destroyed for different fuels for cases with and without solid carbon for constant pressure combustion, reactant temperature of 300 K.

Figure 66 indicates the percentage availability destroyed for different fuels under going a constant pressure combustion process at a reactant temperature of 300 K with and without the inclusion of solid carbon. The inclusion of solid carbon does increase the percentage availability destroyed by a fraction for most fuels. The oxygenated fuels, methanol and ethanol show the least variations in the percentage availability destroyed agreeing with the notion that they are non-sooting fuels as shown in figures 64 and 65.

APPENDIX II

NASA LEWIS POLYNOMIAL COEFFICIENTS FOR FUELS

Table II.1. Coefficients for use with the NASA Lewis polynomials

Fuel	Formula	Range	a1	a2	a3	a4	a5	a6	a7	b1	b2	hf
Methane	CH4	200 - 1000	-1.766851E+05	2.786181E+03	-1.202578E+01	3.917619E-02	-3.619054E-05	2.026853E-08	-4.976705E-12	-2.331314E+04	8.904323E+01	-74600
		1000 - 6000	3.730043E+06	-1.383501E+04	2.049107E+01	-1.961975E-03	4.727313E-07	-3.728815E-11	1.623737E-15	7.532067E+04	-1.219125E+02	
Acetylene	C2H2	200 - 1000	1.598112E+05	-2.216644E+03	1.265708E+01	-7.979651E-03	8.054993E-06	-2.433308E-09	-7.529233E-14	3.712619E+04	-5.244339E+01	228200
		1000 - 6000	1.713847E+06	-5.929107E+03	1.236128E+01	1.314187E-04	-1.362764E-07	2.712656E-11	-1.302066E-15	6.266579E+04	-5.818961E+01	
Ethylene	C2H4	200 - 1000	-1.163606E+05	2.554852E+03	-1.609746E+01	6.625779E-02	-7.885082E-05	5.125225E-08	-1.370340E-11	-6.176191E+03	1.093338E+02	52500
		1000 - 6000	3.408764E+06	-1.374848E+04	2.365898E+01	-2.423804E-03	4.431396E-07	-4.352683E-11	1.775411E-15	8.820429E+04	-1.371278E+02	
Ethane	C2H6	200 - 1000	-1.862044E+05	3.406192E+03	-1.951705E+01	7.565836E-02	-8.204173E-05	5.061136E-08	-1.319282E-11	-2.702933E+04	1.298140E+02	-83851
		1000 - 6000	5.025782E+06	-2.033022E+04	3.322553E+01	-3.836703E-03	7.238406E-07	-7.319183E-11	3.065469E-15	1.115964E+05	-2.039411E+02	
Propylene	C3H6	200 - 1000	-1.912462E+05	3.542074E+03	-2.114879E+01	8.901485E-02	-1.001429E-04	6.267959E-08	-1.637871E-11	-1.529962E+04	1.407641E+02	20000
		1000 - 6000	5.017620E+06	-2.086084E+04	3.644156E+01	-3.881191E-03	7.278677E-07	-7.321205E-11	3.052176E-15	1.261245E+05	-2.195716E+02	
Propane	C3H8	200 - 1000	-2.433144E+05	4.656271E+03	-2.939466E+01	1.188953E-01	-1.376308E-04	8.814824E-08	-2.342988E-11	-3.540335E+04	1.841749E+02	-104680
		1000 - 6000	6.420732E+06	-2.659791E+04	4.534357E+01	-5.020664E-03	9.471217E-07	-9.575405E-11	4.009673E-15	1.455582E+05	-2.818375E+02	
n-Butane	C4H10	200 - 1000	-3.175873E+05	6.176332E+03	-3.891562E+01	1.584654E-01	-1.860050E-04	1.199676E-07	-3.201671E-11	-4.540363E+04	2.379489E+02	-125790
		1000 - 6000	7.682322E+06	-3.256052E+04	5.736733E+01	-6.197917E-03	1.180186E-06	-1.221894E-10	5.250635E-15	1.774527E+05	-3.587919E+02	
n-Pentane	C5H12	200 - 1000	-2.768895E+05	5.834283E+03	-3.617541E+01	1.533340E-01	-1.528396E-04	8.191092E-08	-1.792328E-11	-4.665375E+04	2.265544E+02	-146760
		1000 - 6000	-2.530779E+06	-8.972593E+03	4.536223E+01	-2.626990E-03	3.135136E-06	-5.318729E-10	2.886897E-14	1.484617E+04	-2.516550E+02	
Benzene	C6H6	200 - 1000	-1.677341E+05	4.404500E+03	-3.717378E+01	1.640510E-01	-2.020812E-04	1.307915E-07	-3.444284E-11	-1.035455E+04	2.169853E+02	82880
		1000 - 6000	4.538576E+06	-2.260503E+04	4.694007E+01	-4.206677E-03	7.907994E-07	-7.968302E-11	3.328212E-15	1.391465E+05	-2.868751E+02	
n-Hexane	C6H14	200 - 1000	-5.815927E+05	1.079098E+04	-6.633947E+01	2.523715E-01	-2.904345E-04	1.802202E-07	-4.617224E-11	-7.271545E+04	3.938284E+02	-166920
		1000 - 6000	-3.106626E+06	-7.346088E+03	4.694132E+01	1.693964E-03	2.068997E-06	-4.212142E-10	2.452346E-14	5.237503E+02	-2.549968E+02	

Table II.1. Continued

Fuel	Formula	Range	a1	a2	a3	a4	a5	a6	a7	b1	b2	hf
n-Heptane	C7H16	200 - 1000	-6.127433E+05	1.184085E+04	-7.487189E+01	2.918466E-01	-3.416795E-04	2.159285E-07	-5.655853E-11	-8.013409E+04	4.407213E+02	-187780
		1000 - 6000	9.135632E+06	-3.923320E+04	7.889781E+01	-4.654252E-03	2.071774E-06	-3.442539E-10	1.976835E-14	2.050708E+05	-4.851104E+02	
n-Octane	C8H18	200 - 1000	-6.986647E+05	1.338501E+04	-8.415166E+01	3.271937E-01	-3.777210E-04	2.339837E-07	-6.010893E-11	-9.026223E+04	4.939222E+02	-208750
		1000 - 6000	6.365407E+06	-3.105365E+04	6.969162E+01	1.048060E-02	-4.129622E-06	5.543226E-10	-2.651436E-14	1.500969E+05	-4.169896E+02	
Iso-Octane (l	C8H18	165.79 - 380	1.419158E+05	-2.937251E+03	4.168835E+01	-8.436942E-02	2.894148E-04	-2.200564E-07	7.234226E-11	-2.479399E+04	-1.930220E+02	-259160
Iso-Octane	C8H18	200 - 1000	-1.688759E+05	3.126903E+03	-2.123503E+01	1.489152E-01	-1.151180E-04	4.473216E-08	-5.554882E-12	-4.468061E+04	1.417456E+02	-224010
		1000 - 6000	1.352765E+07	-4.663370E+04	7.795313E+01	1.423730E-02	-5.073594E-06	7.248233E-10	-3.819190E-14	2.541178E+05	-4.933887E+02	
Methanol	CH3OH	200 - 1000	-2.416643E+05	4.032147E+03	-2.046415E+01	6.903698E-02	-7.598933E-05	4.598208E-08	-1.158707E-11	-4.433261E+04	1.400142E+02	-200940
		1000 - 6000	3.411571E+06	-1.345500E+04	2.261408E+01	-2.141029E-03	3.730051E-07	-3.498846E-11	1.366073E-15	5.636082E+04	-1.277814E+02	
Ethanol	C2H5OH	200 - 1000	-2.342791E+05	4.479181E+03	-2.744817E+01	1.088679E-01	-1.305309E-04	8.437346E-08	-2.234559E-11	-5.022229E+04	1.764829E+02	-234950
		1000 - 6000	4.694818E+06	-1.929798E+04	3.447584E+01	-3.236166E-03	5.784948E-07	-5.564600E-11	2.226226E-15	8.601623E+04	-2.034802E+02	
Carbon	C	200 - 1000	6.495031E+02	-9.649011E-01	2.504675E+00	-1.281448E-05	1.980134E-08	-1.606144E-11	5.314483E-15	8.545763E+04	4.747924E+00	716680
		1000 - 6000	-1.289136E+05	1.719529E+02	2.646044E+00	-3.353069E-04	1.742093E-07	-2.902818E-11	1.642182E-15	8.410598E+04	4.130047E+00	
		6000 - 2000	4.432528E+08	-2.886018E+05	7.737108E+01	-9.715282E-03	6.649595E-07	-2.230079E-11	2.899389E-16	2.355273E+06	-6.405123E+02	
Hydrogen	H2	200 - 1000	4.078323E+04	-8.009186E+02	8.214702E+00	-1.269714E-02	1.753605E-05	-1.202860E-08	3.368093E-12	2.682485E+03	-3.043789E+01	0
		1000 - 6000	5.608128E+05	-8.371505E+02	2.975365E+00	1.252249E-03	-3.740716E-07	5.936625E-11	-3.606994E-15	5.339824E+03	-2.202775E+00	
		6000 - 2000	4.966884E+08	-3.147547E+05	7.984122E+01	-8.414789E-03	4.753248E-07	-1.371873E-11	1.605462E-16	2.488434E+06	-6.695728E+02	
Carbon	CO	200 - 1000	1.489045E+04	-2.922286E+02	5.724527E+00	-8.176235E-03	1.456903E-05	-1.087746E-08	3.027942E-12	-1.303132E+04	-7.859241E+00	-110535
Monoxide		1000 - 6000	4.619197E+05	-1.944705E+03	5.916714E+00	-5.664283E-04	1.398815E-07	-1.787680E-11	9.620936E-16	-2.466261E+03	-1.387413E+01	
		6000 - 2000	8.868663E+08	-7.500378E+05	2.495475E+02	-3.956351E-02	3.297772E-06	-1.318410E-10	1.998938E-15	5.701421E+06	-2.060705E+03	

APPENDIX III

ATMOSPHERIC COMPOSITION

Table III.1. “Standard Wet Atmospheric” Composition used in the analyses

Species	Percentage (Mole fractions)
Nitrogen, N_2	0.7565
Oxygen, O_2	0.2029
Carbon dioxide, CO_2	0.0003
Water, H_2O	0.0313
Argon, Ar	0.0090

APPENDIX IV

FUEL AVAILABILITIES

Table IV.1. Availability values for various fuels

FUEL	**FORMULA**	**Fuel availability* (kJ/kg)**
Hydrogen	H_2	115080
Carbon (g)	C	88802
Carbon monoxide	CO	9242
Methane	CH_4	50573
Acetylene	C_2H_2	47484
Propane	C_3H_8	47546
Benzene	C_6H_6	41055
Iso Octane (g)	C_8H_{18}	46244
Methanol	CH_3OH	21836
Ethanol	C_2H_5OH	28735
Carbon (g)	C_2	65161
Carbon (g)	C_3	54371
Solid Carbon	C (gr)	32865
Carbon-Hydrogen	CH	82525
Hydrogen atom	H	318354
Hydroxyl radical	OH	8890
Oxygen atom	O	14758
Nitrogen atom	N	32774
Nitrogen oxide	NO	3088
Nitrogen dioxide	NO_2	1344

* Values calculated from, Fundamentals of Engineering Thermodynamics, Fourth edition, Moran M J and Shapiro H N and Advanced Thermodynamics Engineering, CRC press, Annamalai and Puri.

VITA

Name	Hari Shanker Sivadas
Address	2C, Aishwarya Apartments, 2nd Main Road, CIT Nagar, Chennai – 600037, India.
Education	Master of Science, Mechanical Engineering, August 2007 Texas A&M University, College Station, Texas, USA. Bachelor of Science, Engineering, ANNA University, Chennai, Tamil Nadu, India
Experience	Graduate Research Assistant (January 2006 – May 2007) Dept. of Mechanical Engineering, Texas A&M University, College Station, Texas Studied the effects of EGR, Water/CO_2/N_2 Injection and Oxygen Enrichment on the Availability Destroyed due to Combustion for a Range of Conditions and Fuels. Intern (November 2004 – March 2005) Ashok Leyland Technical Center, Chennai, India Designed a ‘Central Tire Inflation System’ for a STALLION MK II Army Transport Vehicle.